



**Kaunas University of Technology**

Faculty of Electrical and Electronics Engineering

**Technical University of Cartagena**

School of Industrial Engineering

**Human motion estimation and analysing feasible collisions  
between individuals in real settings by using conventional  
cameras and Deep Learning-based algorithms**

Bachelor's Final Degree Project

---

**Rafael Sojo García**

Project author

**Assoc Prof. Dr. Nieves Pavón Pulido**  
**Assoc Prof. Dr. Virginijus Baranauskas**

Supervisor

---

**Cartagena, Kaunas 2022**



**Kaunas University of Technology**

Faculty of Electrical and Electronics Engineering

**Technical University of Cartagena**

School of Industrial Engineering

# **Human motion estimation and analysing feasible collisions between individuals in real settings by using conventional cameras an Deep Learning-based algorithms**

Bachelor's Final Degree Project

Intelligent Robotics Systems (6121EX013)

Industrial Electronics and Automation Engineering (5071)

---

**Rafael Sojo García**

Project author

**Assoc. Prof. Nieves Pavón Pulido**

**Assoc Prof. Dr. Virginijus**

**Baranauskas**

Supervisors

**Assoc. Prof. Dr. Arūnas Lipnickas**

Reviewer

---

**Cartagena, Kaunas 2022**



**Kaunas University of Technology**

Faculty of Electrical and Electronics Engineering

**Technical University of Cartagena**

School of Industrial Engineering

Rafael Sojo García

# **Human motion estimation and analysing feasible collisions between individuals in real settings by using conventional cameras and Deep Learning-based algorithms**

## Declaration of Academic Integrity

I confirm the following:

1. I have prepared the final degree project independently and honestly without any violations of the copyrights or other rights of others, following the provisions of the Law on Copyrights and Related Rights of the Republic of Lithuania, the Regulations on the Management and Transfer of Intellectual Property of Kaunas University of Technology (hereinafter – University) and the ethical requirements stipulated by the Code of Academic Ethics of the University;
2. All the data and research results provided in the final degree project are correct and obtained legally; none of the parts of this project are plagiarised from any printed or electronic sources; all the quotations and references provided in the text of the final degree project are indicated in the list of references;
3. I have not paid anyone any monetary funds for the final degree project or the parts thereof unless required by the law;
4. I understand that in the case of any discovery of the fact of dishonesty or violation of any rights of others, the academic penalties will be imposed on me under the procedure applied at the University; I will be expelled from the University and my final degree project can be submitted to the Office of the Ombudsperson for Academic Ethics and Procedures in the examination of a possible violation of academic ethics.

Rafael Sojo García.

**APPROVED BY:**

KTU Faculty of Electrical and Electronics Engineering

Head of the Department of Automation

Assoc. prof. dr. Gintaras Dervinis

2022 05 04

## TASK OF FINAL PROJECT OF UNDERGRADUATE (BACHELOR) STUDIES

<b>Issued to the Student:</b>	<i>Rafael Sojo García</i>	Group	ERB8/2
<b>1. Project Subject:</b>			
Lithuanian Language:	Žmogaus judėjimo įvertinimas ir galimų susidūrimų analizė tarp asmenų realiomis sąlygomis, naudojant įprastą kamerą ir giliojo mokymosi algoritmus		
English Language:	Human motion estimation and analysing feasible collisions between individuals in real settings by using conventional cameras and Deep Learning-based algorithms		

Approved 2022 April . 29d. Decree of Dean Nr. V25-03-10

<b>2. Goal of the Project:</b>	To develop a collision prevention system
<b>3. Specification of Final Project:</b>	The work must meet the methodological requirements for the preparation of final projects of KTU Faculty of Electrical and Electronics Engineering.

**4. Project's Structure.** *The content is concretized together with supervisor, considering the format of the final project, which is listed in 14 and 15 points of Combined Description of Preparation, Defence and Keeping of Final Projects Methodical Requirements*

4.1 Analyse computer visio, object detection, object tracking algorithms

4.2 Create human detection and tracking algorithm

4.3 Make experimental testings of created algorithm

**5. Economical Part.** *If economical substantiation is needed; content and scope is concretized together with supervisor during preparation of final projects*

none

**6. Graphic Part.** *If necessary, the following schemes, algorithms and assembly drawings; content and scope is concretized together with supervisor during preparation of final projects*

Show experimental results and explane them

### 5. This Task is Integral Part of Final Project of Undergraduate (Bachelor) Studies

**6. The Term of Final Project Submission to Defense Work at a Public Session of Qualification Commission.** *until 2022-05-13*  
(date)

I received this task:	<u><i>Rafael Sojo García</i></u>	<u>2022-02-08</u>
	<i>(student's name, surname, signature)</i>	<i>(date)</i>
Supervisors:	<u>Assoc. Prof. Nieves Pavón Pulido</u> <u>Assoc. Prof. Dr. Virginijus Baranauskas</u>	<u>2022-02-08</u>
	<i>(position, name, surname, signature)</i>	<i>(date)</i>

Sojo García, Rafael. Human motion estimation and analysing feasible collisions between individuals in real settings by using conventional cameras and Deep Learning-based algorithms. Bachelor's Final Degree Project / supervisors: Prof. Dr. Nieves Pavón Pulido, Assoc. Prof. Dr. Virginijus Baranauskas; School of Industrial Engineering; Technical University of Cartagena; Faculty of Electrical and Electronics Engineering, Kaunas University of Technology.

Study field and area (study field group): electronics and electrical engineering, technological science, engineering.

Keywords: Artificial Intelligence, object detection, object tracking, collision prevention, YOLOv5, DeepSORT.

Kaunas, Cartagena, 2022, 93 pages.

### **Summary**

The aim of the final project is to develop a collision prevention system. This project includes: an introduction, which the reader is made aware of the problematic to be addressed; theoretical foundation, with which to provide the necessary knowledge required by the models used, with special emphasis on their mathematical foundations; the proposed method section. Experimental section develops the four main steps 1) camera calibration, 2) correction of possible distortion during image acquisition, 3) detection and tracking of the people involved in the images obtained and 4) obtention of alerts in potentially dangerous situations throughout the test. The experimental section show the results obtained in the process of detection, tracking and obtention of alerts. Conclusions and a list of the bibliographical references are given.

Sojo García, Rafael. Estimación del movimiento humano y analizador de posibles colisiones entre individuos en entornos reales usando cámaras convencionales y algoritmos de Deep Learning. Trabajo de Fin de Grado / supervisores: Prof. Dr. Nieves Pavón Pulido, Prof. Dr. Virginijus Baranauskas; Universidad Politécnica de Cartagena, Facultad de Ingeniería Industrial; Universidad Tecnológica de Kaunas, Facultad de Ingeniería Eléctrica y Electrónica.

Campo de estudio y área: ingeniería electrónica e ingeniería eléctrica, ciencia tecnológica, ingeniería.

Keywords: Inteligencia artificial, detection de objetos, seguimiento de objetos, prevención de colisiones, YOLOv5, DeepSORT

Kaunas, Cartagena 2022, 93 páginas.

### **Sumario**

El objetivo del proyecto final es desarrollar un sistema de prevención de colisiones. Este proyecto incluye: una introducción, con la que se hace partícipe al lector de la problemática que se pretende abordar; una fundamentación teórica, con la que se aportan los conocimientos necesarios que requieren los modelos utilizados, haciendo especial hincapié en sus fundamentos matemáticos; la sección del método propuesto. La sección experimental desarrolla los cuatro pasos principales 1) calibración de la cámara, 2) corrección de la posible distorsión durante la adquisición de la imagen, 3) detección y seguimiento de las personas implicadas en las imágenes obtenidas y 4) obtención de alertas en situaciones potencialmente peligrosas a lo largo de la prueba. El apartado experimental muestra los resultados obtenidos en el proceso de detección, seguimiento y obtención de alertas. Se presentan las conclusiones y una lista de referencias bibliográficas.

Sojo García, Rafael. Žmogaus judėjimo įvertinimas ir galimų susidūrimų analizė tarp asmenų realiomis sąlygomis, naudojant įprastą kamerą ir giliojo mokymosi algoritmus. Bakalauro baigiamasis projektas / vadovai / doc. dr. Virginijus Baranauskas, doc. dr. Nieves Pavón Pulido; Kauno technologijos universitetas, Elektros ir elektronikos fakultetas, Universidad Politécnica de Cartagena, Pramonės inžinerijos fakultetas.

Studijų kryptis ir sritis (studijų kryptių grupė): elektronikos ir elektros inžinerija, technologijos mokslai, inžinerija.

Reikšminiai žodžiai: dirbtinis intelektas, objektų aptikimas, objektų sekimas, susidūrimų vengimas, YOLOv5, DeepSORT.

Kaunas, Cartagena 202. p. 93

### **Santrauka**

Baigiamojo projekto tikslas – sukurti susidūrimų prevencijos sistemą. Darbą sudaro: įvadas, kuriame skaitytojas supažindinamas su problema, kurią reikia spręsti; teorinis pagrindimas, kuris suteikia reikiamų žinių, reikalingų naudojamiems modeliams, ypač pabrėžiant jų matematinius pagrindus; autoriaus siūlomas metodas. Praktinėje dalyje išplėtoti keturi pagrindiniai žingsniai: 1) kameros kalibravimas, 2) galimų iškraipymų koregavimas vaizdo gavimo metu, 3) žmonių, dalyvaujančių gautuose vaizduose, aptikimas ir sekimas ir 4) įspėjimų gavimas, testuojant potencialiai pavojingas situacijas. Eksperimentinėje dalyje rodomi perspėjimų aptikimo, sekimo ir gavimo rezultatai. Pateikiamos išvados ir naudotų literatūros šaltinių sąrašas.

## Table of contents

List of figures .....	10
List of tables .....	12
List of abbreviations and terms .....	13
1. Introduction .....	14
1.1. Objectives .....	14
2. State of Art .....	15
2.1. Accidents involving Forklifts.....	15
2.2. Strategies for addressing the problem .....	17
2.2.1. Autonomous Mobile Robots.....	17
2.2.2. Computer Vision approaches .....	18
2.3. Theoretical concepts .....	19
2.3.1. How does CV work? .....	20
2.3.2. Digital images.....	20
2.3.3. The Convolution.....	21
2.3.4. Pooling.....	22
2.3.5. Linear Regression.....	23
2.3.6. Logistic Regressions.....	24
2.3.7. Cost functions.....	25
2.3.8. Artificial Neural Networks .....	26
2.3.9. Optimization functions.....	28
2.3.10. Activation Functions.....	29
2.3.11. CNNs .....	31
2.4. Object Detection .....	32
2.4.1. Sliding Windows .....	32
2.4.2. DPM .....	33
2.4.3. Region Proposals Network .....	33
2.4.4. YOLO .....	34
2.4.5. YOLOv1 .....	34
2.4.6. YOLOv2 .....	36
2.4.7. YOLOv3.....	38
2.4.8. YOLOv4.....	39
2.5. Object Tracking .....	41
2.5.1. DeepSORT .....	42
2.5.2. Estimation model. Kalman Filter.....	42
2.5.3. Data Association. Hungarian Algorithm.....	43
2.5.4. Track Identities.....	43
2.5.5. Deep Association metric for SORT.....	44
2.5.6. Feature Descriptor.....	45
3. Project Development and Results.....	47
3.1. Asus Xtion Pro Live .....	47
3.2. Programming Language. Python .....	47
3.3. Programming environments .....	47
3.3.1. Visual Studio Code.....	47



3.4. Proposed Solution.....	48
3.4.1. Camera Calibration.....	48
3.4.2. Chessboard Method .....	49
3.4.3. Correcting distortion in images. ....	54
3.4.4. Ground projection.....	56
3.4.5. Homography matrix functions.....	57
3.4.6. Homography error calculations. ....	58
3.4.7. Object Detection and Tracking.....	62
3.4.8. Google Colaboratory implementation .....	66
3.4.9. Tracking preparation .....	68
3.4.10. Local plane coordinates calculation. ....	69
3.4.11. Safety areas calculation .....	70
3.4.12. System of Alerts. ....	72
3.5. Experimental Investigation.....	74
Conclusions .....	90
List of references .....	91
Appendices .....	94
Appendix 1. Tracking file – Test 1.....	94
Appendix 2. Tracking file – Test 2.....	102
Appendix 3. Tracking file – Test 3.....	113
Appendix 4. Tracking file – Test 4.....	136

## List of figures

<b>Fig. 1.</b> Nonfatal injuries involving forklifts, 2011-2017. [2] .....	16
<b>Fig. 2.</b> Fatal injuries involving forklifts, 2011-2017. [2] .....	16
<b>Fig. 3.</b> Accident causes involving forklifts, 2017. [2] .....	17
<b>Fig. 4.</b> VIA Mobile360 Warning and Critical Zones. ....	18
<b>Fig. 5.</b> Warny camera detections. ....	19
<b>Fig. 6.</b> Gray scale digital image.....	20
<b>Fig. 7.</b> RGB image.....	21
<b>Fig. 8.</b> Convolution [9].....	21
<b>Fig. 9.</b> Convolution with zero padding.....	22
<b>Fig. 10.</b> Max and Average Pooling examples. ....	23
<b>Fig. 11.</b> Simple linear regression [11]. ....	24
<b>Fig. 12.</b> Linear regression for a binary classification problem.....	24
<b>Fig. 13.</b> Sigmoid function applied to the linear regression with a threshold of 0.5. ....	25
<b>Fig. 14.</b> Structure of a Neuron.....	26
<b>Fig. 15.</b> Structure of a Deep Neural Network.....	27
<b>Fig. 16.</b> Gradient Descent 3D representation. ....	29
<b>Fig. 17.</b> ReLU and Leaky ReLU activation functions.....	30
<b>Fig. 18.</b> Tanh activation function. ....	31
<b>Fig. 19.</b> Typical structure of a CNN.....	32
<b>Fig. 20.</b> Sliding Window visual example. ....	32
<b>Fig. 21.</b> DPM score process.....	33
<b>Fig. 22.</b> Two examples of selective search at different scales. Note that (b) has detected the girl on the TV. [20] .....	34
<b>Fig. 23.</b> Darknet [21]. ....	35
<b>Fig. 24.</b> Bounding boxes with dimension priors and location prediction [22].....	36
<b>Fig. 25.</b> Darknet 19 [22] .....	37
<b>Fig. 26.</b> Accuracy and speed on VOC 2007 [22] .....	38
<b>Fig. 27.</b> Darknet 53 [24] .....	38
<b>Fig. 28.</b> Object detector [25] .....	39
<b>Fig. 29.</b> CSPDenseNet example. ....	40
<b>Fig. 30.</b> Comparison of the speed and accuracy of different object detectors [25] .....	41
<b>Fig. 31.</b> SORT performance in relation to several baseline trackers. [29] .....	44
<b>Fig. 32.</b> CNN architecture for the feature descriptor [30] .....	45
<b>Fig. 33.</b> DeepSORT tracking results [30].....	46
<b>Fig. 34.</b> Type of distortions [33] .....	48
<b>Fig. 35.</b> Pinhole camera model.....	49
<b>Fig. 36.</b> Two examples of the calibration images with the chessboard at different positions.....	50
<b>Fig. 37.</b> Corners found within the calibration images. ....	52
<b>Fig. 38.</b> Original image. ....	55
<b>Fig. 39.</b> Undistort image.....	56
<b>Fig. 40.</b> Original image ground corners. ....	60
<b>Fig. 41.</b> Upper view of the ground after using the warpPerspective function in the original image	60
<b>Fig. 42.</b> Undistort image ground corners.....	61

<b>Fig. 43.</b> Upper view of the ground after using the warpPerspective function in the undistort image	61
<b>Fig. 44.</b> YOLOv5 variants .....	64
<b>Fig. 45.</b> Frames from test 1, on the left, and test 2, on the right. ....	75
<b>Fig. 46.</b> Frames from test 3, on the left, and test 4, on the right. ....	75
<b>Fig. 47.</b> Detection examples from test 1, on the left, and test 2, on the right.....	76
<b>Fig. 48.</b> Detection examples from test 3, on the left, and test 4, on the right.....	76
<b>Fig. 49.</b> Test 1 localization. ....	80
<b>Fig. 50.</b> Test 2 localization. ....	81
<b>Fig. 51.</b> Test 3 localization. ....	81
<b>Fig. 52.</b> Test 4 localization. ....	82
<b>Fig. 53.</b> Pie chart of warnings. ....	88

## List of tables

<b>Table 1.</b> Fatal accident causes involving forklifts. [1].....	15
<b>Table 2.</b> Detection frameworks on PASCAL VOC 2007 [22] .....	35
<b>Table 3.</b> Average IOU of boxes to closest priors on VOC 2007 [22].....	36
<b>Table 4.</b> Speed/mAP-50 between YOLOv3 and other methods [24] .....	39
<b>Table 5.</b> Loop to get the calibration images.....	50
<b>Table 6.</b> Chessboard preparation. ....	51
<b>Table 7.</b> Camera calibration.....	51
<b>Table 8.</b> Optimal parameters.....	53
<b>Table 9.</b> Camera calibration error. ....	54
<b>Table 10.</b> Image undistortion. ....	54
<b>Table 11.</b> Homography calculation functions.....	57
<b>Table 12.</b> Homography error measurement. ....	58
<b>Table 13.</b> Ground grid function .....	59
<b>Table 14.</b> Original image error.....	62
<b>Table 15.</b> Undistort image error.....	62
<b>Table 16.</b> Mean absolute error of the ground projection .....	62
<b>Table 17.</b> YOLOv5m model summary .....	63
<b>Table 18.</b> OSNet_x0_25 model summary.....	64
<b>Table 19.</b> Cloning repository. ....	66
<b>Table 20.</b> Standing point calculation. ....	66
<b>Table 21.</b> Running command.....	67
<b>Table 22.</b> DeepSORT configuration file.....	67
<b>Table 23.</b> Detection array preparation 1. ....	68
<b>Table 24.</b> Detection array preparation 2. ....	68
<b>Table 25.</b> Real coordinates calculation in the main code.....	69
<b>Table 26.</b> Real coordinates function definition.....	70
<b>Table 27.</b> Safety area calculation in the main code .....	70
<b>Table 28.</b> Safety areas function definition. ....	70
<b>Table 29.</b> Alerting system in the main code. ....	72
<b>Table 30.</b> Alerting system function definition. ....	72
<b>Table 31.</b> Test 1. Detections from the 20 firsts frames.....	77
<b>Table 32.</b> Test 2. Detections from the 20 first frames .....	77
<b>Table 33.</b> Test 3. Detections from the 20 first frames. ....	78
<b>Table 34.</b> Test 4. Detections from the 20 first frames. ....	79
<b>Table 35.</b> Warnings from test 3 .....	82
<b>Table 36.</b> Warnings from test 4 .....	85

## List of abbreviations and terms

### Terms:

**AGV** – Autonomous Guided Vehicles

**AMR** – Autonomous Mobile Robot

**ANN** – Artificial Neural Network

**CmBN** – Cross mini-Batch Normalization

**CNN** – Convolutional Neural Network

**CSPNet** – Cross Stage Partial Network

**DPM** – Deformable Parts Model

**FPN** – Feature Pyramid Network

**FPS** – Frames Per Second

**HSV** – Hue Saturation Value

**IOU** – Intersection Over Union

**mAP** – Mean Average Precision

**PANet** – Path Aggregation Network

**R-CNN** – Region-based Convolutional Neural Network

**ReLU** – Rectified Lineal Unit

**RGB** – Read Green Blue

**ResNet** – Residual Network

**SKU** – Stock-Keeping Unit

**SORT** – Simple Online Real-time Tracking

**SSE** – Sum-Squared Error

**SSP** – Spatial Pyramid Pooling

**VOC** – Visual Object Classes

**YOLO** – You Only Look Once

## **1. Introduction**

Nowadays, Computer Vision (CV), has become a very powerful tool since technological improvements done in recent years are bringing a strong rise in the use and popularity of Artificial Intelligence (AI) systems. Moreover, CV systems have a lot of different possible applications in many fields typically led to the human responsibility, like Health Care or Security Industries. Thus, allowing us to focus our attention in the task of increasing productivity, whereas these systems take care of those aspects in which we are either more likely to commit errors, or just more expensive than the robotization of the job in the long term.

On the other hand, in industrial environments where vehicles are constantly sharing space with pedestrians, any distraction or visibility reduction can end into a forklift-related accident. This is either an economic and a work safety problematic due to the risk for the worker and the subsequent hospitalization costs, which in many cases might end into serious injuries.

Therefore, the aim of this project is to address this problematic through a CV-based human trajectory estimation for collision preventions. This solution takes advantage of some CV and models based on Deep Learning (DL), focused on performing real-time object detections, as well as a mathematical and statistical object tracking implementation with a deep association metric.

This project is entirely focused on human-to-human interactions, but the results are completely extrapolable for human-to-vehicle and vehicle-to vehicle-situations.

### **1.1. Objectives**

This project aims to develop a collision prevention system, whose function is to contribute to the work safety in the manufacturing industry. For that reason, this system should be able to return warnings depending on the location of several individuals within a predefined area.

To accomplish this goal, the following partial objectives are set:

- Camera calibration: for the camera parameters extraction.
- Image undistortion: for the correct data acquisition.
- Object detection and tracking: based on YOLOv5 and DeepSORT.
- Security area definition: setting the angle, radius and orientation of a circular sector in front of each human at each frame.
- Warning system definition: the alerts are given depending on the trajectories and locations of the individuals.

## 2. State of Art

### 2.1. Accidents involving Forklifts.

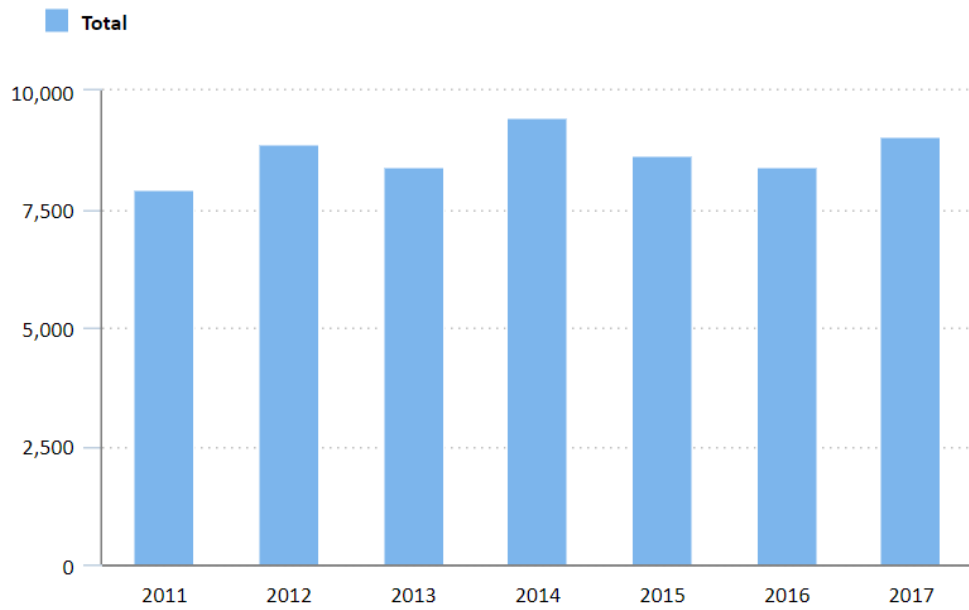
Industrial environments are characterized by the fact that work safety has an important role in every task, since the machinery is capable of causing enormous amounts of energy. However, the workers and vehicles moving around are something that may go unnoticed, but according to the Occupational Safety and Health Administration (OSHA) in 1995, up to 34.900 serious injuries, 61.800 non-serious injuries and around 85 fatalities, were caused by forklifts trucks in the United States since 1981 on annual average. At least a 10% of the fatal accidents as a result of people being struck by a forklift, see Table 1.

Type accident	Percent
Crushed by tipping vehicle	42
Crushed between vehicle and a surface	25
Crushed between two vehicles	11
Struck or run over by vehicle	10
Struck by falling material	8
Fall from platform on forks	4
Accidental activation of controls	2

**Table 1.** Fatal accident causes involving forklifts. [1]

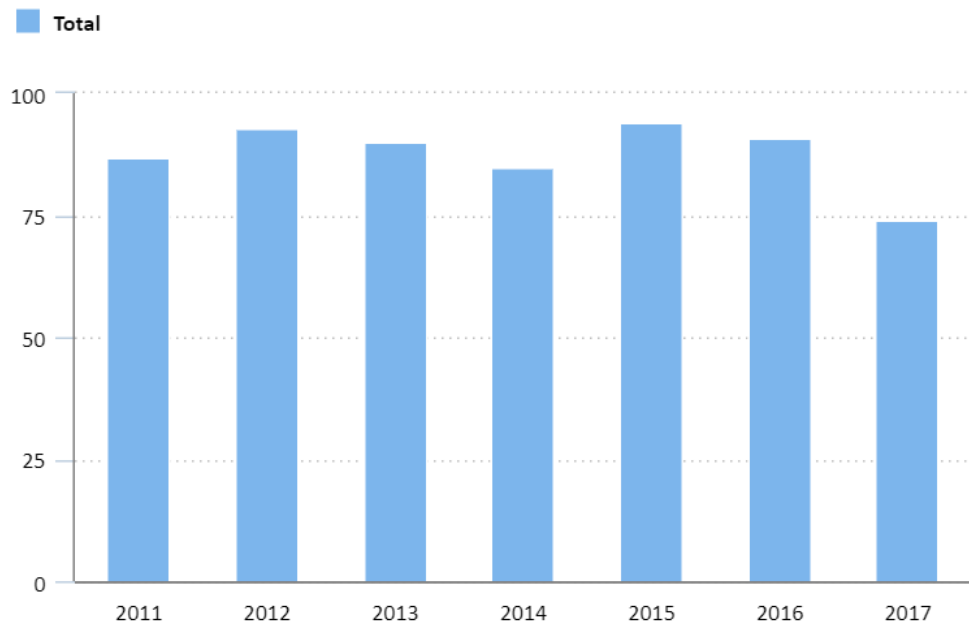
More recently, the Bureau of Labor Statistics, U.S. Department of Labor, shared in 2019 that more than 8.500 nonfatal injuries involving forklifts still occurring on average every year, resulting in several days out of work. Furthermore, with barely no change in the number of fatal injuries and nearly the 20% of them as a direct cause of forklift struck, see Fig 1 and Fig 2.

### Nonfatal occupational injuries and illnesses involving forklifts, 2011-17



**Fig. 1.** Nonfatal injuries involving forklifts, 2011-2017. [2]

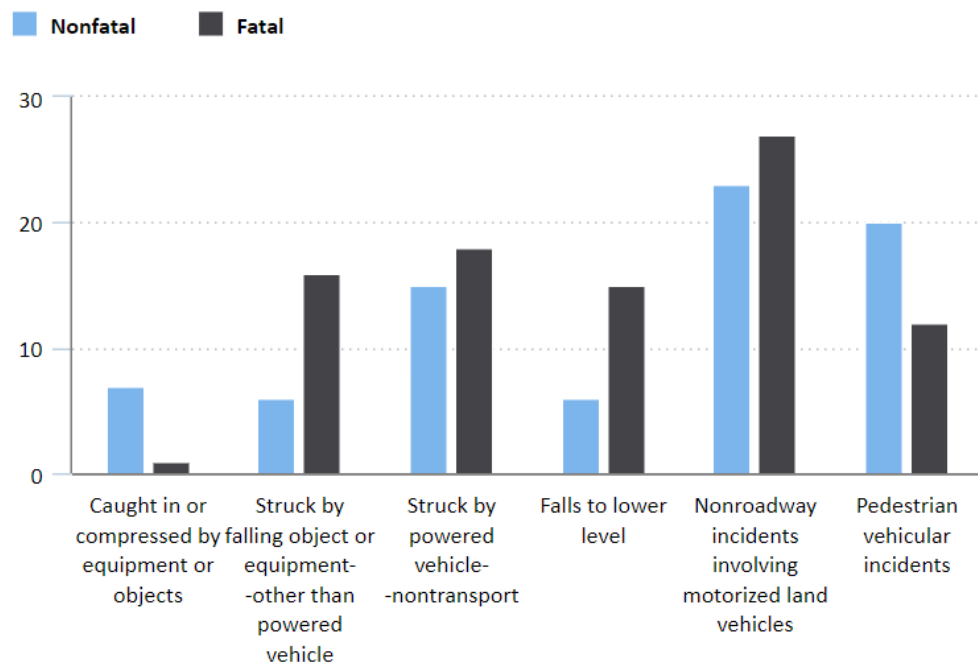
### Fatal occupational injuries involving forklifts, 2011-17



**Fig. 2.** Fatal injuries involving forklifts, 2011-2017. [2]



**Percentage of fatal injuries and nonfatal injuries and illnesses involving forklifts by selected events, 2017**



**Fig. 3.** Accident causes involving forklifts, 2017. [2]

## 2.2. Strategies for addressing the problem

Forklifts struck are one of the principal cause of accidents in the manufacturing industry as it was shown above. However, there are different ways of addressing the problem for reducing the number of injuries. Some of the most promising strategies are the use of autonomous robots and the application of CV approaches.

### 2.2.1. Autonomous Mobile Robots

According to Intel’s description, “an autonomous mobile robot is a type of robot that can understand and move through its environment independently” [3]. These robots, use artificial intelligence systems to calculate the best route based on the environmental inputs received from their sensors and cameras. This behavior increases the fluency of travelling, since they are able to avoid obstacles and find faster routes depending on the situation without the need of an operator, as with the classical AGVs, which independency was subject to the conditions of the tracks and the correct oversight.

Furthermore, an AMR can be used for different tasks than simply moving inventory, like assisting in the picking process or performing sortation, thus, increasing productivity and order accuracy. Due to the fact that an AMR model can be equipped with different handling technologies, the sortation usability is managed by a barcode reader on the robot, and a rapid displacement to the storage location, where the item is tilted.

For the assistance in the picking process, there are two ways of using the AMRs:

- Conventional picking.

- Goods-to-Person Picking.

In the picking process, an operator must move from location to location, losing a big amount of time. When using an AMR, it is possible to equip the robot with an order basket, so that the robot can perform these movements while the operator of every location takes the inventory. The Goods-to-Person Picking, on the contrary, consist on the movement of the entire shelve to the pick station. Then, the robot indicates the correct picks and quantities.

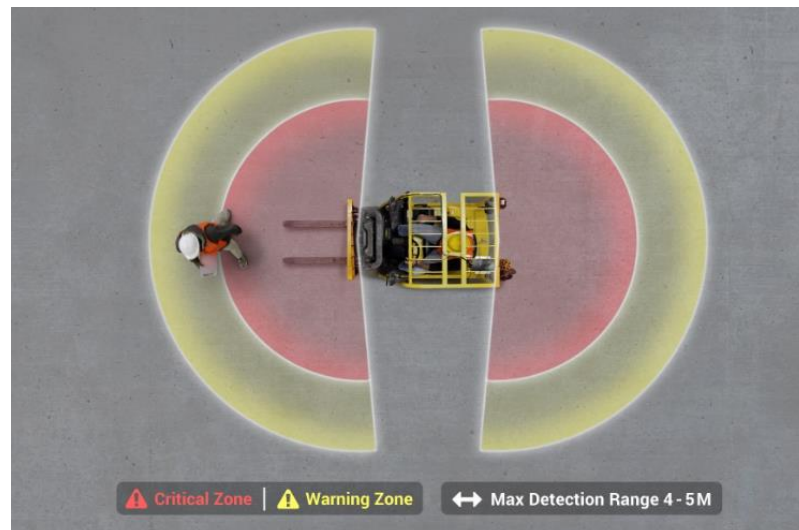
In any case, a fleet of AMRs can significantly reduce the number of forklift-related accidents within a warehouse if the number of SKUs is big enough [4].

## 2.2.2. Computer Vision approaches

### 2.2.2.1. VIA Mobile360

The company VIA Technologies, Inc., announced in October of 2021 the VIA Mobile360 Forklift Safety System [5]. The system uses voice and sounds alerts to warn the forklift driver of possible collisions through three IP67 HD cameras, two of them wide-angle cameras situated in front and rear of the forklift, and one inside the cabin.

According to the company, the area coerture has a radius of 4-5 meters far, which can be configured with either two or one warning zones. The alert is given if either a pedestrian is to close of the forklift safety zone (see Fig. 4), or the cabin camera detects signs of fatigue, smartphone usage or smoking.



**Fig. 4.** VIA Mobile360 Warning and Critical Zones.

### 2.2.2.2. Warny

Warny [6] is a product developed by the Australian computer vision company Bigmate, focused on reducing the number of heavy vehicles-related accidents, as well as unexpected situations. They provide a full ecosystem to enhance work safety through three applications:

- Vehicle collision avoidance
- Safety zone alerting
- Thermal analysis of people and industrial systems

Warny (see Fig. 5), is capable of detecting combustions, fires, equipment overheating, and especially, a real time movement analysis, for example, alerting operators out of the sight of an upcoming driver. The system takes images from multiple standard CCTV cameras, which are used to calculate the ground-truth position of the object detected. Once the real positions are obtained, their velocities and relative distances are calculated in real time, thus, performing an analysis of the situation and giving the corresponding alert to the worker's device.

According to the article published in VentureBeat website, "Early into installation, one factory in Singapore saw a 22% drop in incidents (...) Across the board, on average, Bigmate is seeing a 80% drop in incidents in their clients' work environment" [7]. They ensure a network with nearly 100% accuracy and milliseconds of latency for the alerts. All the data is also collected to allow workplace analysis.

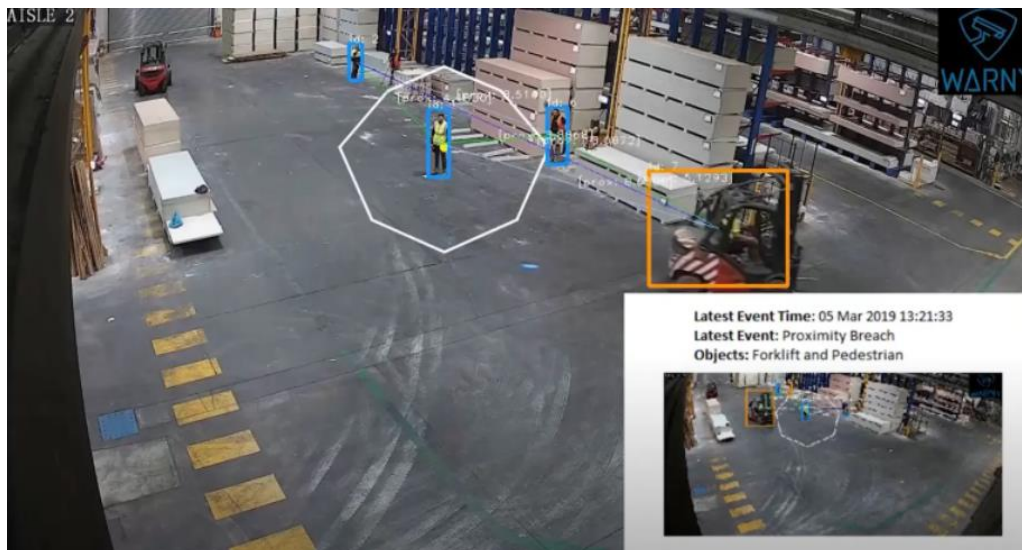


Fig. 5. Warny camera detections.

### 2.3. Theoretical concepts

In previous sections, two CV-based approaches to ensure work safety were presented. IBM gives the following description to this term. "Computer vision is a field of artificial intelligence (AI) that enables computers and systems to derive meaningful information from digital images, videos and

other visual inputs — and take actions or make recommendations based on that information. If AI enables computers to think, computer vision enables them to see, observe and understand” [8]. Therefore, CV is the branch of artificial intelligence that teaches computer systems how to extract and understand visual information from the environment.

### 2.3.1. How does CV work?

In order to extract this information, CV-based systems take advantage of a DL concept called CNN, which is used to get features from the image in a set of convolutional layers, whose level of complexity increases with the depth of the architecture. These layers are used to create a feature map with the most meaningful information of the image. Then, the model takes this feature map to understand the context of the image through a classification model.

### 2.3.2. Digital images

First, it is important to know what a digital image is. A digital image is a matrix of elements from 0 to 255, in which the 0 represents the minimum level of luminosity and 255 de maximum. For example, in gray scale images, the 0 is a black pixel, whereas 255 is a white pixel, see Fig. 6.

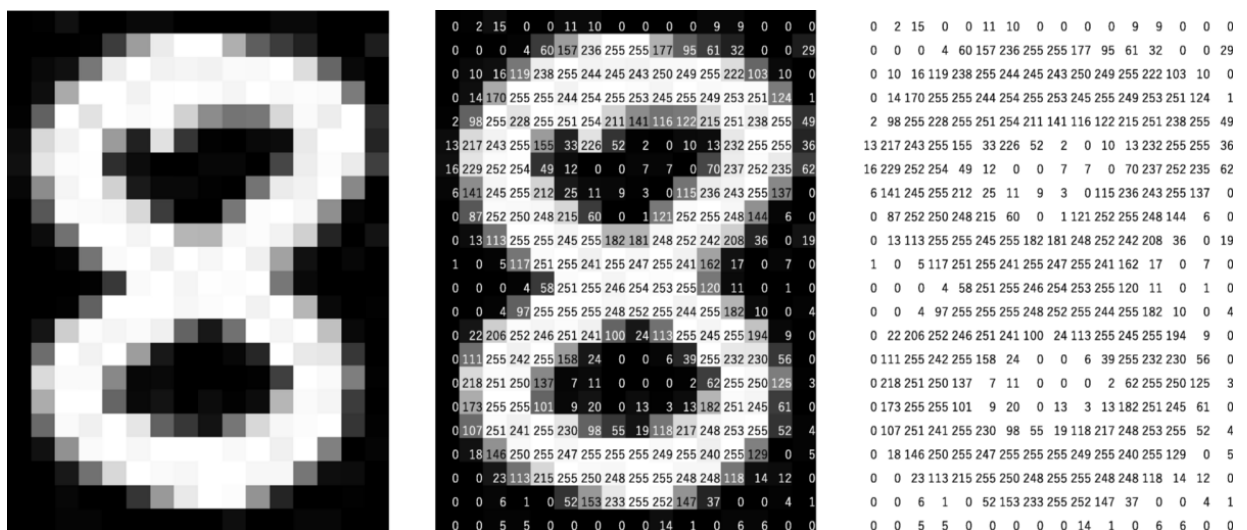


Fig. 6. Gray scale digital image.

However, digital images are usually composed by different color channels, where the scale does not necessarily mean the brightness, but some source of information. The most common color space for visualization is RGB (see Fig. 7), where each channel corresponds to the brightness of each color (red, green, and blue). Other color spaces like HSV, LAB or LUV are not suitable for visualization, but they contain useful information to increase the robustness against light changes in CV-based applications, like hue or saturation channels in HSV space.

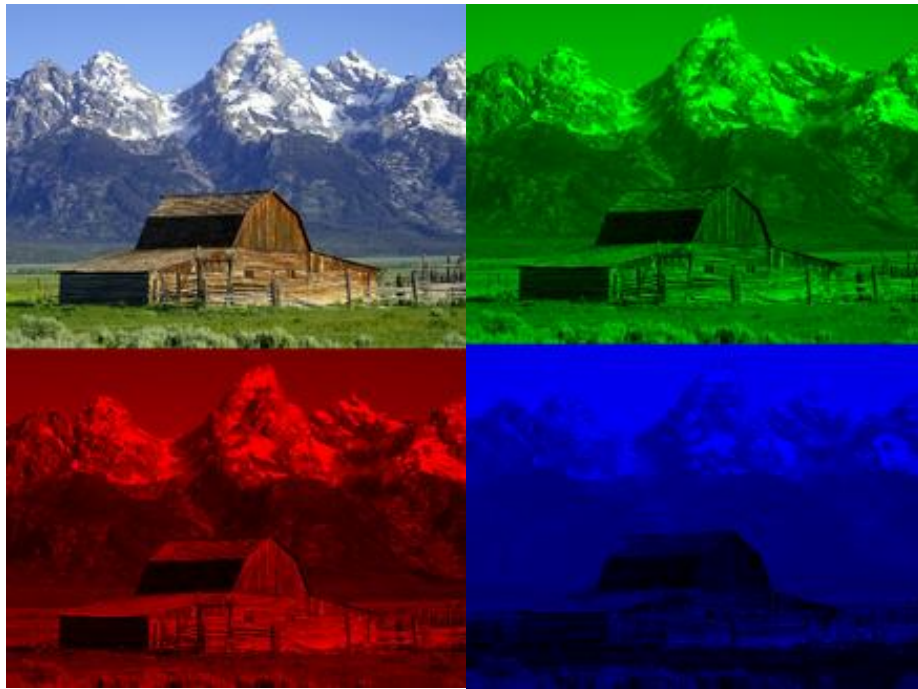


Fig. 7. RGB image.

### 2.3.3. The Convolution

A convolution is a sum of element-wise products between two matrixes. In computer vision, these two matrixes are the raw image and the kernel (see Fig. 8), where the kernel is an odd smaller matrix, whose elements are used to highlight some features of the raw image. The kernel is also named as filter.

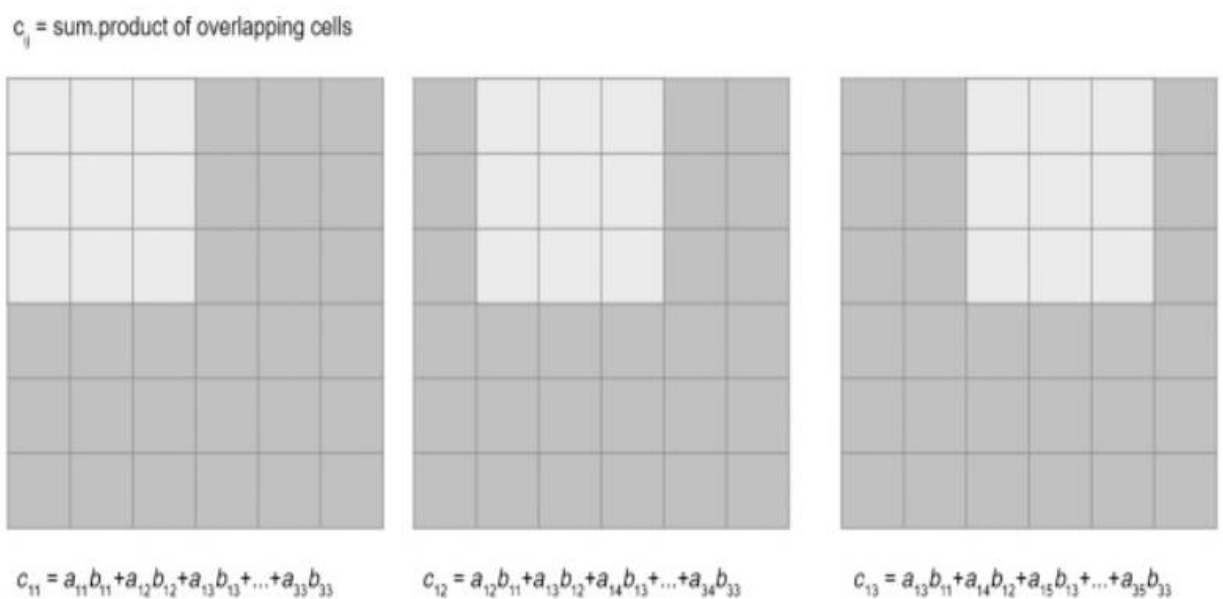
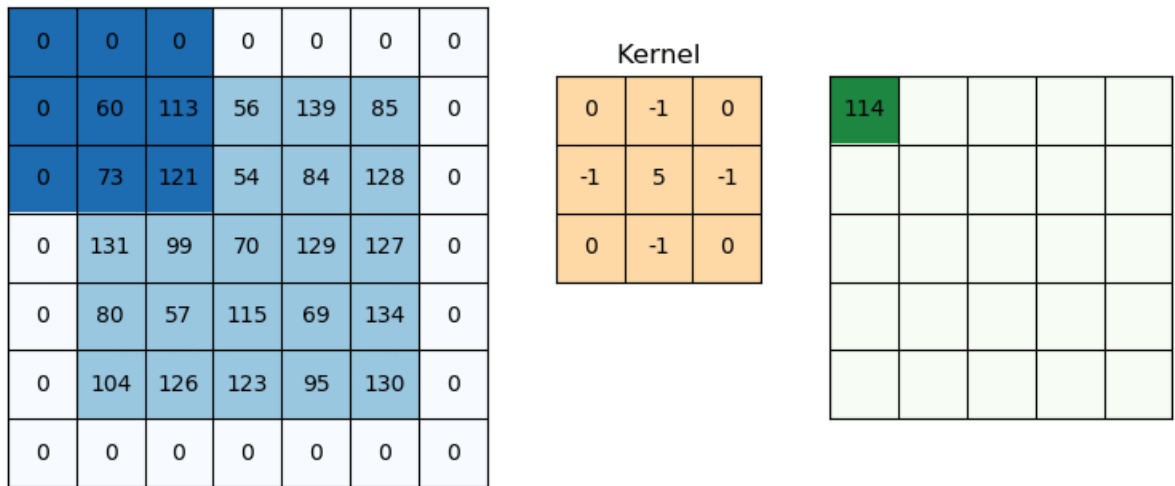


Fig. 8. Convolution [9]

Then, the kernel convolves through the different cells replacing the number that falls in the center of the overlapped elements. However, this will result in a reduction of the input size. To avoid so, a padding process is applied to the image during the convolution. This padding process consist of adding pixels to the border of an image, for example, a 3x3 kernel operation might want to use 1-unit padding, which will add one extra pixel to each one of the edges. There are different types of paddings, but the most common is the zero padding, which fills these extra cells with zeros, see Fig. 9.



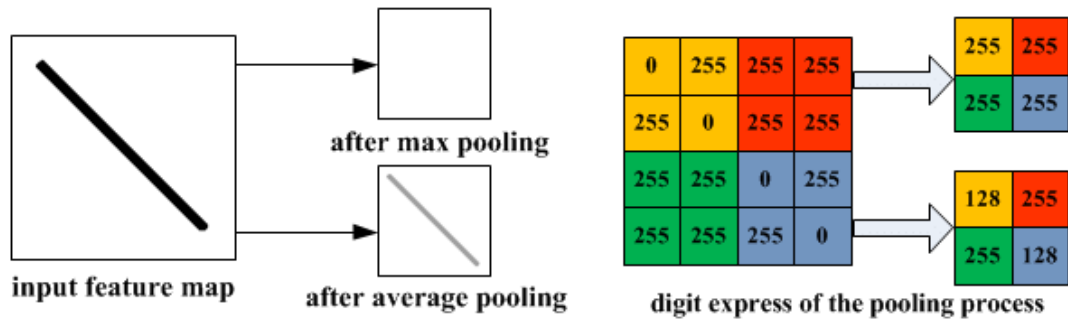
**Fig. 9.** Convolution with zero padding.

Another important parameter in relation to the output size is the stride, which is defined as the number of cells that the kernel moves after each iteration.

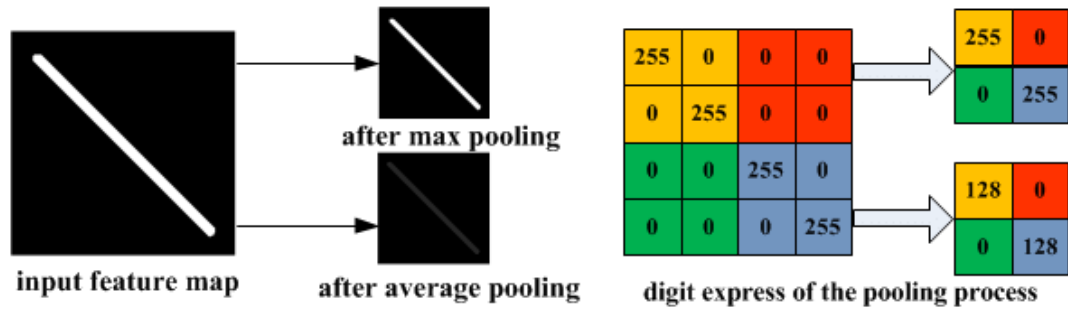
### 2.3.4. Pooling

Sometimes, in CV-based systems it may be desirable to get rid of non-significant information, resulting in a smaller summarized picture. This is done with the pooling operation, which fuses meaningful information across the image using a filter. Depending on how this operation is performed, one result or another will be obtained, two main types are Max Pooling and Average Pooling.

The max pooling takes the maximum value of the area covered by the filter, thus, extracting the most significant features of each region, while the average pooling takes the mean [10]. In Fig. 10, there is an example of both.



(a) Illustration of max pooling drawback



(b) Illustration of average pooling drawback

Fig. 10. Max and Average Pooling examples.

### 2.3.5. Linear Regression

The concepts shown above are important to understand how the features of an image can be extracted. Nevertheless, the following sections are more related to learning process in AI systems.

Linear regressions are one of the most important and basic concepts in supervised Machine Learning (ML). Basically, a linear regression is a statistic model that tries to find the line that best fits a set of supposedly related values, where the y-axis corresponds to the dependent variable, and the x-axis the independent variable. In supervised machine learning problems, the aim is to predict this y value, given a single x input, or set of inputs. Therefore, there are simple, equation 1, and multiple linear regressions, equation 2.

$$y = b_0 + w_1x \quad (1)$$

$$y = b_0 + w_1x_1 + w_2x_2 + \dots + w_nx_n \quad (2)$$

The line that best fits the model (see Fig. 11) is obtained through the slope and the intercept, which are usually referred as weight (w) and bias (b). These two parameters are calculated for a given training set as the optimal values for which the error is minimum, where the error is the distance between the predicted and the actual value. Then, the accuracy of the model is validated in a test set.

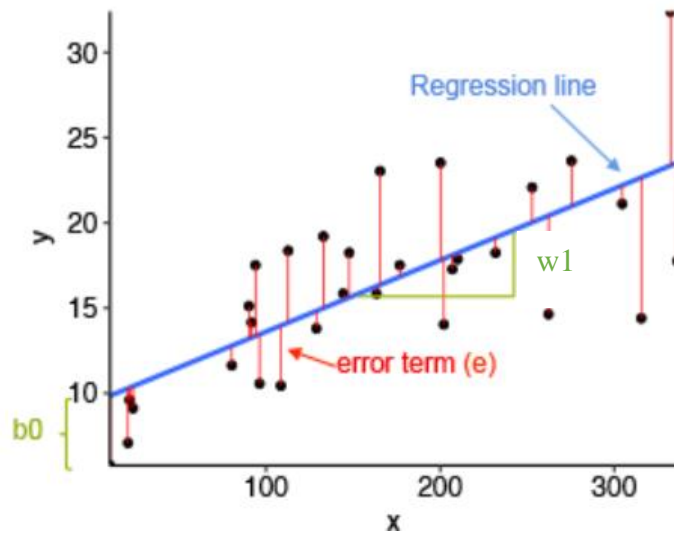


Fig. 11. Simple linear regression [11].

### 2.3.6. Logistic Regressions

However, in some problems it would be necessary to predict the probability of belonging to a certain class, since the dependent variable can be categorical, for example, in binary classifications. Here, a linear regression approach might cause some problems by the fact, that a linear model allows the result to be out of the boundaries of the problem, i.e. probabilities higher than one and lower than zero, see Fig. 12. It can also bring problems with the outliers, since the line that best fits the model can be shifted to decrease the distance error between the farthest outliers and the rest of the data, causing miss-classifications.

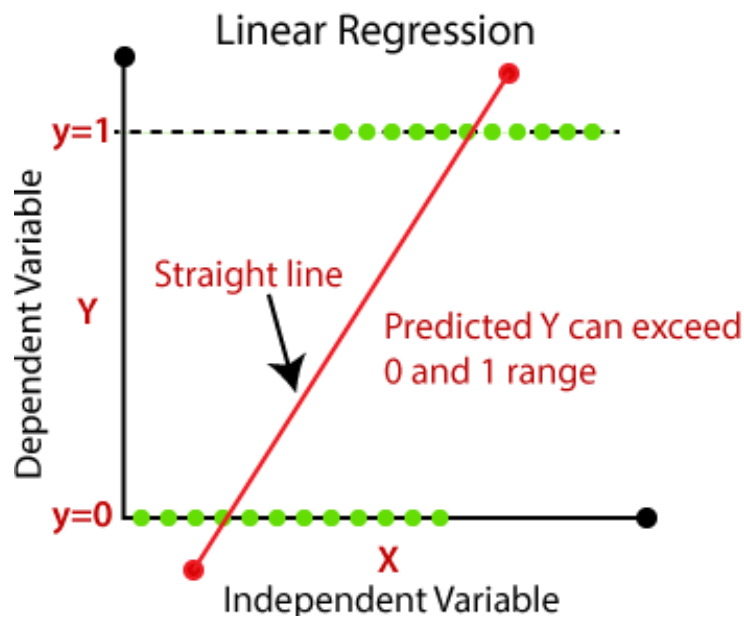


Fig. 12. Linear regression for a binary classification problem.



Therefore, a logistic regression approach is more suitable for this type of problems, where rather than a straight line it is used an S-curve, so the predictions can fall within the boundaries of the problem, and the farthest outliers do not affect much to the model [12]. To do so, a logistic function must be applied to the linear calculations.

$$\sigma(z) = \frac{1}{1+e^{-z}} \quad (3)$$

For example, equation 3, corresponds to the sigmoid function, it makes the output of the linear prediction to fall between 0 and 1, thus, resulting in a much more accurate model. A threshold value it is also set to classify the predictions, see Fig. 13.

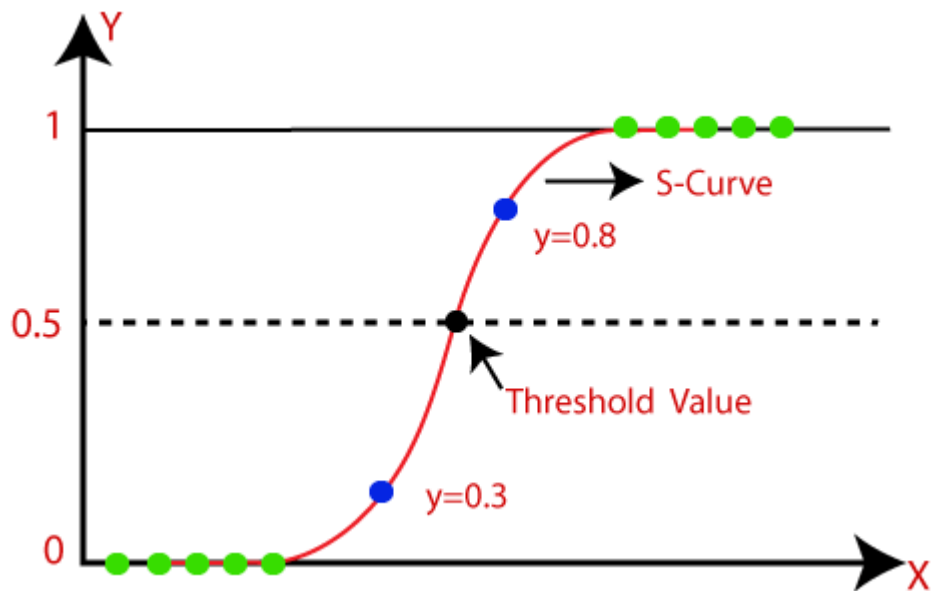


Fig. 13. Sigmoid function applied to the linear regression with a threshold of 0.5.

### 2.3.7. Cost functions.

To train a model in supervised learning algorithms, the output has to be evaluated iteratively until it reaches a good accuracy. This is done with a cost function, either called loss. The cost function compares the output of the model with the real output of the dataset in order to get the error of the prediction. To do so, there are many approaches depending on the type of problem, but for regression problems, the loss is a distance-based error calculation.

Based on this distance, there are two famous approaches, the MSE (equation 4), or L2 loss, and, MAE (equation 5), or L1 loss [13].

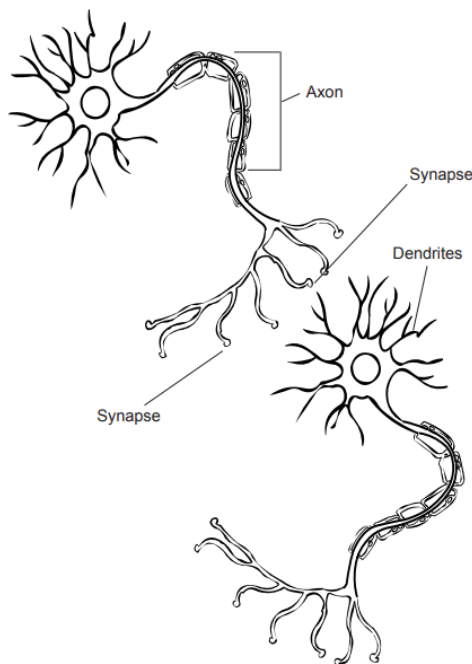
$$MSE = \frac{1}{N} \cdot \sum_{i=0}^n (y - y')^2 \quad (4)$$

$$MAE = \frac{1}{N} \cdot \sum_{i=0}^n |y - y'| \quad (5)$$

The fact that the L2 loss is squared, means that it penalizes higher the outliers of the dataset. However, the L1 loss is more robust in this aspect and also performs well with noisy data.

### 2.3.8. Artificial Neural Networks

An Artificial Neural Network is a deep learning model architecture directly inspired from the human central nervous system. The information in the human body flows in form of electrical impulses through billions of interconnected cells called neurons, see Fig. 14.

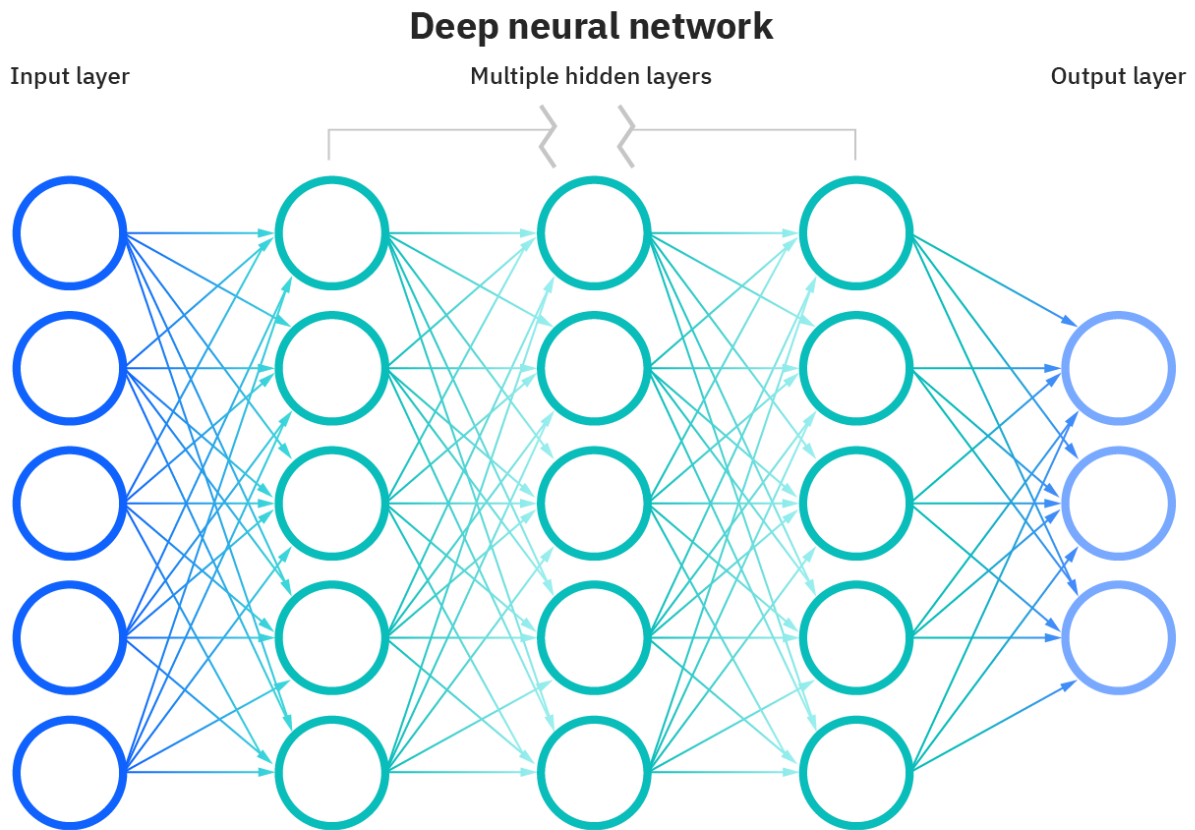


**Fig. 14.** Structure of a Neuron

Every single neuron has a cell body from which a set of small branches called dendrites grow, as well as a long fiber known as the axon. The information flows from the whiskers of the axon, i.e. the synapses, to the dendrites of another neuron. Then, the information from many neurons is processed in its body cell and joined together to be sent to a new neuron. Thus, constantly activating

certain neuron connections over the others, the brain learns which neurons will be more likely to use to get the expected output.

An artificial neural network works pretty much the same way, where there is a neuron that receives inputs from many different others, and send a response according to them. Its architecture is composed by an input layer, a set of hidden layers and the outputs, see Fig. 15.



**Fig. 15.** Structure of a Deep Neural Network

The hidden layers can be understood as the central nervous system, where the inputs of the neuron are the dendrites and the outputs the synapses. Every neuron of an artificial neural network performs a linear regression followed by an activation function, which can be either linear, hyperbolic or logistic as seen above. On the contrary, rather than electrical impulses, the information flows in form of weighted values, which are adjusted depending on the neuron. The output of a neuron is defined in equation 6.

$$o = f(z) = f\left(\sum_i w_i x_i + b\right) \quad (6)$$

Each neuron might find different associations for the input data that can end into the expected value or not. For this reason, after reaching the output layer and calculate the loss, the error of the neurons

is back-propagated to search the path that has had the biggest implication in the result to reinforce it. This process is known as backpropagation.

The weights and bias of the neurons are randomly initialized and automatically adjusted through this backpropagation algorithm. Once the network has arrived with a result, is more efficient to search the error implications of each neuron backwards than calculating forward every change in the net. Therefore, if every neuron in the final layer has an implication in the error, it will be more likely to have a neuron that has contributed more in the result than de others. This process can be repeated for each layer discarding the neurons with less contribution in the result, thus, back propagating the error until the first layer. This way can be obtained the parameters for the calculations of the gradient descent in the training process [15], see equation 7.

$$\frac{\partial C}{\partial b^L}, \frac{\partial C}{\partial w^L} \rightarrow l = 0,1,2, \dots, L; \quad (7)$$

Here,  $\frac{\partial C}{\partial b^L}$  and  $\frac{\partial C}{\partial w^L}$  are the partial derivatives of the cost with respect the bias and weight respectively.

### 2.3.9. Optimization functions.

After the cost calculations, the parameters of the function must be optimized to find the minimum possible error. In convex functions, it can be obtained matching the cost derivative to zero, but for non-convex functions, this approach faces the problem of finding several points where the slope can be zero, like peaks or saddle points. Hence, the Stochastic Gradient Descent or ADAM approaches are better methods for the optimization task, especially in ANNs.

The Stochastic Gradient Descent consists on a partial derivative calculation of the parameters of the function. This gradient can be subtracted on a certain percent, the learning rate, to find a minimum in the function [14].

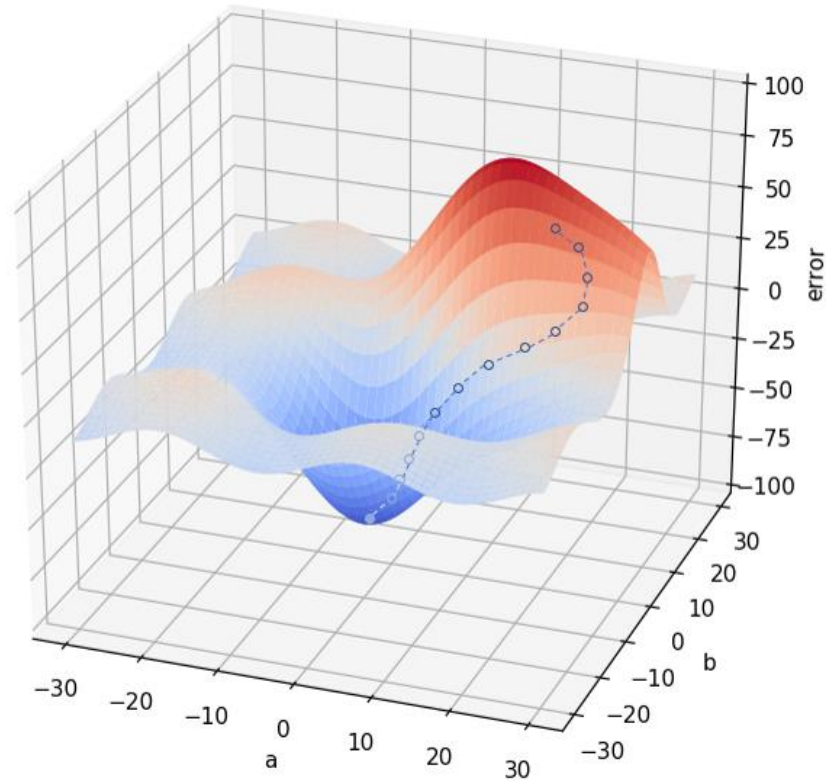
$$\theta_{n+1} = \theta - \eta \nabla f \quad \forall 0 < \eta < 1 \quad (8)$$

Where

$$\nabla f = \begin{bmatrix} \frac{\partial C}{\partial \theta_1} \\ \frac{\partial C}{\partial \theta_2} \\ \dots \\ \frac{\partial C}{\partial \theta_n} \end{bmatrix} \quad (9)$$

Here,  $\eta$  is the learning rate.

For small learning rates, the algorithm might never converge, while for larger ones the jump after each iteration can be such, that it turns impossible to find the minimum. The following picture, Fig 16, shows a 3-Dimensional representation of this process.



**Fig. 16.** Gradient Descent 3D representation.

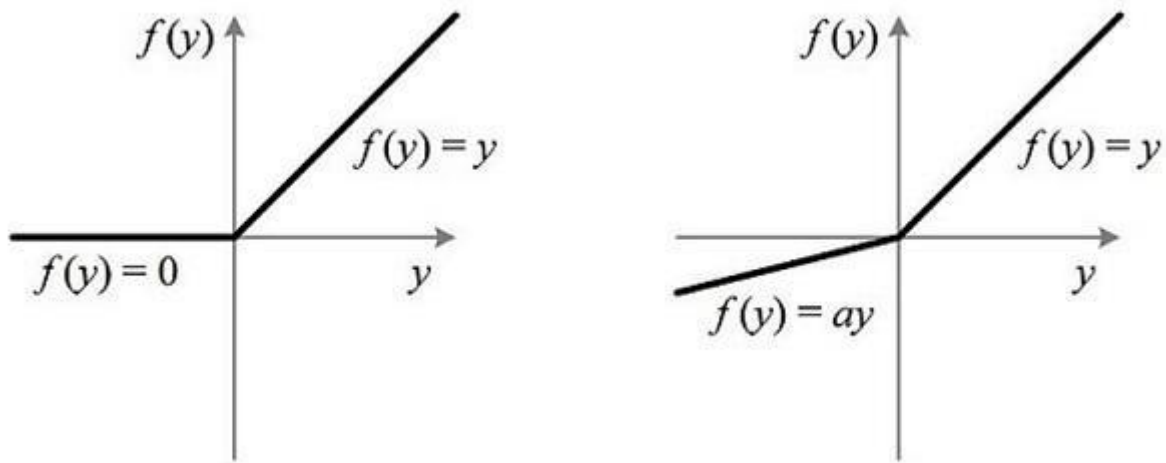
### 2.3.10. Activation Functions.

As mentioned above, every linear regression in a neuron comes with an activation function. However, a common issue in deep neural networks is the vanishing gradient problem during backpropagation. Here, the chain rule is used for the gradient descent calculations, this means that after multiple concatenations, the gradients from the first layers will be inevitably smaller than the lasts, tending to vanish at a certain point if the activation output is also constrained within small boundaries. Hence, the activation function has a direct implication in the performance of the network. For this reason, there are some functions which are more likely to perform better under certain circumstances than others. Non-linear functions tend to give better results, for example, a very popular activation function in CNNs is ReLU, which maximizes positive inputs, but returns zero otherwise, i.e.  $R(z) = \max(0, z)$ .

$$R(z) = \begin{cases} 0, & x \leq 0 \\ x, & x > 0 \end{cases} \quad (10)$$

It performs well in most of the cases and avoids the vanishing gradient problem. Nevertheless, negative neurons are completely forgotten during the training. Leaky ReLU (see Fig. 17) solves this problem multiplying all negative inputs for a small factor,  $\alpha$ , while keeps maximizing positive inputs [16].

$$LR(z) = \begin{cases} \alpha x, & x \leq 0 \\ x, & x > 0 \end{cases} \quad (11)$$



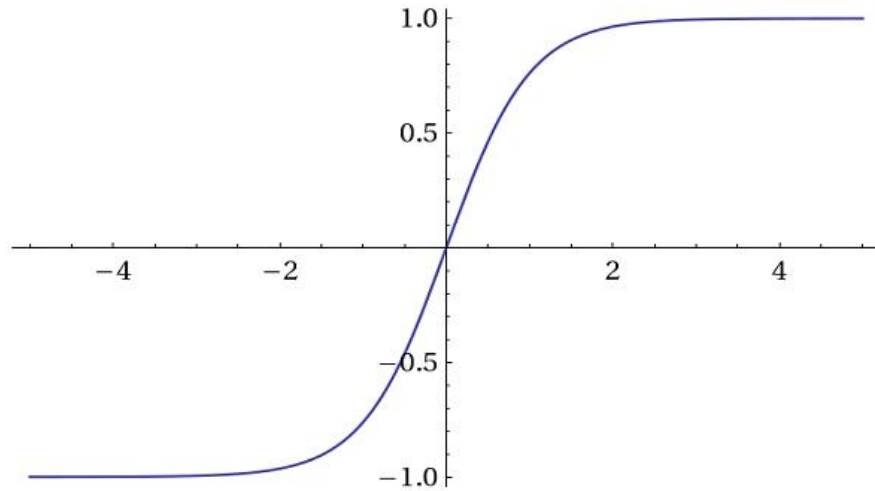
**Fig. 17.** ReLU and Leaky ReLU activation functions.

Another famous activation function that has been already explained is the Sigmoid function. It works well for binary classification problems, but despite of its popularity, it is computationally expensive and converges slower than, for example, the Tanh activation function (see Fig. 18), which is zero-centered between -1 and 1.

$$\tanh(z) = \frac{2}{1 + e^{-2z}} - 1 \quad (12)$$

On the contrary, for multi-classification problems, Softmax gives better results, so it is used at the end of the network. It returns a probability between 0 and 1 like the sigmoid [17].

$$Softmax(z) = \frac{e^{z_i}}{\sum_{j=1}^K e^{z_j}} \quad (13)$$

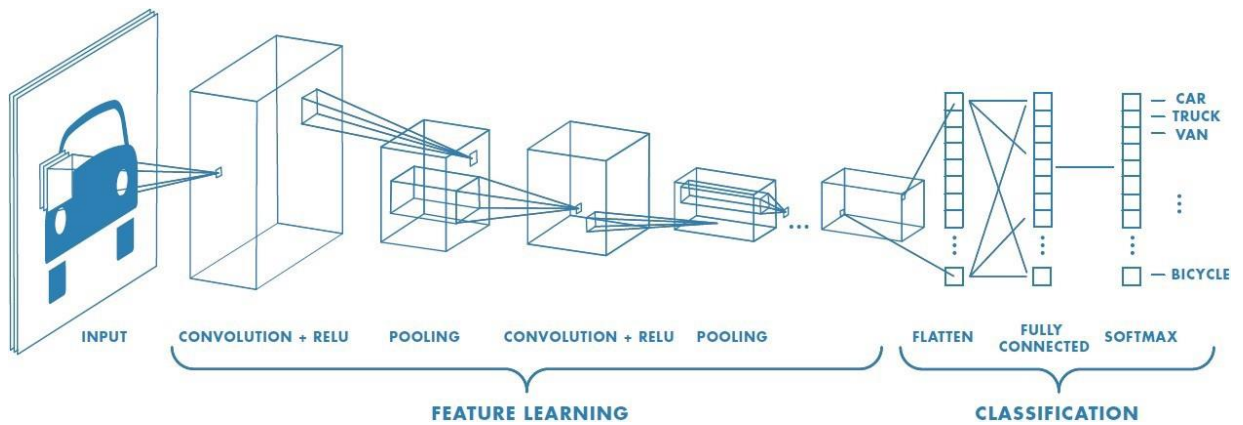


**Fig. 18.** Tanh activation function.

### 2.3.11. CNNs

All things consider, a DL model can be configured in multiples ways so that the network learns to perform different tasks based on the functions used and the connections of its layers. There are dozens of different configurations and ways of building an ANN, one of the most famous is named CNN and is fundamental for CV-based applications, as it was mentioned in previous sections.

“The first work on modern convolutional neural networks occurred in 1990, Gradient Based Learning Applied to Document Recognition“ [18] . In this paper, it was found that the concatenation of filters throughout different layers ended in a progressive transformation from simple to complex feature maps. These feature maps being incremented along with the depth of the network. In this approach, the increment was from 6 to 16 after the first subsampling, but in modern CNNs the final layers are made by hundreds of them. Then, the feature map is usually flattened and each cell is used as an input for the classification model. A ReLU activation function is commonly used here as well as during the convolutional layers, but the process usually ends with a logistic function for the object classification, for example, the Softmax function if there are multiple classes. Therefore, two parts can be distinguished in a CNN, a feature learning, and a classification part. Here is a visual representation of the structure just explained, see Fig. 19.



**Fig. 19.** Typical structure of a CNN

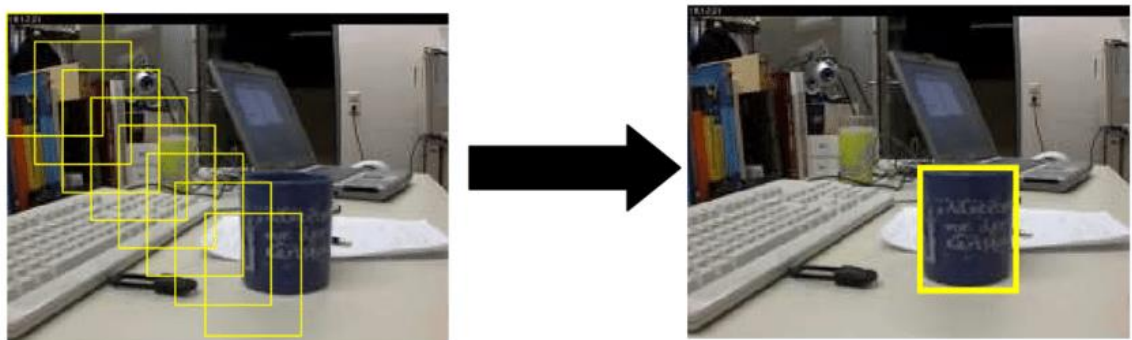
The learning process for the image classification requires a dataset of labeled images. These images must be different and should have different angles and different levels of luminosities, so that the network could learn to perform in different scenarios.

## 2.4. Object Detection

For the time being, the process of image classification has been explained, but this networks are still unable to know where the object is. To do find the object, there is something called object detection, which by making use of a proposal area or bounding box, teaches the network to also locate the object. In this section, an overview of some approaches to this problem are going to be presented, as well as the object detector used.

### 2.4.1. Sliding Windows

The first method ever used to find the location of an object was done by the sliding-windows technique. This technique, consists on taking a crop of the image to predict whether a particular object is on that window or not. Then, the window is moved along the image with different strides and sizes performing this predictions until the network ends finding a window that contains the object that was looked for, see Fig. 20.



**Fig. 20.** Sliding Window visual example.



### 2.4.2. DPM

One of the classical approaches that use this technique is Deformable Parts Model (DPM). This approach takes into account that either a person or an object can have different shapes, poses and colors. In real situations, an object can be partially occluded, what might lead into an accuracy reduction. DPM, uses the sliding windows technique to find the bounding box of an object and then, doubles the size of the image to take a crop of the different parts within that bounding box from where to extract more features. Within these crops, it is later computed how far are the parts from the body of the object. The following picture, Fig. 21, shows a diagram of this process.

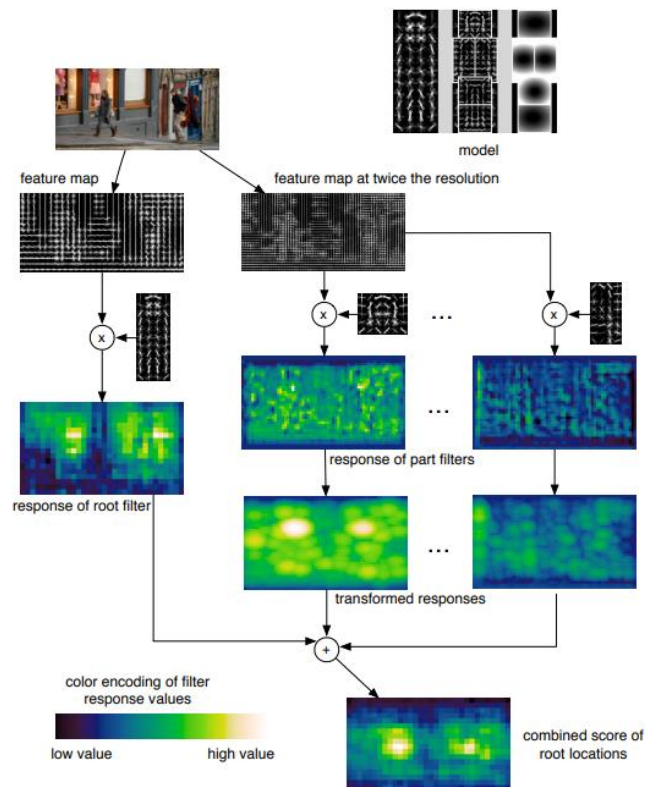


Fig. 21. DPM score process.

### 2.4.3. Region Proposals Network

Another famous technique for choosing possible bounding boxes within an image, is a region proposal method, which is done by a selective search of areas at different scales ratios. These areas, are found through a segmentation at different scales, resulting on a variety of several shapes for which the bounding box that fits that region is proposed. The regions are proposed by an hierarchical grouping of the most similar regions at different color spaces. Then, the color similarities are computed through their histogram intersections, as well as the textures similarities using SIFT measurements and Gaussian derivatives. The size of the region is also computed, allowing the smaller regions to merge earlier. Finally, the way in which each region fits into the

other is taken into account for the filling process. Fig. 22 shows an example of this process at different scales.



**Fig. 22.** Two examples of selective search at different scales. Note that (b) has detected the girl on the TV. [20]

A famous approach that implements this region proposal network is the R-CNN family, a two stages object detector where the bounding boxes for the feature extraction are got using this selective search, and a SVM algorithm is used for the classification process.

#### 2.4.4. YOLO

The main problem with these object detection models, is the high computational cost of their methods, which makes them incredibly slow. Even the improvements done by Fast R-CNN and Faster-RCNN, were so far away from being real-time approaches. This is the purpose for which YOLO was intended. The developers of this approach, managed to solve this frame rate problem by reframing it as “a single regression problem” [21], with a lot less bounding boxes instead of the conventional region-based and sliding windows techniques.

YOLO is the choice for the object detection task in this project, but in order to comprehend how it works nowadays, it is important to first walk through its different versions.

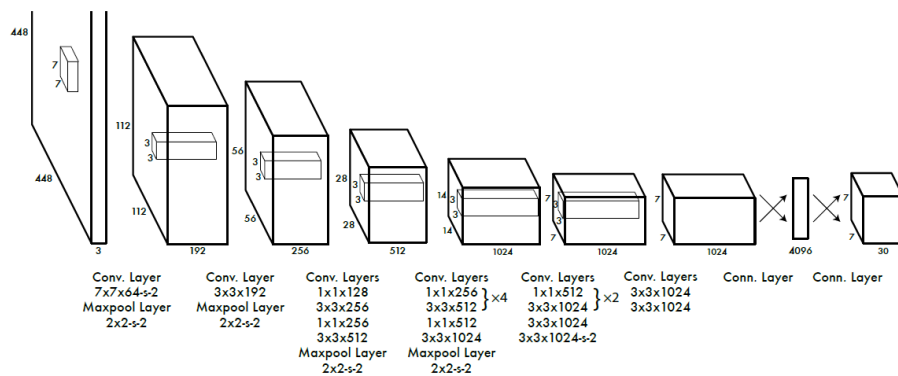
#### 2.4.5. YOLOv1

The first version of this algorithm, began “simultaneously predicting bounding boxes and class probabilities for those boxes” [21]. It worked over the entire image, thus, resulting on the encoding of the contextual information linked to the prediction. This was a great feature, because it allowed the model to be more generalizable in a wide range of situations while maintaining larger frame rates.

To accomplish this achievement, YOLO introduced an  $S \times S$  grid whose cells were responsible for providing these predictions. Every cell returned a  $B$  number of bounding boxes and a  $C$  number of class probabilities. Each bounding box contains the information of the  $x$  and  $y$  coordinates relatives

to that cell, the width and height relatives to the entire image and the IOU confidence that there was an object, ideally 1. Therefore, the prediction was an  $S \times S \times (B * 5 + C)$  tensor limited to one object per cell. This limitation in the number of objects that can be detected was important, because it directly affected to the performance with smaller objects.

Nevertheless, what made YOLO extremely fast was not only the reduction in the number of bounding boxes proposals compared to other techniques, but its network design, which was closely based on the GoogLeNet architecture. The main difference here, remained in the fact that YOLOv1 uses just  $1 \times 1$  reduction layers before the  $3 \times 3$  convolutional layers instead of the inception modules. This was named Darknet. Darknet’s architecture was built under “24 convolutional layers followed by 2 fully connected layers” [21] and took  $448 \times 448$  RGB images as inputs, see Fig. 23.



**Fig. 23.** Darknet [21].

Proceeding with the activation functions, a linear activation function was used for the final layer and a leaky rectified linear activation was used for the rest.

This first approach was trained with a grid size of  $S = 2$ , using the Pascal VOC Dataset, which contains a list of 20 different classes, each grid cell returning  $B = 2$  bounding boxes, making a total of 98 proposals, much less than the thousands of proposals in previous methods. Finally, the model was optimized with the sum-squared error loss.

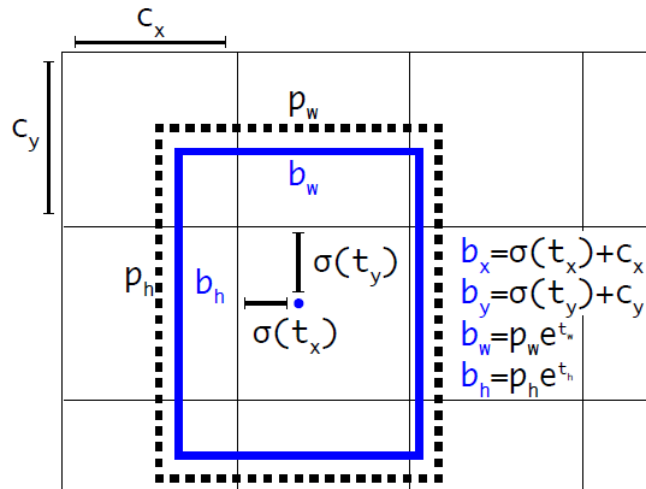
The results were quite impressive in terms of speed, achieving around 45 FPS, but it lacked in terms of recall and mAP, see Table 2.

Detection Frameworks	Train	mAP	FPS
Fast R-CNN	2007+2012	70.0	0.5
Fast R-CNN VGG-16	2007+2012	73.2	7
Fast R-CNN ResNet	2007+2012	76.4	5
YOLO	2007+2012	63.4	45
SSD300	2007+2012	74.3	46
SSD500	2007+2012	76.8	19

**Table 2.** Detection frameworks on PASCAL VOC 2007 [22]

### 2.4.6. YOLOv2

Later, YOLOv2 was released and with it, several changes within its architecture. One of the most significant changes made in YOLOv2 with respect to YOLOv1 to improve the location problems, was the implementation of anchor boxes (see Fig. 24) instead of predicting the coordinates directly.



**Fig. 24.** Bounding boxes with dimension priors and location prediction [22]

This anchor boxes allow the network to slightly adjust their size, which is much easier than predicting bounding boxes from scratch. These anchors, are chosen running a “k-means clustering on the training set bounding boxes to automatically find good priors” [22], thus, improving the results in the average IOU compared to hand-picked priors, see Table 3.

Box Generation	#	Avg IOU
Cluster SSE	5	58.7
Cluster IOU	5	61.0
Anchor Boxes	9	60.9
Cluster IOU	9	67.2

**Table 3.** Average IOU of boxes to closest priors on VOC 2007 [22]

Here, it is showed how, indeed, the clusters can achieve the same results than the hand-picked priors but using almost half of them.

However, since the anchor boxes led to model instability, the approach made in YOLOv1 was kept in terms of maintaining location coordinates relative to each grid cell. Therefore,  $t_x, t_y, t_w, t_h$  and  $t_o$  were defined as the new five predictions for each bounding box, whose x and y coordinates, width, height and IOU correspond to the following terms.

$$b_x = \sigma(t_x) + c_x \quad (14)$$

$$b_y = \sigma(t_y) + c_y \quad (15)$$

$$b_w = p_w e^{t_w} \quad (16)$$

$$b_h = p_h e^{t_h} \quad (17)$$

$$\Pr(\text{object}) * IOU(b, \text{object}) = \sigma(t_o) \quad (18)$$

Where  $p_w$  and  $p_h$  are the width and height of the anchor box and  $c_x$  and  $c_y$  the offsets of that cell.

Another important change made in YOLOv2, was the new network design, Darknet 19 (see Fig. 25), in which the class predictions were “decouple (...) from the spatial location” [22]. This meant, that the prediction then became an  $S \times S \times B(5 + C)$  tensor. This fact indicated that the loss would not only depend on the cell, but the index of the anchor too. On the other hand, the fully connected layers were also removed due to the use of anchor boxes for the bounding box predictions, and the input resolution was reduced to 416, downsampling the output image by a factor of 32. This way, allowing the implementation of a multi-scale training for multiples of 32 from 320 to 608. The multi-scale training, allowed YOLOv2 to learn how to perform in different scenarios, becoming faster at lower resolutions, and more accurate at higher, see Fig. 26.

Type	Filters	Size/Stride	Output
Convolutional	32	$3 \times 3$	$224 \times 224$
Maxpool		$2 \times 2/2$	$112 \times 112$
Convolutional	64	$3 \times 3$	$112 \times 112$
Maxpool		$2 \times 2/2$	$56 \times 56$
Convolutional	128	$3 \times 3$	$56 \times 56$
Convolutional	64	$1 \times 1$	$56 \times 56$
Convolutional	128	$3 \times 3$	$56 \times 56$
Maxpool		$2 \times 2/2$	$28 \times 28$
Convolutional	256	$3 \times 3$	$28 \times 28$
Convolutional	128	$1 \times 1$	$28 \times 28$
Convolutional	256	$3 \times 3$	$28 \times 28$
Maxpool		$2 \times 2/2$	$14 \times 14$
Convolutional	512	$3 \times 3$	$14 \times 14$
Convolutional	256	$1 \times 1$	$14 \times 14$
Convolutional	512	$3 \times 3$	$14 \times 14$
Convolutional	256	$1 \times 1$	$14 \times 14$
Convolutional	512	$3 \times 3$	$14 \times 14$
Maxpool		$2 \times 2/2$	$7 \times 7$
Convolutional	1024	$3 \times 3$	$7 \times 7$
Convolutional	512	$1 \times 1$	$7 \times 7$
Convolutional	1024	$3 \times 3$	$7 \times 7$
Convolutional	512	$1 \times 1$	$7 \times 7$
Convolutional	1024	$3 \times 3$	$7 \times 7$
Convolutional	1000	$1 \times 1$	$7 \times 7$
Avgpool		Global	1000
Softmax			

**Fig. 25.** Darknet 19 [22]

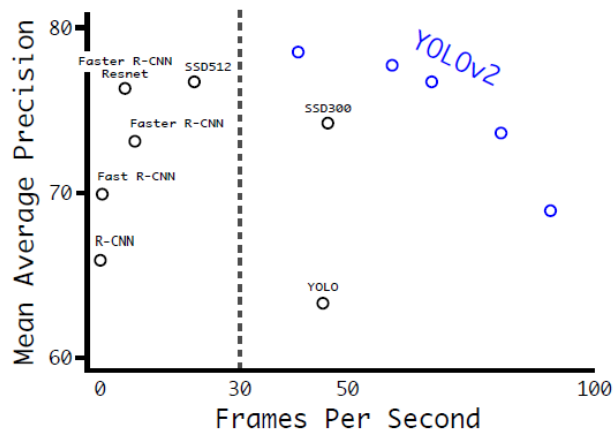


Fig. 26. Accuracy and speed on VOC 2007 [22]

### 2.4.7. YOLOv3

In YOLOv3 there is just one important change with respect to YOLOv2, since the implementation of the anchor boxes, the new Darknet 19 and the multi-scale training were incredibly successful on improving recall and mAP without losing speed in the process. It was a new version of Darknet, Darknet-53 (see Fig. 27), which merged the previous structure used in Darknet-19 with the residual blocks introduced in ResNet [23] within an FPN. These residual blocks, allow the network to become deeper while solving the vanishing gradient problem. This is the main reason of the new three different levels of predictions, where the feature map is upsampled after each one of them. Thus, allowing the net to perform better with smaller boxes. For the class predictions, each bounding box may now have a multilabel classification, using independent logistic classifiers, and the binary cross-entropy loss during training.

Table 4 shows how YOLOv3 reaches the same mAP than other methods, but clearly overcoming them in terms of speed.

Type	Filters	Size	Output
Convolutional	32	3 × 3	256 × 256
Convolutional	64	3 × 3 / 2	128 × 128
1×	Convolutional	32	1 × 1
	Convolutional	64	3 × 3
Residual			128 × 128
Convolutional	128	3 × 3 / 2	64 × 64
2×	Convolutional	64	1 × 1
	Convolutional	128	3 × 3
Residual			64 × 64
Convolutional	256	3 × 3 / 2	32 × 32
8×	Convolutional	128	1 × 1
	Convolutional	256	3 × 3
Residual			32 × 32
8×	Convolutional	512	3 × 3 / 2
	Convolutional	256	1 × 1
8×	Convolutional	512	3 × 3
	Residual		
			16 × 16
4×	Convolutional	1024	3 × 3 / 2
	Convolutional	512	1 × 1
4×	Convolutional	1024	3 × 3
	Residual		
			8 × 8
Avgpool		Global	
Connected		1000	
Softmax			

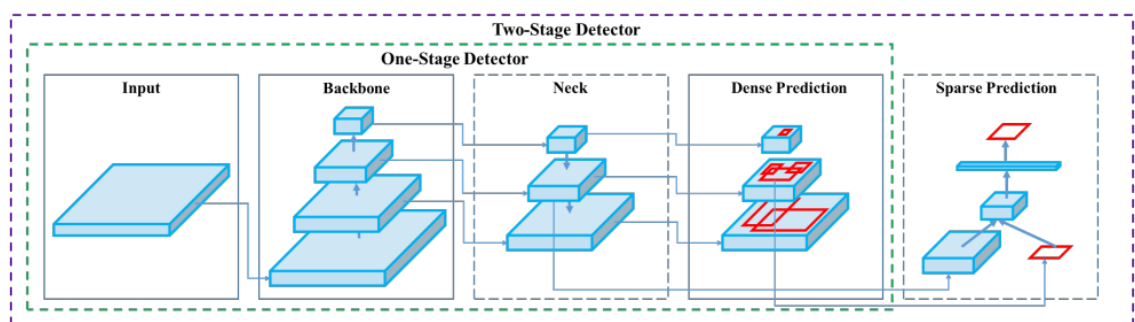
Fig. 27. Darknet 53 [24]

Method	mAP-50	time(ms)
SSD321	45.4	61
DSSD321	46.1	85
R-FCN	51.9	85
SSD513	50.4	125
DSSD513	53.3	156
FPN FRCN	59.1	172
RetinaNet-50-100	50.9	73
RetinaNet-101-500	53.1	90
RetinaNet-101-800	57.2	198
YOLOv3-320	51.5	22
YOLOv3-416	55.3	29
YOLOv3-608	57.9	51

**Table 4.** Speed/mAP-50 between YOLOv3 and other methods [24]

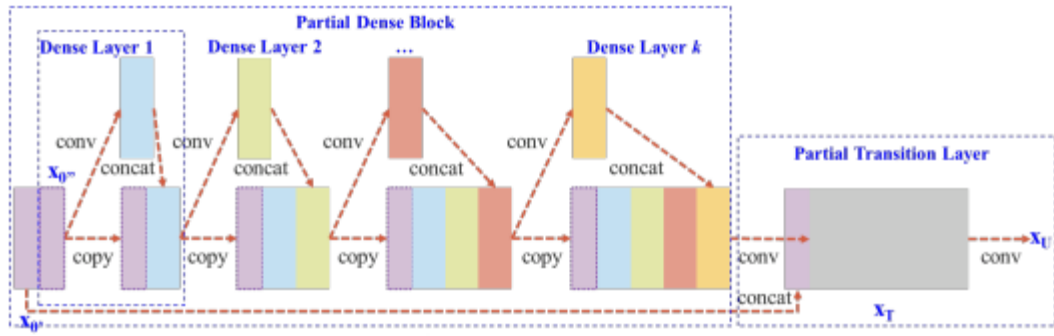
#### 2.4.8. YOLOv4

Previously, it was mentioned that object classifiers are composed by two main parts, in object detection, these two parts are named as backbone, which extract the features, and head, which perform predictions, but ever since most recent develops in object detection are including a way of mix together feature maps from different stages, a “neck” has started to take part in the structure. Thus, the last version of YOLO, YOLOv4, implemented several new features to Darknet-53 to improve its performance on single conventional GPUs. The following picture, Fig. 28, shows this structure.



**Fig. 28.** Object detector [25]

The new backbone in YOLOv4 maintained Darknet-53, but merging it with a CSPNet on top of its basis. The CSPNet, takes just one portion of each output before the next convolutional layer, thus, resulting in lighters convolutional blocks. The rest, is concatenated in the transition layers, see Fig. 29.



**Fig. 29.** CSPDenseNet example.

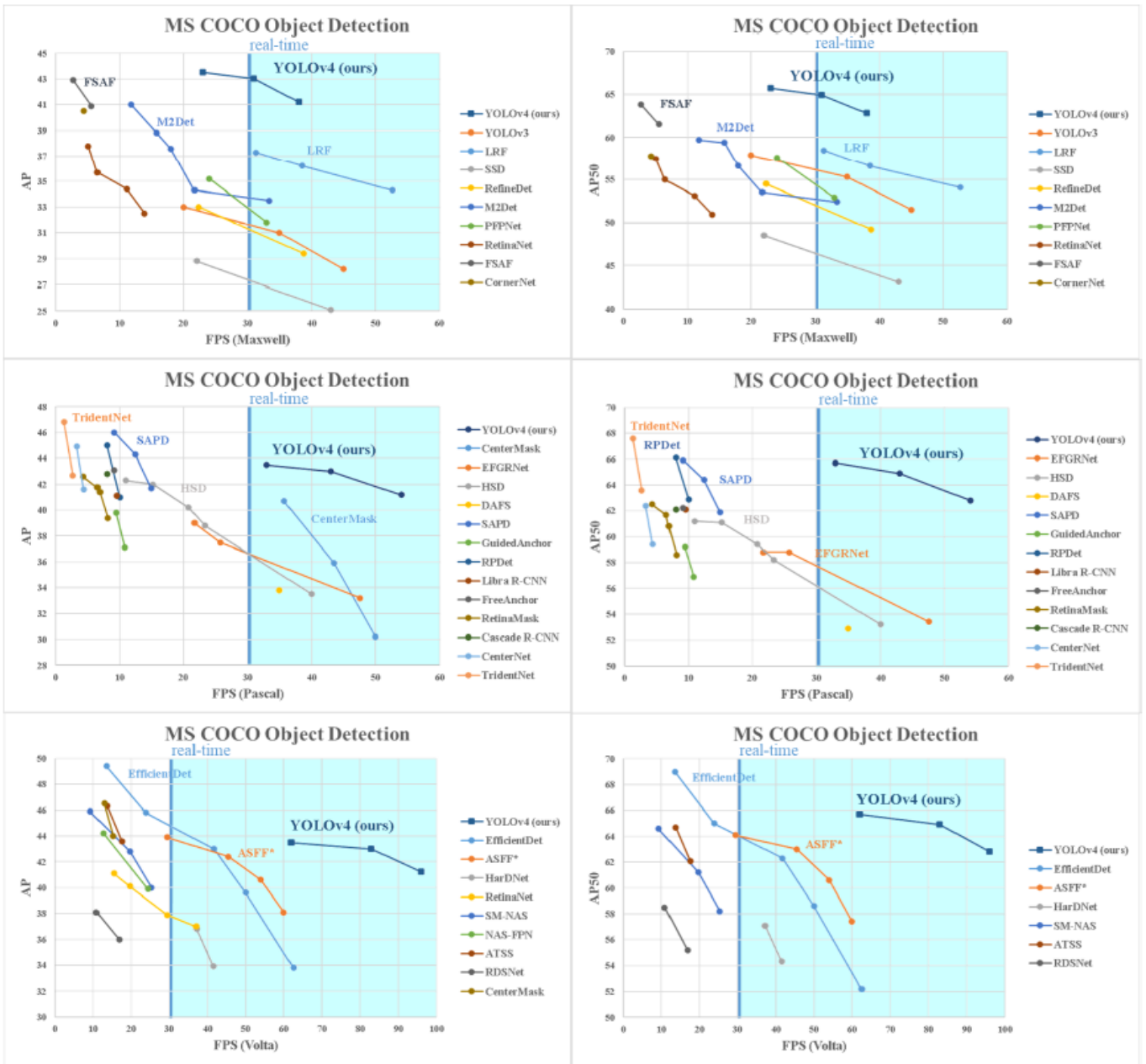
Usually, network lightening leads to worst performances, but on the contrary, this technique results in a reduction of the computational cost from 10% to 20% and still outperforming in terms of accuracy, also reducing memory costs and “removing computational bottlenecks” [26]

Furthermore, YOLOv4 adds a modified version of the SPP model to its model neck, setting a multi-scale max pooling with different kernel sizes but stride 1, and a subsequential concatenation of those outputs. This block not only improves the receptive field but screens the most significant context features with nearly 0 speed reduction. The neck also includes a modified PANet [27] for the aggregation of parameters, using element concatenations instead of element-wise additions. The head remains the same as in YOLOv3

Ultimately, a Mosaic data augmentation was included, next to a Self-Adversarial Training and a modified version of the CBN, it was called CmBN. Mosaic data augmentation helps to add more context information within one image, reducing the necessity of larger mini-batch. This new mosaic data augmentation works well with Cross Batch Normalization, as the tendency of higher resolution images has grown in recent years. In this case, the CmBN “collects statistics only between mini-batches with a single batch” [25].

Fig. 30 shows YOLOv4 performance.





**Fig. 30.** Comparison of the speed and accuracy of different object detectors [25]

This figure shows how YOLOv4 outperforms different object detectors in terms of speed and works in par in terms of AP due to its previously explained model design, being a very balance and suitable option for real-time object detections.

## 2.5. Object Tracking

Object detection is often coupled with object tracking for many reasons, since we may not only need to know where a certain object is, but its trajectory. This has become a very important task that must be taken into consideration if we talk, for example, about autonomous vehicles or security systems for collision avoidances.

### 2.5.1. DeepSORT

One of these approaches often coupled with YOLO is DeepSORT, a deep learning improvement of a famous object tracker released in 2007 called SORT.

SORT

The methodology followed by SORT, takes advantage of the nice performance of another two famous methods for motion estimation and combinational optimization, the Kalman Filter [28] and Hungarian algorithm.

SORT methodology has 4 main steps:

1. Detection;
2. Estimation;
3. Association;
4. Creation and Deletion of Track identities.

The detections can be made by any object detector, the better detections, the greater performance in SORT.

### 2.5.2. Estimation model. Kalman Filter.

The Kalman Filter is a probabilistic state estimator that fuses information from different sources to give a final estimate for unknown states. The estimate is calculated through both the predicted motion model and measurement model distributions, taking into consideration a certain noise for each one of them.

The estimation model is done by the Kalman filter using the following state vector.

$$X = [u, v, s, r, vu, vv, vs]^T \quad (19)$$

Where  $u$  and  $v$  are the horizontal and vertical centre coordinates of the target,  $s$  is the scale area of the bounding box and  $r$  the aspect ratio of that bounding box. The rest of the parameters are their respective velocities.

For a 1-Dimensional state, the predictions are given by.

$$x_k^{pred} = F_k x_{k-1} + B_k u_k \quad (20)$$

$$P_k^{pred} = F_k P_{k-1} F_k^T + Q_k \quad (21)$$

Where

$$F_k = \begin{pmatrix} 1 & \delta t \\ 0 & 1 \end{pmatrix} \quad (22)$$

$$G_k = \begin{pmatrix} \frac{1}{2} \delta t^2 \\ \delta t \end{pmatrix} \quad (23)$$

Where  $x_k$  is the state vector,  $P_k$  the covariance,  $u_k$  a control input noise, and  $F_k$ ,  $B_k$  and  $Q_k$  are the transition, control and covariance noise matrix, respectively.

Then, the measurement is used to correct the prediction based on the innovation and some gain. This kalman gain is also used to propagate the state covariance.

$$x_k^{corrected} = x_k^{pred} + K_k * Innovation \quad (24)$$

$$P_k^{corrected} = (I - K_k H_k) P_k^{pred} \quad (25)$$

Where

$$K_k = P_k^{pred} H_k^T (H_k P_k^{pred} H_k^T + R_k)^{-1} \quad (26)$$

$$Innovation = (y_k - H_k x_k^{pred}) \quad (27)$$

Here,  $y_k$  corresponds to the measurement,  $K_k$  is the Kalman Gain,  $H_k$  is the relation matrix between the predicted state and the measurements in case of having different input units, and  $R_k$  is the measurement covariance noise.

### 2.5.3. Data Association. Hungarian Algorithm.

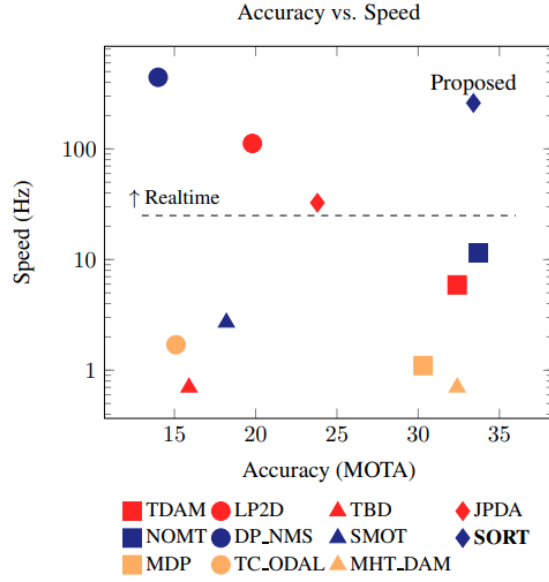
For the data association, a cost matrix is calculated based on the IOU distance between all the predicted and detected objects. Later, the Hungarian algorithm matches the bounding boxes.

The Hungarian algorithm is an optimization algorithm which finds the minimum values for each not repeated row and column within a given  $N \times N$  matrix in assignment problems. The fundamental of this problem is that the optimal assignment for a reduced cost matrix, is also the optimal assignment for the original cost matrix.

### 2.5.4. Track Identities.

Finally, the new identities are created only if their IOU is greater than a fixed minimum distance and remain for a certain amount of time. Then, if the identity is lost for a  $T_{Lost}$  number of frames, it is eliminated.

Fig. 31 shows SORT performance.



**Fig. 31.** SORT performance in relation to several baseline trackers. [29]

As shown, SORT had a nice performance in comparison to other object trackers. The problem in SORT was the high number of switches, since it does not perform well under high state uncertainties, for example, during occlusions.

### 2.5.5. Deep Association metric for SORT

To improve this behavior, in 2017 was introduced a deep association metric for SORT. They included an appearance feature descriptor to consider along with the state estimation in order outperform SORT previous results. There are also some little changes with respect the original SORT, for example, the state vector.

$$y_i = (u, v, \gamma, h, vu, vv, v\gamma, vh) \quad (28)$$

Where  $\gamma$  is the aspect ratio and  $h$  the height of the bounding box.

Besides, the squared Mahalanobis distance is used instead of the Hungarian algorithm due to that change.

$$d_{i,j}^{(1)} = (d_j - y_i)^T S_i^{-1} (d_j - y_i) \quad (29)$$

Here,  $S_i$  is de covariance matrix and  $d_j$  is the bounding box detection.

The problem with the Euclidean distance to perform the data association, is that it does not work well when covariances are involve. Therefore, Manhalanobis distance is a better choice for rescaling the problem, so that these covariances can vanish. In this case, it is used a threshold of 95% the Manhalanobis distance instead of the IOU minimum.

### 2.5.6. Feature Descriptor.

However, as used to happen in the original SORT, the Mahalanobis distance is not suitable enough under high uncertainties, since the Kalman filter estimates are not so accurate. This is where the appearance descriptor vector takes part in.

Fig. 32 shows the architecture of the obtention of the feature descriptor.

Name	Patch Size/Stride	Output Size
Conv 1	$3 \times 3/1$	$32 \times 128 \times 64$
Conv 2	$3 \times 3/1$	$32 \times 128 \times 64$
Max Pool 3	$3 \times 3/2$	$32 \times 64 \times 32$
Residual 4	$3 \times 3/1$	$32 \times 64 \times 32$
Residual 5	$3 \times 3/1$	$32 \times 64 \times 32$
Residual 6	$3 \times 3/2$	$64 \times 32 \times 16$
Residual 7	$3 \times 3/1$	$64 \times 32 \times 16$
Residual 8	$3 \times 3/2$	$128 \times 16 \times 8$
Residual 9	$3 \times 3/1$	$128 \times 16 \times 8$
Dense 10		128
Batch and $\ell_2$ normalization		128

**Fig. 32.** CNN architecture for the feature descriptor [30]

The feature descriptor is obtained throughout the above architecture, for which the nearest neighbor queries are used to process the relation between the measurement and the existing track, using the smallest cosine distance as the metric and a binary variable for the unlikely associations.

$$d_{i,j}^{(2)} = \min\{1 - r_j^T r_k^{(i)} \mid r_k^{(i)} \in R_i\} \quad (30)$$

Where  $r_j$  is the appearance descriptor for the bounding box and  $r_k^{(i)}$  the associate appearance descriptor for the  $i$ -th track.

Then, both state and appearance metrics are combined using a weighted sum.

$$c_{i,j} = \lambda d_{i,j}^{(1)} + (1 - \lambda) d_{i,j}^{(2)} \quad (31)$$

Nevertheless, the creation and deletion of identities follows the same logic as the original SORT.

Fig. 33 shows some DeepSORT results.

		MOTA $\uparrow$	MOTP $\uparrow$	MT $\uparrow$	ML $\downarrow$	ID $\downarrow$	FM $\downarrow$	FP $\downarrow$	FN $\downarrow$	Runtime $\uparrow$
KDNT [16]*	BATCH	68.2	79.4	41.0%	19.0%	933	1093	11479	45605	0.7 Hz
LMP_p [17]*	BATCH	<b>71.0</b>	<b>80.2</b>	<b>46.9%</b>	21.9%	434	<b>587</b>	7880	<b>44564</b>	0.5 Hz
MCMOT_HDM [18]	BATCH	62.4	78.3	31.5%	24.2%	1394	1318	9855	57257	35 Hz
NOMTwSDP16 [19]	BATCH	62.2	79.6	32.5%	31.1%	<b>406</b>	642	<b>5119</b>	63352	3 Hz
EAMTT [20]	<b>ONLINE</b>	52.5	78.8	19.0%	34.9%	910	<b>1321</b>	<b>4407</b>	81223	12 Hz
POI [16]*	<b>ONLINE</b>	<b>66.1</b>	79.5	<b>34.0%</b>	20.8%	805	3093	5061	<b>55914</b>	10 Hz
SORT [12]*	<b>ONLINE</b>	59.8	<b>79.6</b>	25.4%	22.7%	1423	1835	8698	63245	<b>60 Hz</b>
Deep SORT (Ours)*	<b>ONLINE</b>	61.4	79.1	32.8%	<b>18.2%</b>	<b>781</b>	2008	12852	56668	40 Hz

**Fig. 33.** DeepSORT tracking results [30]

It can be seen a reduction in the lost percentage and number of identity switches with respect the original SORT, and an increase in the tracked percentage while maintaining a real-time runtime. Definitely, a more robust and accurate version than SORT, and still faster than other options. Therefore, the choice for the object tracking.

### **3. Project Development and Results**

The images used on this project are recorded with an Asus Xtion Pro Live and the further post processing is done in Python using Google Colaboratory and Visual Studio Code. Here, there is a brief explanation of these working tools.

#### **3.1. Asus Xtion Pro Live**

The Asus Xtion Pro Live [31] is an RGB camera with a depth measurement sensor for distances in between 0.8 m and 3.5 m. It is thought to operate indoor and has a field of view of 58° H, 45° V, 70° D (Horizontal, Vertical, Diagonal). It has a power consumption below 2.5 W and uses OpenNI2 as software.

For this project, the image acquisition was done at a resolution of 640x480 and 30 FPS.

#### **3.2. Programming Language. Python**

“Python is an interpreted, object-oriented, high-level programming language“ [32] with dynamic typing and programming structure. It is popular because of its portability and simple syntax, which facilitates the readability of the code and the learning process. It has one of the largest programming communities, hence, there are a lot of different libraries available for almost every scenario. It has multiple applications in artificial intelligence and computer vision problems.

#### **3.3. Programming environments**

Although the aim of this project is to develop a collision avoidance algorithm, first, an object detection and tracking must be done. For that reason, Google Colaboratory is used. However, the rest of the project has been developed using Visual Studio Code instead.

Google Colaboratory is a free Jupyter Notebook based environment for cloud programming released by Google, and enabled for everybody with an internet connection without the need of installing anything. It is given the possibility of using a random GPU or TPU from their servers for deep learning applications. Therefore, it is perfect for the object detection and tracking tasks of the individuals appeared in this project.

##### **3.3.1. Visual Studio Code**

Visual Studio Code, on the other hand, is a free code editor from Microsoft. It supports almost any programming language and allows the customization of its interface throughout an extension store. It also includes git connection, a debugging window, and a command prompt. Hence, one of the best choices for app and web developing.

Due to the fact that Google Colaboratory is run on the cloud, it has some limitations with respect other code editors, like for example some OpenCV functions. Thus, it is justified the use of Visual Studio Code during the rest of the project, i.e. camera calibration, image acquisition, error measurement and collision avoidance scripts.

### 3.4. Proposed Solution

In this section, the proposed solution for the collision avoidance between humans and vehicles will be explained. That said, during the introduction, it was mentioned that this solution was focused on human-human interactions. However, later it will be explained how it could be applied for human-vehicle situations.

First of all, a calibration must be done to get the intrinsic parameters of the camera. It will be done running a calibration script which returns a YAML file with the OpenCV calculations. Then, these parameters will be used to correct the distortion of the image, and calculate the error on the ground projection between the original and the undistort images.

After the camera calibration and error calculations for the ground projections, a set of frames will be recorded as inputs for the object detection and tracking scripts. The model is taken from a public github repository from Mikel Brostrom, it will be later explained in more detail.

Finally, the standing points of the individuals detected corresponding to the tracked bounding boxes will be mapped from the pixel coordinate system to the ground plane. This ground projections, will be used to set the orientation of a safety area according to the trajectory of the detection. Therefore, the collision alerts will be given depending on these safety areas and their trajectories.

#### 3.4.1. Camera Calibration

In computer vision applications, it is important to perform a camera calibration from the operating point of the camera, since the image might have a positive or negative radial distortion, which is related to the field of view of the camera lens, see Fig. 34.



Fig. 34. Type of distortions [33]

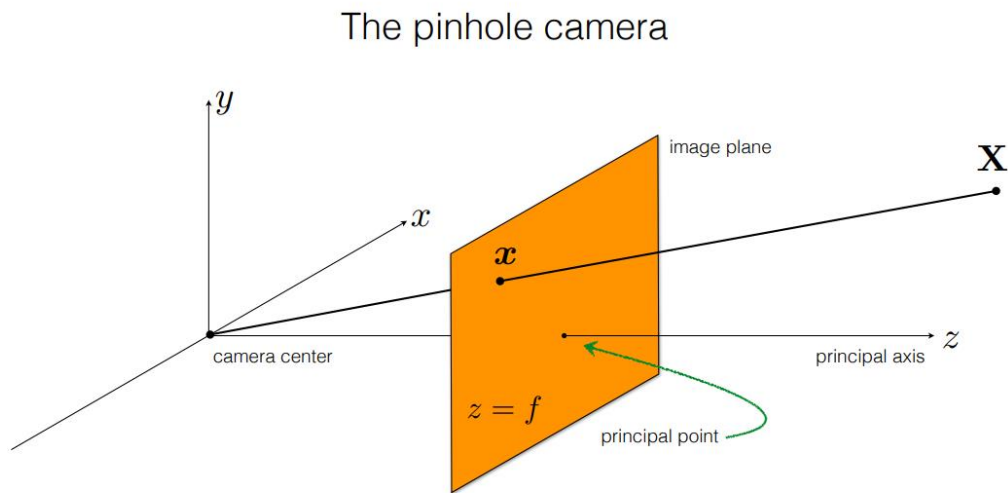
This calibration is used to get the intrinsic parameters of the camera, as well as the distortion parameters, and rotation and translation vectors, so that any possible distortion on the image could be corrected beforehand in order to perform accurate measurements or any needed calculation.



This is possible due to the fact that the camera performs a 2D representation of the 3D world, which in fact, is directly related to their intrinsic parameters like the focal length and the location of its optical center. The pinhole camera model (see Fig. 35) mathematically describes this relationship as:

$$s \begin{bmatrix} u \\ v \\ 1 \end{bmatrix} = \begin{bmatrix} f_x & 0 & c_x \\ 0 & f_y & c_y \\ 0 & 0 & 1 \end{bmatrix} \begin{bmatrix} r_{11} & r_{12} & r_{13} & t_1 \\ r_{21} & r_{22} & r_{23} & t_2 \\ r_{31} & r_{32} & r_{33} & t_3 \end{bmatrix} \begin{bmatrix} X \\ Y \\ Z \\ 1 \end{bmatrix} \quad (32)$$

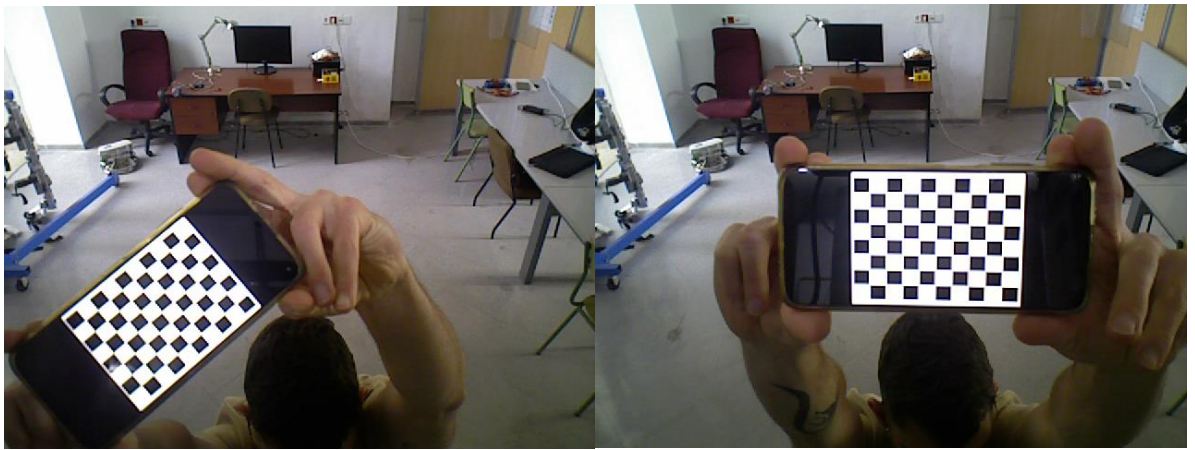
Where  $(f_x, f_y)$  are the focal lengths in pixels,  $(c_x, c_y)$  are the coordinates of principal point, and the  $r_{mn}$  parameters are part of the rotation-translation matrix, which is related to the scene.



**Fig. 35.** Pinhole camera model.

### 3.4.2. Chessboard Method

OpenCV has some functions to calculate these intrinsic and extrinsic parameters throughout the corners of a chessboard and their relationship within a set of images at different positions, see Fig. 36.



**Fig. 36.** Two examples of the calibration images with the chessboard at different positions

Table 5 shows to get the images for the calibration process.

**Table 5.** Loop to get the calibration images.

```

1. # initialize the camera
2. openni2.initialize("C:\Program Files\OpenNI2\Redist")
3. dev = openni2.Device.open_any()
4.
5. color_stream = dev.create_color_stream()
6. color_stream.set_video_mode(c_api.OniVideoMode(pixelFormat =
   c_api.OniPixelFormat.ONI_PIXEL_FORMAT_RGB888, resolutionX = int(640),
7.                               resolutionY = int(480), fps = 30))
8. color_stream.start()
9.
10. i=0
11. start = time.time()
12. while True:
13.
14. cframe = color_stream.read_frame()
15. cframe_data = cframe.get_buffer_as_uint8()
16. cimg = np.ndarray((cframe.height, cframe.width, 3), dtype=np.uint8,
17.                   buffer=cframe_data)
18. cimg = cv.cvtColor(cimg, cv.COLOR_BGR2RGB)
19.
20. end = time.time()
21.
22. #stores the frame every 5 seconds
23. if int(round(end-start,2)) == 5:
24.     cv.imwrite("calibration_images/"+str("{}".format(i)+"chessboard") +
25.               ".png",cimg)
26.     i+=1
27.     start = end
28. cv.imshow("color", cimg)
29.
30. #breaks the loop after 10 images

```

```

31. if len(glob.glob('calibration_images/*.png')) == 10:
32.     break
33.
34. if cv.waitKey(10) & 0xFF == ord('q'):
35.     break
36. color_stream.stop()
37. openni2.unload()
38. cv.destroyAllWindows()

```

For this process, ten chessboard images were got in loop, storing a frame every five seconds so that the chessboard could be situated at different positions. To measure the time, the function time is used. In line 23, is set the statement for which, if the difference between the end variable, line 20, and start variable, line 11, is equal to five, it would mean that five seconds were spent.

After that, some preparation for the calibration process is needed. Table 6 shows the code for this preparation.

**Table 6.** Chessboard preparation.

```

1. chessboardSize = (9,7)
2. frameSize = (640,480)
3.
4. # prepare object points, like (0,0,0), (1,0,0), (2,0,0) ....,(6,5,0)
5. objp = np.zeros((chessboardSize[0] * chessboardSize[1], 3), np.float32)
6. objp[:, :2] = np.mgrid[0:chessboardSize[0],
7.                        0:chessboardSize[1]].T.reshape(-1,2)
8.
9. size_of_chessboard_squares_mm = 10
10. objp = objp * size_of_chessboard_squares_mm
11. # Arrays to store object points and image points from all the images.
12. objpoints = [] # 3d point in real world space
13. imgpoints = [] # 2d points in image plane.

```

The window size and the number of x and y-axis corners of the chessboard should be defined. These corners are also used to prepare an array with the location in millimeters of each one of them. Moreover, two empty lists are defined to store the image and real world corners in case they are found, see lines 12 and 13. Now, in Table 7 is presented the code for the calibration process.

**Table 7.** Camera calibration.

```

1. # termination criteria
2. criteria = (cv2.TERM_CRITERIA_EPS + cv2.TERM_CRITERIA_MAX_ITER, 30, 0.001)

```

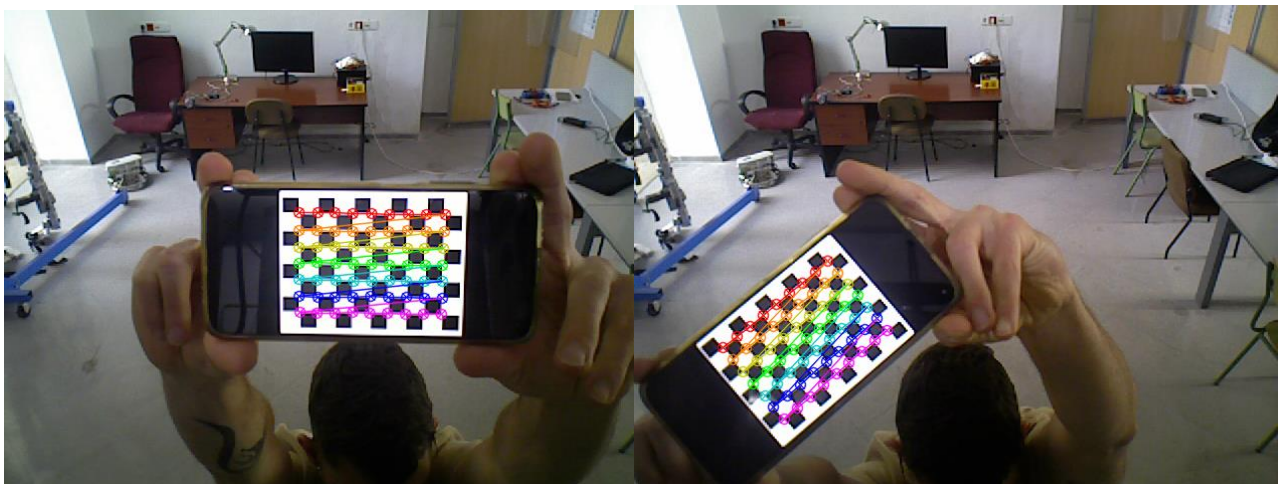
```

3. images = glob.glob('calibration_images/*.png')
4.
5. for i, image in enumerate(images):
6.     img = cv2.imread(image)
7.     gray = cv2.cvtColor(img, cv2.COLOR_BGR2GRAY)
8.
9.     # Find the chess board corners
10.    ret, corners = cv2.findChessboardCorners(gray, chessboardSize, None)
11.
12.    # If found, add object points, image points (after refining them)
13.    if ret == True:
14.
15.        objpoints.append(objjp)
16.        corners2 = cv2.cornerSubPix(gray, corners, (11,11), (-1,-1), criteria)
17.        imgpoints.append(corners)
18.        # Draw and display the corners
19.        cv2.drawChessboardCorners(img, chessboardSize, corners2, ret)
20.
21.        cv2.imwrite("calibration_images/calibrated/"+str("{}").format(i)+"calib")
22.                    + ".png",img)
23.    cv2.destroyAllWindows()
24. # CALIBRATION
25.    ret, cameraMatrix, Distortion_Params, Rotation_vec, Translation_vec =
        cv2.calibrateCamera(objpoints, imgpoints, frameSize, None, None)

```

The calibration process works as follows. After the chessboard is prepared, a rough estimation of the corners in the calibration image is done, line 10. If this estimation is done correctly, the corners locations are refined with another function in line 16. Then, both 3D and 2D lists of chessboard corners are stored for each calibration image. These two lists as well as the frame size, are used as inputs for the camera calibration function in line 25.

Fig. 37 shows the calibration points.



**Fig. 37.** Corners found within the calibration images.

The functions used to get the chessboard corners were:

**cv2.findChessboardCorners(image, patternSize[, corners[, flags]])** [34]: It finds the positions of internal corners of the chessboard.

- Image: source chessboard view. It must be an 8-bit grayscale or color image.
- patternSize: number of inner corners per a chessboard row and column.
- corners: output array of detected corners.
- flags: various operation flags.

**cv2.cornerSubPix(image, corners, winSize, zeroZone, criteria)** [35]: It refines the corner locations.

- image: input single-channel, 8-bit or float image.
- corners: initial coordinates of the input corners.
- winSize: half of the side length of the search window.
- zeroZone: half of the size of the dead region in the middle of the search zone over which the summation in the formula below is not done.
- criteria: criteria for termination of the iterative process of corner refinement.

Finally, the optimal camera matrix is obtained and everything is stored in a YAML file. Table 8 shows the code for this process.

**Table 8.** Optimal parameters.

```
1. # GETTING OPTIMAL PARAMETERS
2. h, w = img.shape[:2]
3. newCameraMatrix, roi = cv2.getOptimalNewCameraMatrix(cameraMatrix,
4.                                                     Distortion_Params, (w,h), 1, (w,h))
5.
6. print('Saving parameters !')
7. cv_file = cv2.FileStorage('cameraIntrinsic.yaml', cv2.FILE_STORAGE_WRITE)
8. cv_file.write('Camera_Matrix', cameraMatrix)
9. cv_file.write('newCamera_Matrix', newCameraMatrix)
10. cv_file.write('Roi',roi)
11. cv_file.write('Distortion_Params', Distortion_Params)
12. cv_file.write('Rotation_Vec', np.array(Rotation_vec))
13. cv_file.write('Translation_Vec', np.array(Translation_vec))
```

The functions used in the calibration process were:

**cv2.calibrateCamera(objectPoints, imagePoints, imageSize, cameraMatrix, distCoeffs[, rvecs[, tvecs[, flags[, criteria]]]])** [36]: It finds the camera intrinsic and extrinsic parameters from several views of a calibration pattern.

- objectPoints: it is a vector of vectors of calibration pattern points in the calibration pattern coordinate space.
- imagePoints: it is a vector of vectors of the projections of calibrating pattern points.
- imageSize: size of the image used to initialize the camera intrinsic matrix.
- cameraMatrix: input/output 3x3 floating-point camera intrinsic matrix
- distCoeffs: input/output vector of distortion coefficients.
- rvecs: output vector of rotation vectors.
- tvecs: output vector of translation vectors.
- flags: different flags.
- criteria: termination criteria for the iterative optimization algorithm.

**cv2.getOptimalNewCameraMatrix(cameraMatrix, distCoeffs, imageSize, alpha[, newImgSize[, centerPrincipalPoint]])** [37]: It returns the new camera intrinsic matrix based on the free scaling parameter.

- cameraMatrix: input camera intrinsic matrix.
- distCoeffs: input vector of distortion coefficients.
- imageSize: original image size.
- alpha: free scaling parameter between 0 and 1.
- newImgSize: image size after rectification.
- centerPrincipalPoint: optional flag that indicates whether in the new camera intrinsic matrix the principal point should be at the image center or not.

In this case, I got a mean error during the calibration of 0.09005, see Table 9

Calibration Error
0.09005

**Table 9.** Camera calibration error.

### 3.4.3. Correcting distortion in images.

Now, since the camera calibration has been performed, the following task is to use the camera parameters to undistort the image, see Table 10.

**Table 10.** Image undistortion.

```
1. frame = cv2.imread('error_measurement/test0/1color.png')
```

```

2. frame_copy = frame.copy()
3.
4. # Undistort image
5. dst = cv2.undistort(frame_copy, cameraMatrix, Distortion_Params, None,
6.                     newCameraMatrix)
7.
8. # crop the image
9. x, y, w, h = roi
10. dst = dst[y[0]:y[0]+h[0], x[0]:x[0]+w[0]]
11. dst = cv2.resize(dst, (640,480))

```

In line 5, the image is undistorted, and right after, it is cropped to eliminate the resulting black borders. Both images are shown in Fig. 38 and Fig. 39.

The function which performs the undistortion is:

**cv2.undistort(src, cameraMatrix, distCoeffs[, dst[, newCameraMatrix]])** [38]: It transforms an image to compensate radial and tangential lens distortion.

- src: input image..
- dst: output corrected image.
- cameraMatrix: input camera Matrix.
- distCoeffs: input vector of distortion coefficients.
- newCameraMatrix: camera matrix of the distorted image.



**Fig. 38.** Original image.



**Fig. 39.** Undistort image

#### 3.4.4. Ground projection.

Now, to get the actual location of the individuals, it would be necessary to map the image coordinates to another reference system, there are multiple ways to do so.

One of those ways, is via homography calculations, which is commonly used to relate 2D images of the same view at different angles. In this case, the idea is to use the homography matrix to project any falling point within the boundaries of a ground layout in the input image, into an upper view of the same area, so that the actual location could be accurately obtained .

Therefore, the new coordinates could be calculated as follows.

$$\begin{bmatrix} x_a \\ y_a \\ z_a \end{bmatrix} = H_{3 \times 3} \cdot \begin{bmatrix} x_1 \\ y_1 \\ 1 \end{bmatrix} \quad (33)$$

$$\begin{bmatrix} x_2 \\ y_2 \\ 1 \end{bmatrix} = \begin{bmatrix} x_a \\ y_a \\ z_a \end{bmatrix} \cdot \frac{1}{z_a} \quad (34)$$

Where  $(x_1, y_1, 1)$  are the coordinates within the boundaries of the original image and  $H_{3 \times 3}$  is the homography matrix.



OpenCV has two functions to do so:

**cv2.findHomography(srcPoints, dstPoints[, method[, ransacReprojThreshold[, mask[, maxIters[, confidence]]]])** [39]: It finds a perspective transformation between two planes.

- srcPoints: coordinates of the points in the original plane
- dstPoints: coordinates of the points in the target plane
- method: method used to compute a homography matrix
- ransacReprojThreshold: maximum allowed re-projection error to treat a point pair as an inlier
- mask: optional output mask set by a robust method
- maxIters: the maximum number of RANSAC iterations
- confidence: confidence level

**cv2.warpPerspective(src, M, dsize[, dst[, flags[, borderMode[, borderValue]]])** [40]: It transforms the source image using the specified matrix

- src: input image
- M: 3x3 transformation matrix
- dsize: size of the output image
- dst: output image
- flags: combination of interpolation methods (INTER\_LINEAR or INTER\_NEAREST) and the optional flag WARP\_INVERSE\_MAP, that sets M as the inverse transformation (dst→src)
- borderMode: pixel extrapolation method.
- borderValue value used in case of a constant border.

### 3.4.5. Homography matrix functions.

Here, two homography functions are defined. The first, is set for the original image, whereas the second is for the undistort one. See Table 11.

**Table 11.** Homography calculation functions.

```
1. width,height = (640,480)
2. n,m = (246,320)
3.
4. def homography()
5.     #corners of the ground layout
6.     corners = np.array([[178,105], [465,105], [0,height], [width, height]])
7.     #corners of the new perspective
8.     cornersN = np.array([[0,0],[n,0],[0,m],[n,m]])
9.     corners=np.int64(corners)
10.    cornersN=np.int64(cornersN)
```

```

11.
12. h,_=cv2.findHomography(corners,cornersN)
13.
14. return h, corners
15.
16. def homography_dist():
17.
18. corners = np.array([[161,95], [461,95], [0,height], [width, height]])
19. cornersN = np.array([[0,0],[n,0],[0,m],[n,m]])
20. corners=np.int64(corners)
21. cornersN=np.int64(cornersN)
22.
23. h,_=cv2.findHomography(corners,cornersN)
24.
25. return h, corners

```

In relation to the homography calculations, the real plane has a width and height measures of 246x320 cm, these measurements are used to define the window size of the new perspective, which means that the scale is 1:1 for the upper view

### 3.4.6. Homography error calculations.

The next step, is to measure the error in the location estimation after finding the homography between the upper view of the real plane and the original image taken from the camera point of view. To do so, both original and undistort images are loaded and reframed to the new perspective. Then, a set of 20 points with respect the measurement of the slabs in the real plane is drawn, and the deviation within the x and y-axis is measured.

Table 12 corresponds to this process.

**Table 12.** Homography error measurement.

```

1. #load test images
2. frame = cv2.imread('error_measurement/test0/1color.png') #distort
3. dst = cv2.imread('error_measurement/test0/0color.png') #undistort
4. wrap_dist = frame.copy()
5. wrap_undist = dst.copy()
6.
7. #show ground corners
8. h, layout = homography()
9. cv2.circle(frame, layout[0], 5, (0,0,255), 2)
10. cv2.circle(frame, layout[1], 5, (0,255,0), 2)
11. cv2.circle(frame, layout[2], 5, (255,0,255), 2)
12. cv2.circle(frame, layout[3], 5, (255,0,0), 2)
13.

```

```

14. h1, layout2 = homography_dist()
15. cv2.circle(dst, layout2[0], 5, (0,0,255), 2)
16. cv2.circle(dst, layout2[1], 5, (0,255,0), 2)
17. cv2.circle(dst, layout2[2], 5, (255,0,255), 2)
18. cv2.circle(dst, layout2[3], 5, (255,0,0), 2)
19.
20. #ground perspective
21. ground=cv2.warpPerspective(wrap_dist,h,(n,m),flags=cv2.INTER_LINEAR)
22. ground_undist=cv2.warpPerspective(wrap_undist,h1,(n,m),
23.                                 flags=cv2.INTER_LINEAR)
24. #set 20 ground points in the intersection of the slabs
25. ground_grid(ground)
26. ground_grid(ground_undist)

```

In lines 8 and 14, the homography matrixes are obtained and used to reframe the view in lines 21 and 22. Then, the ground points for the error measurement are set in lines 25 and 26, This is done throughout the following function, see Table 13.

**Table 13.** Ground grid function

```

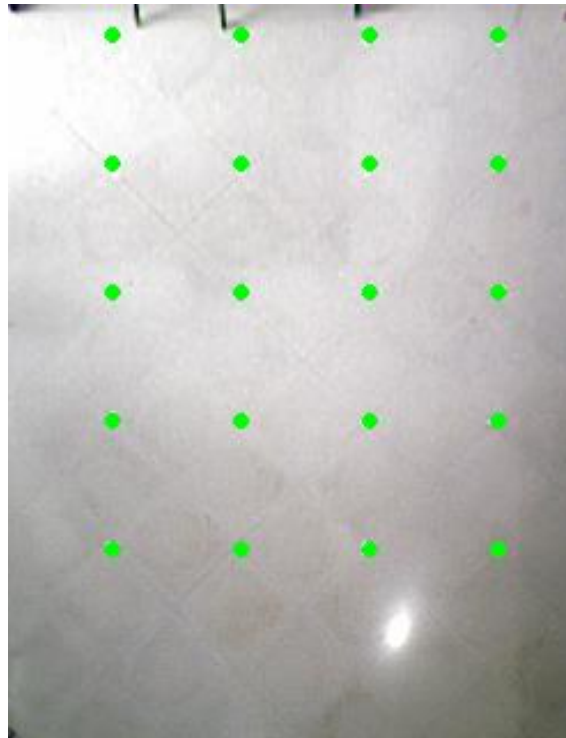
1. def ground_grid(image):
2.     pt1 = (45, 13) #offset to the first corner
3.     slab = 56
4.
5.     for row in range(0,4):
6.         for col in range(0,5):
7.             ptx = (pt1[0]+slab *row, pt1[1]+slab *col)
8.             cv2.circle(image,(int(ptx[0]),int(ptx[1])),2,(0,255,0),2)

```

Every slab is a 56 cm square, and the first corner is situated at a distance of 45 cm in the x-axis and 13 cm in the y-axis with respect the origin point, which is the top left corner of the original image. The following Fig. 40 and Fig. 41 correspond to the original image and its ground projection, while Fig. 42 and Fig. 43 correspond to the undistort ones.



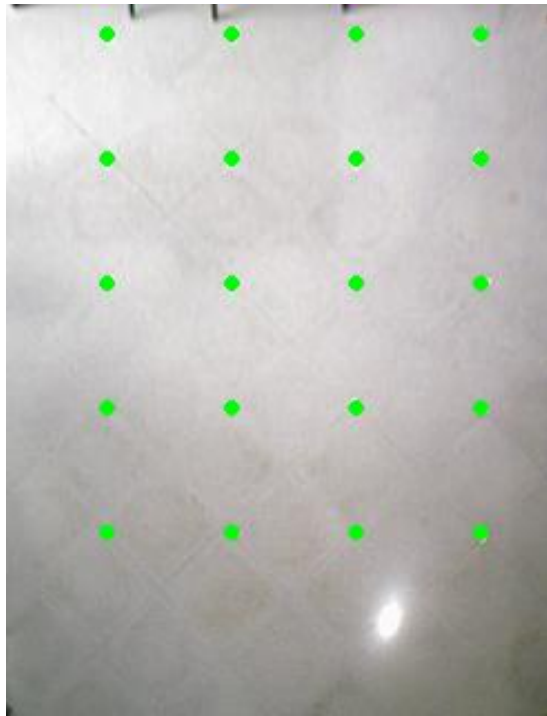
**Fig. 40.** Original image ground corners.



**Fig. 41.** Upper view of the ground after using the warpPerspective function in the original image



**Fig. 42.** Undistort image ground corners



**Fig. 43.** Upper view of the ground after using the warpPerspective function in the undistort image

For the original image, the following x and y deviations in centimeters were obtained, see Table 14. Likewise, for the undistort image those are shown in Table 15.

<b>Table 14. Original image error</b>	
$X_{dev}^{original} = \begin{bmatrix} -3 & 0 & 0 & 0 \\ -3.5 & 0 & 0 & 0 \\ 0 & 0 & 0 & 2.5 \\ 0 & 0 & 2 & 3 \\ 2 & 0 & 4.5 & 5 \end{bmatrix} ; Y_{dev}^{original} = \begin{bmatrix} 0 & 0 & 0 & 0 \\ 0 & 4 & 4 & 3.5 \\ 0 & 2.5 & 1.5 & 1.5 \\ 0 & 0 & 2.5 & 3 \\ 0 & 0 & 1 & 1.5 \end{bmatrix}$	

<b>Table 15. Undistort image error</b>	
$X_{dev}^{undistort} = \begin{bmatrix} 0 & -2 & -2 & -2 \\ 0 & 0 & 0 & 0 \\ 2.5 & 0 & 0 & 0 \\ 0 & 0 & 0 & 0 \\ 2 & 0 & 1.5 & 0 \end{bmatrix} ; Y_{dev}^{undistort} = \begin{bmatrix} -1 & -2 & -2 & -2.5 \\ -0.5 & 0 & 0 & 0 \\ -1.5 & -2.5 & -1 & -2 \\ 0 & 0 & 0 & -1.5 \\ 0 & 0 & 1 & 0 \end{bmatrix}$	

Table 16 shows the error of the ground projections.

<b>Image</b>	<b>Mean Absolute Error X axis</b>	<b>Mean Absolute Error Y axis</b>
Undistort	0.6	0.875
Original	1.275	1.25

**Table 16.** Mean absolute error of the ground projection

Since the original image had nearly zero distortion, the mean absolute error in both cases is really small. There are various points with no deviation, while the rest are deviated less than 5 centimeters in one or both axis. However, the maximum deviation reached in the original image is slightly higher. In any case, it is a good accuracy for the location estimation.

### 3.4.7. Object Detection and Tracking

The object detection is done with YOLOv5, whose model structure is the same as YOLOv4, but entirely built in Pytorch and using a focus CSPDarknet53 as backbone, see Table 17.

**Table 17.** YOLOv5m model summary

Layer (type:depth-idx)	Output Shape	Param #
Model	--	--
└─Sequential: 1	--	--
├─┬─Detect: 2	--	--
│ │ └─ModuleList: 3-1	--	343,485
├─┬─Conv: 2-1	[2, 48, 160, 160]	--
│ │ └─Conv2d: 3-2	[2, 48, 160, 160]	5,184
│ │ └─BatchNorm2d: 3-3	[2, 48, 160, 160]	96
│ │ └─SiLU: 3-4	[2, 48, 160, 160]	--
├─┬─Conv: 2-2	[2, 96, 80, 80]	--
│ │ └─Conv2d: 3-5	[2, 96, 80, 80]	41,472
│ │ └─BatchNorm2d: 3-6	[2, 96, 80, 80]	192
│ │ └─SiLU: 3-7	[2, 96, 80, 80]	--
	(...)	
├─┬─Conv: 2-22	[2, 384, 10, 10]	--
│ │ └─Conv2d: 3-59	[2, 384, 10, 10]	1,327,104
│ │ └─BatchNorm2d: 3-60	[2, 384, 10, 10]	768
│ │ └─SiLU: 3-61	[2, 384, 10, 10]	--
├─┬─Concat: 2-23	[2, 768, 10, 10]	--
├─┬─C3: 2-24	[2, 768, 10, 10]	--
│ │ └─Conv: 3-62	[2, 384, 10, 10]	295,680
│ │ └─Sequential: 3-63	[2, 384, 10, 10]	2,952,192
│ │ └─Conv: 3-64	[2, 384, 10, 10]	295,680
│ │ └─Conv: 3-65	[2, 768, 10, 10]	591,360
├─┬─Detect: 2-25	[2, 6300, 85]	--
Total params: 21,190,557		
Trainable params: 21,190,557		
Non-trainable params: 0		
Total mult-adds (G): 12.22		
Input size (MB): 2.46		
Forward/backward pass size (MB): 371.06		
Params size (MB): 84.76		
Estimated Total Size (MB): 458.28		

Fig. 44 shows a comparison of the different versions in YOLOv5.

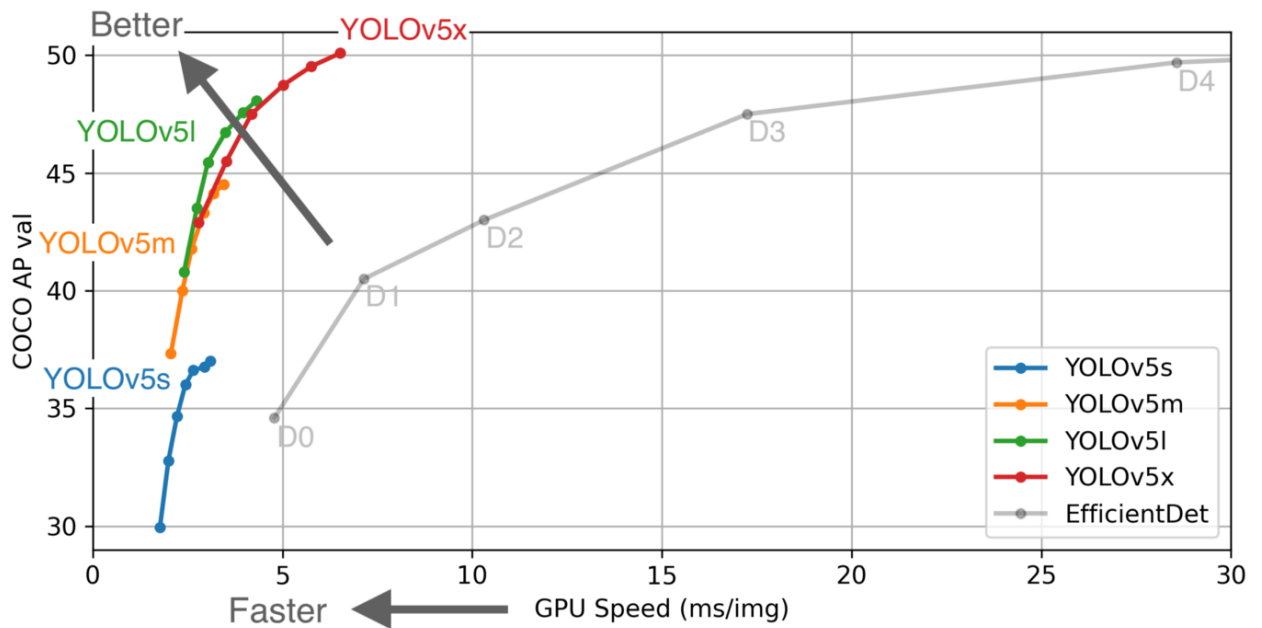


Fig. 44. YOLOv5 variants

More specifically, this project uses the weights from the variant YOLOv5m, which sets a good balance between speed and AP, as can be seen above. Its size is estimated in about 458 MB and has a total 21,190,557 trainable parameters

On the other hand, the object tracking and re-identification is done with DeepSORT in combination with OSNet, see Table 18.

Table 18. OSNet\_x0\_25 model summary

Layer (type:depth-idx)	Output Shape	Param #
OSNet	--	--
└─ConvLayer: 1-1	[2, 16, 160, 160]	--
└─┬─Conv2d: 2-1	[2, 16, 160, 160]	2,352
└─┬─BatchNorm2d: 2-2	[2, 16, 160, 160]	32
└─┬─ReLU: 2-3	[2, 16, 160, 160]	--
└─MaxPool2d: 1-2	[2, 16, 80, 80]	--
└─Sequential: 1-3	[2, 64, 40, 40]	--
└─┬─OSBlock: 2-4	[2, 64, 80, 80]	--
└─┬─┬─Conv1x1: 3-1	[2, 16, 80, 80]	288
└─┬─┬─LightConv3x3: 3-2	[2, 16, 80, 80]	432
└─┬─┬─Sequential: 3-3	[2, 16, 80, 80]	864
└─┬─┬─Sequential: 3-4	[2, 16, 80, 80]	1,296



└─Sequential: 3-5	[2, 16, 80, 80]	1,728
└─ChannelGate: 3-6	[2, 16, 80, 80]	49
└─ChannelGate: 3-7	[2, 16, 80, 80]	(recursive)
└─ChannelGate: 3-8	[2, 16, 80, 80]	(recursive)
└─ChannelGate: 3-9	[2, 16, 80, 80]	(recursive)
└─Conv1x1Linear: 3-10	[2, 64, 80, 80]	1,152
└─Conv1x1Linear: 3-11	[2, 64, 80, 80]	1,152
└─OSBlock: 2-5	[2, 64, 80, 80]	--
└─Conv1x1: 3-12	[2, 16, 80, 80]	1,056
└─LightConv3x3: 3-13	[2, 16, 80, 80]	432
└─Sequential: 3-14	[2, 16, 80, 80]	864
└─Sequential: 3-15	[2, 16, 80, 80]	1,296
└─Sequential: 3-16	[2, 16, 80, 80]	1,728
└─ChannelGate: 3-17	[2, 16, 80, 80]	49
└─ChannelGate: 3-18	[2, 16, 80, 80]	(recursive)
└─ChannelGate: 3-19	[2, 16, 80, 80]	(recursive)
└─ChannelGate: 3-20	[2, 16, 80, 80]	(recursive)
└─Conv1x1Linear: 3-21	[2, 64, 80, 80]	1,152
	(...)	
└─Conv1x1: 1-6	[2, 128, 20, 20]	--
└─Conv2d: 2-12	[2, 128, 20, 20]	16,384
└─BatchNorm2d: 2-13	[2, 128, 20, 20]	256
└─ReLU: 2-14	[2, 128, 20, 20]	--
└─AdaptiveAvgPool2d: 1-7	[2, 128, 1, 1]	--
└─Sequential: 1-8	[2, 512]	--
└─Linear: 2-15	[2, 512]	66,048
└─BatchNorm1d: 2-16	[2, 512]	1,024
└─ReLU: 2-17	[2, 512]	--
-----		
Total params: 201,864		
Trainable params: 201,864		
Non-trainable params: 0		
Total mult-adds (M): 514.20		
=====		
Input size (MB): 2.46		
Forward/backward pass size (MB): 249.06		
Params size (MB): 0.81		
Estimated Total Size (MB): 252.32		
=====		

The OSNet model chosen for the re-identification task is its tiniest version, OSNet\_x0\_25. In the above table, it can be seen that it has a size of 252 MB and a total of 201.864 trainable parameters. Both detection and tracking models, are already trained in humans with the COCO VOC Dataset.

### 3.4.8. Google Colaboratory implementation

As mentioned previously, this object detector and tracker is taken from a public repository from Mikel Brostrom, so the first step is to clone the repository and install the dependencies. The following code from Table 19, corresponds to the first cell from Google Colaboratory.

**Table 19.** Cloning repository.

```
1. !git clone -recurse-
   submodules https://github.com/mikelbrostrom/Yolov5_DeepSort_OSNet.git
2. # clone repo
3. %cd Yolov5_DeepSort_OSNet
4. %pip install -qr requirements.txt # install dependencies
```

Now, to get the actual position of the detections, it is made the assumption that the middle point of the width and the highest value of the height, corresponds to the standing point of the human in the image, which is the closer location to the feet. Table 20 shows the calculation of this standing point.

**Table 20.** Standing point calculation.

```
1. # draw boxes for visualization
2. if len(outputs[i]) > 0:
3.     for j, (output) in enumerate(outputs[i]):
4.
5.         bboxes = output[0:4]
6.         id = output[4]
7.         cls = output[5]
8.         conf = output[6]
9.
10.    if save_txt:
11.        # to MOT format
12.        bbox_left = output[0]
13.        bbox_top = output[1]
14.        bbox_w = output[2] - output[0]
15.        bbox_h = output[3] - output[1]
16.        bbox_groundx = bbox_w/2 + output[0]
17.        bbox_groundy = output[3]
18.        # Write MOT compliant results to file
19.        with open(txt_path + '.txt', 'a') as f:
20.            f.write('%g ' * 10 + '\n') % (frame_idx + 1, id,
21.                bbox_groundx, bbox_groundy, bbox_w, bbox_h))
```

In the following table, it can be seen a modified fragment from the track.py file from Yolov5\_DeepSort\_OSNet folder obtained after cloning the repository. Here, the variables from lines 12 and 13 were stored in line 21, line 206 of the original code. However, since the needed values are the ones corresponding to the standing point of the object detected, the variables calculated in lines 16 and 17 are saved instead.

To run the model, it can be done throughout the track.py file, see Table 21.

**Table 21.** Running command.

```
1. !python track.py --yolo_model yolov5m.pt
2.                   --source '/content/drive/MyDrive/TFG/prueba0/*'
3.                   --save-vid
4.                   --save-txt
5.                   --classes 0
```

By default, the weights from YOLOv5s and OSNet\_x0\_25 are set. Therefore, the YOLO model is changed to YOLOv5m, whereas the DeepSORT model is left by default. Likewise, there are many other default parameters that can be changed by typing some commands in the running line. In this case, the detections are limited to the class 0 corresponding to humans, and the commands --save-vid and --save-txt are specified so that the video and text record could be obtained. In relation to the text record, the information is stored in rows per detection, as seen in table 18. The first two positions of each row, corresponding to the frame number and tracking id of the object detected, and the next four, to the standing x and y points, and the width and height lengths of the bounding box respectively.

To end the section, it is important to mention another set of parameters corresponding to the DeepSORT configuration file, see Table 22.

**Table 22.** DeepSORT configuration file.

```
1. DEEPSORT:
2. MODEL_TYPE: "osnet_x_25"
3. MAX_DIST: 0.2
4. MAX_IOU_DISTANCE: 0.7
5. MAX_AGE: 30
6. N_INIT: 3
7. NN_BUDGET: 100
```

Here, in lines 3, 4 and 5, it is set a maximum distance for the ID matching of 0.2, an IOU threshold of 0.7 and 30 frames of ID storing after losing the detection. Furthermore, the minimum number of matching frames for considering a valid ID is set to 3 and the maximum size of the appearance descriptor is fixed to 100.

### 3.4.9. Tracking preparation

Finally, the last step is to use these results to set the orientation of the safety zones for the collision alerting.

To do so, the tracking file is loaded, split and saved as a numpy array. Then, this array is split into another two, so that the frame numbers and detection information could be separated, see the following code from Table 23.

**Table 23.** Detection array preparation 1.

```
1. #import object detection info
2. f = open('detections/test3/tracks/prueba3.txt').read()
3. detections = f.split('\n')[:-1]
4.
5. record = np.zeros((len(detections),6))
6. for i, rec in enumerate(detections):
7.     rec = np.array(rec.split())
8.     record[i:] = rec
9.
10. #prepare the number tracks per frames
11. frames = np.array([np.array(list(j)).astype(int) for i, j in
12. groupby(record[:,0])], dtype=object)
13. max_detects = max([len(frame) for frame in frames])
14.
15. ground_points = record[:,1:].astype(int)
16. tracks = np.zeros((3,frames.shape[0], max_detects), dtype = object)
```

In line 3, the tracking record is split per row, but it is also needed to split the columns, which are 6. This is done in the for loop from line 6. Then, once this process has finished, the frames, whose number is the same, are clustered together. The objective here, is to separate the detections that were done at each frame. After that, the maximum number of detections made at certain point and the number of frames, are used to define a 3-Dimensional array. This array, containing the ground location of all the human detections at each frame and their corresponding ID.

Table 24 shows the last part of the tracking array preparation.

**Table 24.** Detection array preparation 2.

```
1. row = 0
2. for n1, frame in enumerate(frames):
3.     ids = list(ground_points[row:row+len(frame),0])
4.     tx = list(ground_points[row:row+len(frame),1])
5.     ty = list(ground_points[row:row+len(frame),2])
6.
7.     tracks[0,n1,:len(frame)] = tx
8.     tracks[1,n1,:len(frame)] = ty
9.     tracks[2,n1,:len(frame)] = ids
```

```

10.
11. if len(frame) < max_detects:
12.     tracks[0,n1,len(frame):] = np.nan
13.     tracks[1,n1,len(frame):] = np.nan
14.     tracks[2,n1,len(frame):] = np.nan
15.     row += len(frame)

```

Depending on the length of each frame, there will be more or less detections. This information is used to separate the IDs, as well as the ground locations, as it can be seen in lines 3,4 and 5 from the above code. However, due to the fact that number of columns is fixed to a maximum value, in case of less number of detections, the last position is always set to a None value, see line 11.

### 3.4.10. Local plane coordinates calculation.

Now, in Table 25 the real coordinates are obtained from the ground projections.

**Table 25.** Real coordinates calculation in the main code.

```

1. images = glob.glob('tests/prueba3/*.png')
2. images = natsort.natsorted(images)[6:]
3. for i, image in enumerate(images):
4.
5.     if i <= tracks.shape[1]-1:
6.         img = cv2.imread(image)
7.         ground = np.zeros_like(img)
8.         ground=cv2.warpPerspective(ground, h,(n,m), flags=cv2.INTER_LINEAR)
9.
10.        for person in range(0,len(frames[i])):
11.            if np.isnan(tracks[0,i,person]) != True:
12.
13.                x = tracks[0,i,person]
14.                y = tracks[1,i,person]
15.                id = tracks[2,i,person]
16.
17.                xy_pixels = np.array([x,y],dtype=int)
18.
19.                xyreal = real_coords(xy_pixels,h)
20.                xyreal = xyreal.reshape(1,2).astype(int)[0]
21.
22.                cv2.circle(img, xy_pixels, 2, (0,0,255),2)

```

After the tracking array preparation, the ground location of each detection is got, see lines 10 to 15. This location is converted to the ground projection throughout the homography matrix, as mentioned in section 3.4.4. For that reason, the function in line 19 is defined as follows in Table 26.

**Table 26.** Real coordinates function definition

```

1. def real_coords(px1_point,h):
2.   coords = np.array([[px1_point[0]], [px1_point[1]], [1]])
3.
4.   real_coords = np.dot(h, coords)
5.   real_coords = real_coords/real_coords[2]
6.   return real_coords[:2]

```

Notice that, as it was shown in formula 34, to get the new positions the coordinates are divided by the z value. Now, these real coordinates can be used to get direction of the human detected.

### 3.4.11. Safety areas calculation

Table 27 correspond to the obtention of the security areas.

**Table 27.** Safety area calculation in the main code

```

1.   if id not in tracks_dict.keys():
2.     tracks_dict[id] = xyreal
3.
4.   else:
5.     t1 = tracks_dict[id]
6.     t2 = xyreal
7.     tracks_dict[id] = xyreal
8.
9.     xy_edges,xy_half_edges = limits_safety_zone(t2, t1, ground)
10.    tracks_edges[id] = xy_edges, xy_half_edges
11.    cv2.circle(ground, xyreal, 2, (0,0,255),2)

```

First of all, two locations are needed, for that reason, an if-else conditional is set to check whether or not the algorithm has seen the current identity of the loop. In case of a new identity, its first location is stored, otherwise, both previous and current positions are named as t1 and t2, see lines 5 and 6. Then, a circular sector of 50 degrees is got in the same direction of the movement. This sector is obtained throughout the function defined in line 9, see Table 28.

**Table 28.** Safety areas function definition.

```

1. def limits_safety_zone(xyreal_t2,xyreal_t1, ground):
2.   xydiag = xyreal_t2 - xyreal_t1
3.
4.   diag = np.sqrt(xydiag[0]**2 + xydiag[1]**2)
5.   x = xydiag[0]
6.   y = xydiag[1]
7.
8.   if diag==0:

```

```

9.     return [],[]
10.
11. theta = math.acos(x/diag)
12. theta = theta*180/math.pi
13.
14. if (x >= 0 and y >= 0) or (x <= 0 and y >= 0): #1 quadrant(4), 2 quadrant(3)
15.     start2 = 335-theta
16.     end2 = start2 + 50
17.
18. else: #3 quadrant(2), #4 quadrant(1)
19.     start2 = theta - 25
20.     end2 = start2 + 50
21.
22. xy_edges = np.zeros((int(int(end2)-int(start2-1)), 2))
23. xy_half_edges = np.zeros_like(xy_edges)
24.
25. for i,angle in enumerate(range(int(start2),int(end2))):
26.     rads = angle*(math.pi/180)
27.
28.     # external edge
29.     xedge = xyreal_t2[0] + 100 *np.cos(rads)
30.     yedge = xyreal_t2[1] - 100 *np.sin(rads)
31.
32.     xy=np.array([int(xedge),int(yedge)])
33.     xy_edges[i,:] = xy
34.
35.     # middle edge
36.     xedge = xyreal_t2[0] + 50*np.cos(rads)
37.     yedge = xyreal_t2[1] - 50*np.sin(rads)
38.
39.     xy_half=np.array([int(xedge),int(yedge)])
40.     xy_half_edges[i,:] = xy_half
41.
42.     cv2.circle(ground, xy,2,(255,255,0),2)
43.     cv2.circle(ground, xy_half,2,(0,0,255),2)
44.
45. return xy_edges, xy_half_edges

```

Here, the distance from t1 to t2 is calculated, but if t1 and t2 are equals, then two empty lists are returned, see line 9. Nevertheless, when these two variables are different, the angle of displacement is obtained as the arccosine of the triangle formed between these two points. This angle is eventually used to get the starting and ending points with respect to that orientation, see lines 11 to 20.

Finally, a set points with a separation of one degree each, are situated at two different radius of distance. These two radius corresponding to the limits of the security area, one being the half of the other. In this case, since the ground area is not so big, this radius is set to one meter long. Notice

that in lines 30 and 37, the radius is subtracted from the current y position instead of being added. This is due to the fact, that the y-axis of the window grows downward.

### 3.4.12. System of Alerts.

Finally, the alerting system is defined in Table 29.

**Table 29.** Alerting system in the main code.

```
1.     ids = tracks[2,i,:]
2.     for id_list in ids:
3.         if id_list in tracks_edges.keys() and id != id_list:
4.             alert = alerts(tracks_edges, alert, id, id_list)
5.             #actual id of the loop, other ids
6.
7.             if alert[2][id] >= 6:
8.                 print('ALERT 2: imminent collision for object {}'.format(id) )
9.                 cv2.putText(img, 'ALERT', (50, 50), cv2.FONT_HERSHEY_SIMPLEX, 1,
10.                    (0, 0, 255), 2, cv2.LINE_AA)
11.            elif alert[1][id] >= 6:
12.                print('ALERT 1: object {} is on the way to collide
13.                    alert'.format(id) )
14.                cv2.putText(img, 'ALERT', (50, 50), cv2.FONT_HERSHEY_SIMPLEX, 1,
15.                    (0, 255, 255), 2, cv2.LINE_AA)
16.            elif alert[0][id] >= 6:
17.                print('ALERT 0: object {} has someone close, take care'.format(id))
18.                cv2.putText(img, 'ALERT', (50, 50), cv2.FONT_HERSHEY_SIMPLEX, 1,
19.                    (0, 255, 0), 2, cv2.LINE_AA)
```

For the alerting system, there are three different alerts depending on the distance between the limits of the security areas. In lines 7, 11, and 15, it is showed that they are named as ALERT 2, ALERT 1 and ALERT 0 respectively, for which the danger increases with the number of the alert.

The alerts are given throughout the alert function in line 4, see Table 30. It takes as inputs a dictionary with the arrays containing the limits of the safety areas of each individual, the previous alert dictionary, the current id, and an id from the list of identities seen in that instance. The idea is to compare the position of the current safety area with the rest of areas from the map, so that the system could know which identity is in danger with which other. Besides, it is set a minimum number of 6 consecutive alerts, to avoid fake warnings. he alert function definition.

**Table 30.** Alerting system function definition.

```
1. def alerts(tracks_edges, alert, id, id_list):
2.     alrt_ID0 = alert[0]
3.     alrt_ID1 = alert[1]
4.     alrt_ID2 = alert[2]
```



```

5.
6. id_xyedges, id_xy_halfedges = tracks_edges[id]
7. id_list_xyedges, id_list_xy_halfedges = tracks_edges[id_list]
8.
9. if len(id_xyedges) == len(id_list_xyedges) and len(id_xyedges) != 0:
10.
11.     distance_far_edges = id_xyedges - id_list_xyedges
12.     distance_farclose_edges_1 = id_xyedges - id_list_xy_halfedges
13.     distance_farclose_edges_2 = id_xy_halfedges - id_list_xyedges
14.
15.     euclid_far_distance = np.sqrt(distance_far_edges[:,0]**2 +
16.                                   distance_far_edges[:,1]**2)
17.     euclid_farclose_distance_1 = np.sqrt(distance_farclose_edges_1[:,0]**2 +
18.                                           distance_farclose_edges_1[:,1]**2)
19.     euclid_farclose_distance_2 = np.sqrt(distance_farclose_edges_2[:,0]**2 +
20.                                           distance_farclose_edges_2[:,1]**2)
21.
22.     dist_mean_far = np.mean(euclid_far_distance)
23.     dist_mean_farclose_1 = np.mean(euclid_farclose_distance_1)
24.     dist_mean_farclose_2 = np.mean(euclid_farclose_distance_2)
25.
26.     if dist_mean_farclose_2 < 50 or dist_mean_farclose_1 < 50 :
27.
28.         #ALERTS 2
29.         if id not in alrt_ID2.keys():
30.             alrt_ID2[id] = 1
31.             alert[2] = alrt_ID2
32.         else:
33.             n = alrt_ID2[id]
34.             n += 1
35.             alrt_ID2[id] += n
36.             alert[2] = alrt_ID2
37.
38.     elif dist_mean_far < 90:
39.
40.         #ALERTS 1
41.         if id not in alrt_ID1.keys():
42.             alrt_ID1[id] = 1
43.             alert[1] = alrt_ID1
44.
45.         else:
46.             n = alrt_ID1[id]
47.             n += 1
48.             alrt_ID1[id] += n
49.             alert[1] = alrt_ID1
50.
51.     elif dist_mean_far < 120:
52.         #ALERTS 0
53.         if id not in alrt_ID0.keys():
54.             alrt_ID0[id] = 1
55.             alert[0] = alrt_ID0

```

```

56.
57.     else:
58.         n = alrt_ID0[id]
59.         n += 1
60.         alrt_ID0[id] += n
61.         alert[0] = alrt_ID0
62.     else:
63.         alrt_ID0[id] = 1
64.         alrt_ID1[id] = 1
65.         alrt_ID2[id] = 1
66.
67.         alert[0] = alrt_ID0
68.         alert[1] = alrt_ID1
69.         alert[2] = alrt_ID2
70.
71.     else:
72.         alrt_ID0[id] = 1
73.         alrt_ID1[id] = 1
74.         alrt_ID2[id] = 1
75.         alert[0] = alrt_ID0
76.         alert[1] = alrt_ID1
77.         alert[2] = alrt_ID2
78.
79.     return alert

```

Here, the Euclidean distances between the external, and between the external and internal limits of the security areas are calculated. After that, the mean of each set of distances is obtained and the results are used to get a rough estimation of the overall distance, see lines 22, 23 and 24. Considering the distances between the external and internal boundaries as the most important, if any of those values is less than 50 cm, it would mean that the hazard of collision is higher than any other. Likewise, if the distance is not that close, but the external limits are less than 90 cm, then, a medium alert in the scale of danger is given, whereas if the distance is in between 90 and 120, the alert is just a suggestion of velocity moderation, because another human is close.

On the other hand, the count in the number of consecutive alerts is done individually at each level of danger. If the dictionary of a certain alert for the given current id has saved that id previously, its value is incremented, otherwise is set to one. Moreover, the count of the three types of alerts is reset for the given id every time that there is not a hazard, what forces a minimum continuity to avoid fake warnings, see lines 72 to 77. These three dictionaries are saved within another dictionary named as alert, which is the output of the function. Now that this function is clearer, it is better understood the alerting system from Table 30.

### 3.5. Experimental Investigation.

To evaluate the collision avoidance system, four tests for which the distortion has been corrected have been recorded. In these tests, the trajectories are within the boundaries of the area defined previously, i.e. a rectangle of 246 cm width and 320 cm height. The first two tests, correspond to a

single person walk and there are a total number of 465 and 617 frames, whereas for the remaining two, there are two people at the same time and a total 707 and 419 frames respectively.

The following figures, Fig. 45 and Fig. 46, are examples of the image acquisition process.



**Fig. 45.** Frames from test 1, on the left, and test 2, on the right.



**Fig. 46.** Frames from test 3, on the left, and test 4, on the right.

As mentioned previously, the detections are done in Google Colaboratory with the weights from the YOLOv5m model and OSNet\_x0\_25. Likewise, the DeepSORT configuration file is set as it was showed in table 20.

Some examples of human detections are presented in Fig. 47 and Fig. 48, followed by an extract of the 20 firsts detections made at each test in Tables 31, 32, 33 and 34.



**Fig. 47.** Detection examples from test 1, on the left, and test 2, on the right.



**Fig. 48.** Detection examples from test 3, on the left, and test 4, on the right.

**Table 31.** Test 1. Detections from the 20 firsts frames

1. 3 1 388 475 260 391
2. 4 1 384 474 256 400
3. 5 1 380 476 250 408
4. 6 1 376.5 477 233 415
5. 7 1 374 478 220 424
6. 8 1 371.5 478 205 437
7. 9 1 367.5 479 201 448
8. 10 1 363.5 477 199 451
9. 11 1 360.5 476 197 455
10. 12 1 357 464 200 455
11. 13 1 359 451 194 449
12. 14 1 361 448 194 448
13. 15 1 363 446 192 446
14. 16 1 368.5 445 191 445
15. 17 1 375 445 190 445
16. 18 1 385.5 444 189 444
17. 19 1 394.5 440 187 440
18. 20 1 401.5 429 185 429

**Table 32.** Test 2. Detections from the 20 first frames

1. 1 281.5 478 349 207
2. 4 1 290 478 336 221
3. 5 1 300 478 336 234
4. 6 1 307 478 334 243
5. 7 1 313 479 332 251
6. 8 1 320.5 478 325 260
7. 9 1 330 478 320 268
8. 10 1 340.5 478 317 276
9. 11 1 355 479 316 282
10. 12 1 365.5 479 313 284
11. 13 1 382 479 314 284
12. 14 1 397 479 310 286
13. 15 1 404 479 310 288
14. 16 1 406.5 479 309 289
15. 17 1 409.5 479 299 294
16. 18 1 409 479 298 300
17. 19 1 406 479 290 310
18. 20 1 398.5 479 245 343

**Table 33.** Test 3. Detections from the 20 first frames.

1. 3 1 167.5 478 311 302
2. 3 2 587.5 356 103 355
3. 4 1 166.5 478 311 306
4. 4 2 583 351 112 350
5. 5 1 166 479 312 308
6. 5 2 578.5 344 121 343
7. 6 1 166 479 308 307
8. 6 2 575.5 340 127 340
9. 7 1 164.5 479 301 307
10. 7 2 572.5 338 133 338
11. 8 1 164.5 479 293 306
12. 8 2 570 336 138 335
13. 9 1 164 479 280 308
14. 9 2 568 335 142 333
15. 10 1 162 479 268 312
16. 10 2 567.5 333 143 331
17. 11 1 161.5 479 253 319
18. 11 2 567.5 332 141 329
19. 12 1 160.5 479 247 327
20. 12 2 568 332 140 329
21. 13 1 158.5 478 231 336
22. 13 2 568.5 331 139 328
23. 14 1 154.5 479 207 354
24. 14 2 568.5 332 141 328
25. 15 1 152 478 204 363
26. 15 2 568 332 142 326
27. 16 1 150 478 186 375
28. 16 2 568.5 333 141 324
29. 17 1 148 478 184 388
30. 17 2 568.5 334 139 328
31. 18 1 146 479 190 396
32. 18 2 568.5 335 141 333
33. 19 1 145.5 479 267 421
34. 19 2 568 335 142 329
35. 20 1 139 479 270 432
36. 20 2 568.5 335 139 332

**Table 34.** Test 4. Detections from the 20 first frames.

1. 1 136 479 264 336
2. 2 540 308 144 307
3. 4 1 127.5 479 247 350
4. 4 2 544.5 304 151 303
5. 5 1 116.5 479 227 364
6. 5 2 547 303 154 301
7. 6 1 108 479 216 372
8. 6 2 548.5 302 157 300
9. 7 1 95.5 479 187 381
10. 7 2 548.5 300 157 298
11. 8 1 96 479 192 391
12. 8 2 548 298 154 297
13. 9 1 93.5 479 187 400
14. 9 2 545.5 297 147 296
15. 10 1 95 479 190 406
16. 10 2 543.5 298 145 297
17. 11 1 97 479 194 411
18. 11 2 542.5 298 145 298
19. 12 1 100.5 478 201 419
20. 12 2 542 298 144 298
21. 13 1 102.5 478 205 428
22. 13 2 542 297 142 297
23. 14 1 103.5 479 207 434
24. 14 2 541 298 140 298
25. 15 1 110.5 479 221 436
26. 15 2 541.5 299 143 299
27. 16 1 117 479 234 438
28. 16 2 542.5 301 147 301
29. 17 1 120.5 479 241 439
30. 17 2 543 303 146 303
31. 18 1 123 479 246 441
32. 18 2 543.5 304 147 304
33. 19 1 125 478 250 450
34. 19 2 545 304 152 304
35. 20 1 126 478 252 454
36. 20 2 546.5 305 153 305

Some information can be extracted from the detections made. In all the cases, the detection confidence is above 80%, even if the most distant individuals cannot be fully seen.

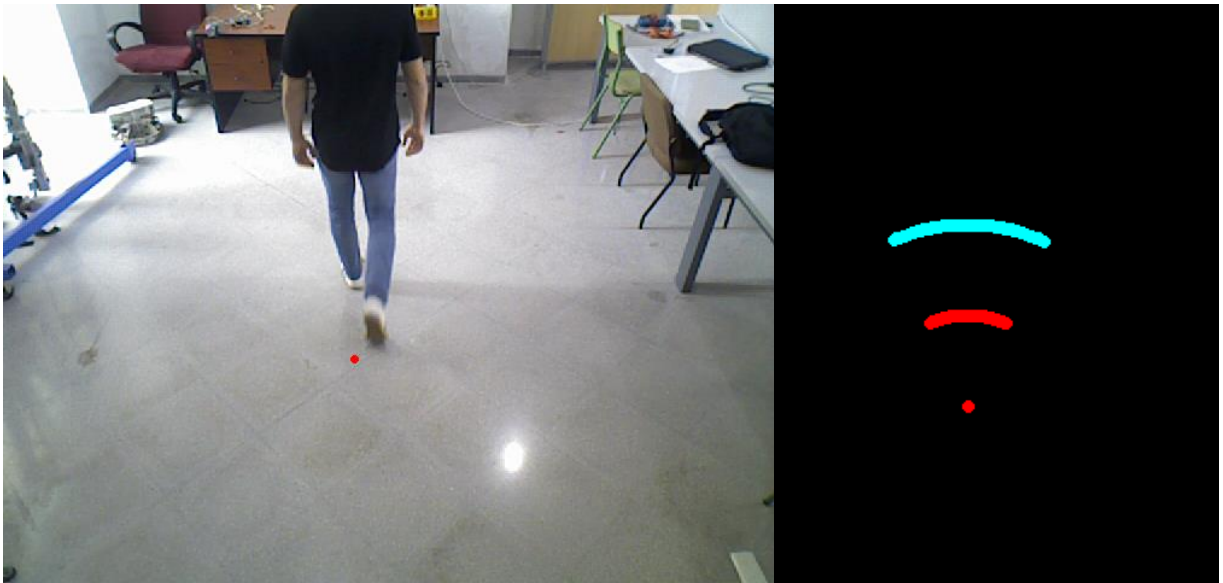
On the other hand, the tracking identities of test 3 and 4, remained the same during the first 20 frames. However, DeepSORT eventually ended switching these identities due to some long occlusions occurred during both tests. In test 3, these identities ended as human 3 and human 8, while in test 4, the identities ended as human 3 and human 5 respectively. Nevertheless, this was not a problem, since after each switch, that identity remained enough time.

With respect to the visualization of the standing points and safety areas, as it was mentioned previously, there are two radii of danger, one being the half of the other, where the longest radius is one-meter long. Here, there are some examples from each test, see Fig. 49, Fig. 50, and Fig. 51.

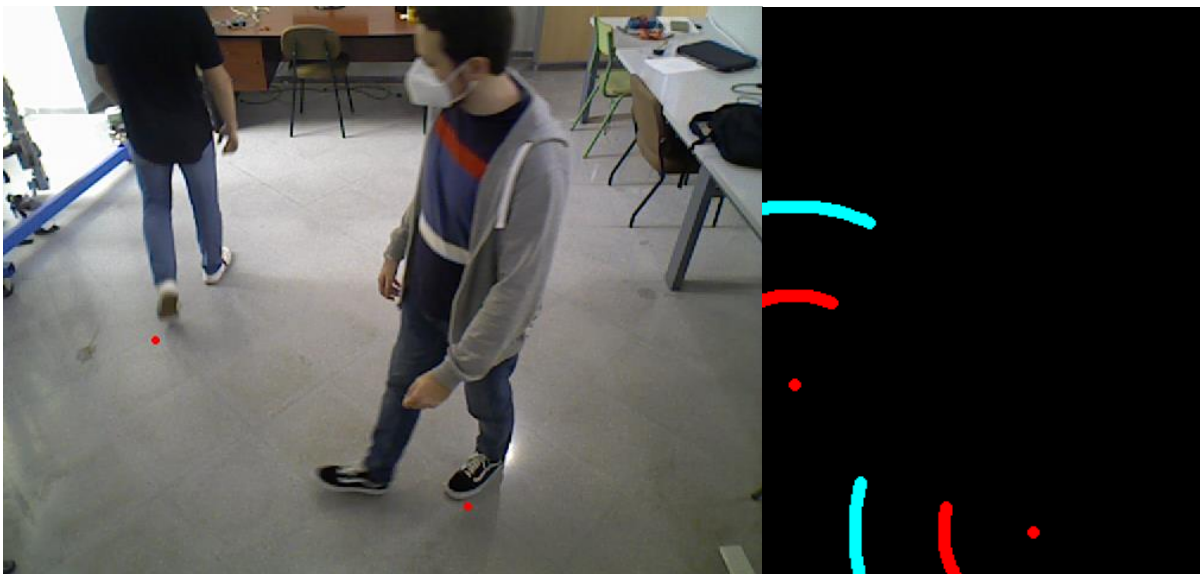


**Fig. 49.** Test 1 localization.





**Fig. 50.** Test 2 localization.






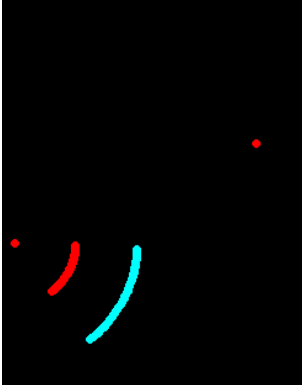
**Fig. 51.** Test 3 localization.


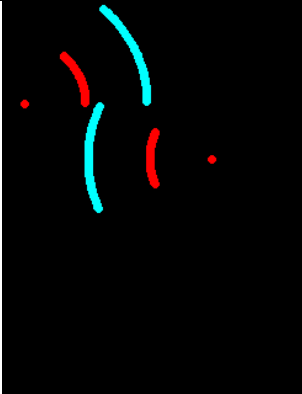
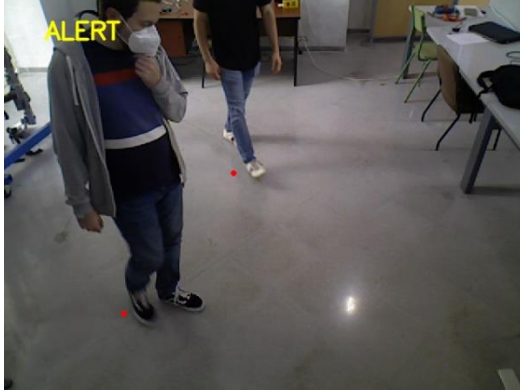
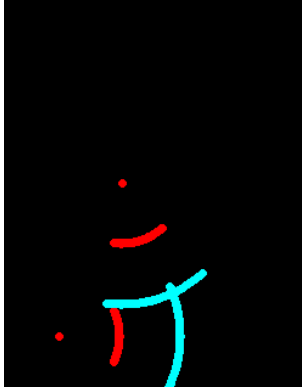

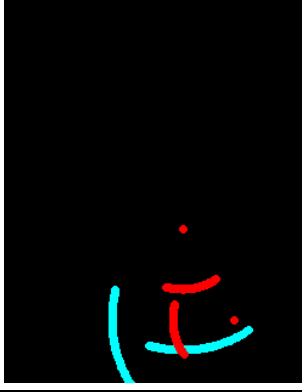




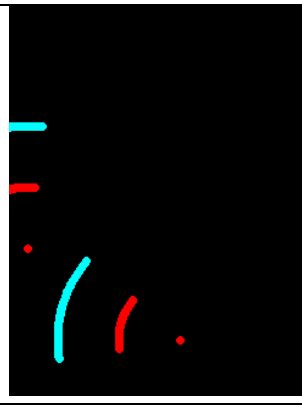
**Fig. 52.** Test 4 localization.

Finally, three types of warning are given depending on the distance and trajectory of the individuals, as it was explained in section 3.4.12. In Tables 35 and 36, the results obtained for the dangerous situations in both test 3 and 4 are shown, where the type-0 is drawn in green letters, type-1 in yellow and type-2 in red.

**Table 35.** Warnings from test 3






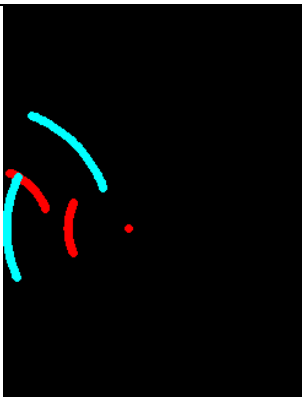

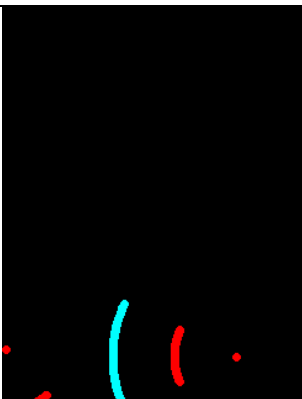
Image	Ground	Type and Frame
		Type-0. Frame 33.
		Type-0. Frame 118.

		<p>Type-1. Frame 231.</p>
		<p>Type-1. Frame 237.</p>
		<p>Type-2. Frame 478.</p>
		<p>Type-1. Frame 533.</p>

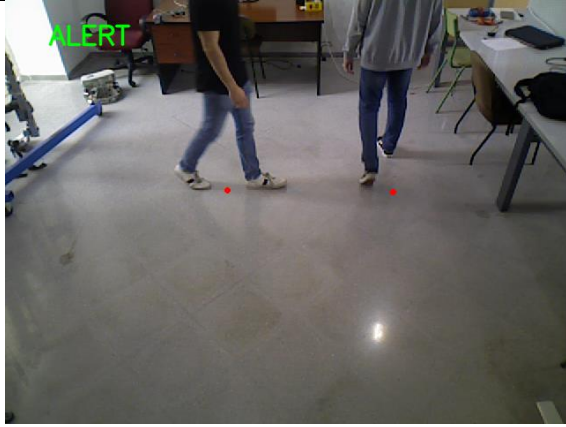






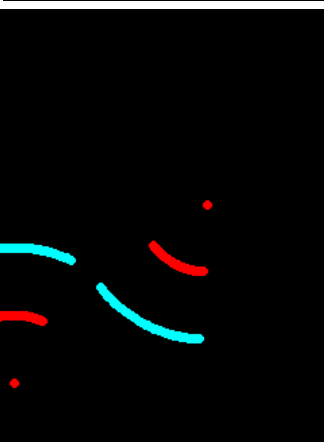


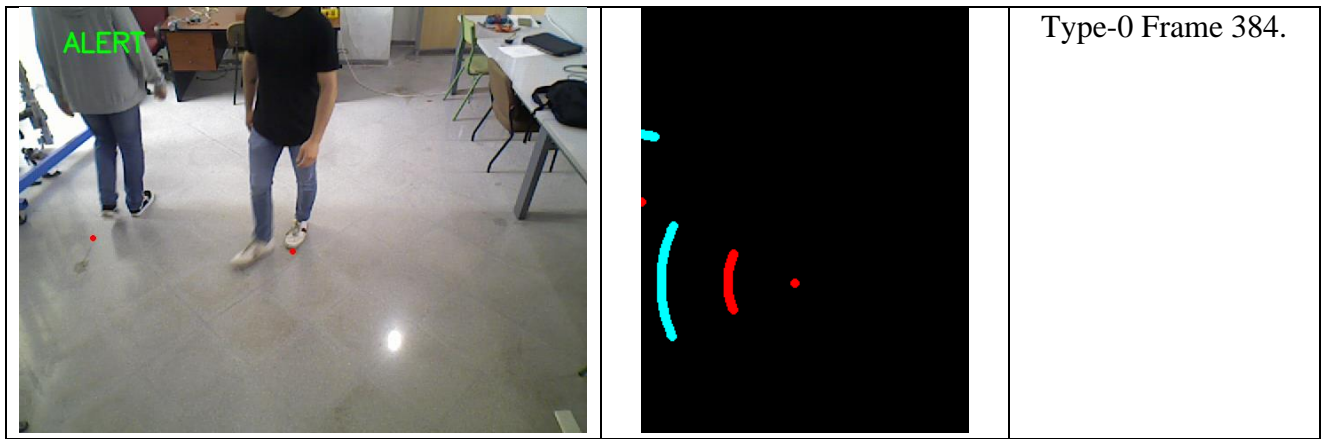
Type-2. Frame 538.

**Table 36.** Warnings from test 4

		Type-0. Frame 13.
		Type-0. Frame 117.
		Type-2. Frame 124.
		Type-0. Frame 197.

		<p>Type-2. Frame 206.</p>
		<p>Type-1. Frame 241.</p>
		<p>Type-1. Frame 249.</p>
		<p>Type-1 Frame 261.</p>

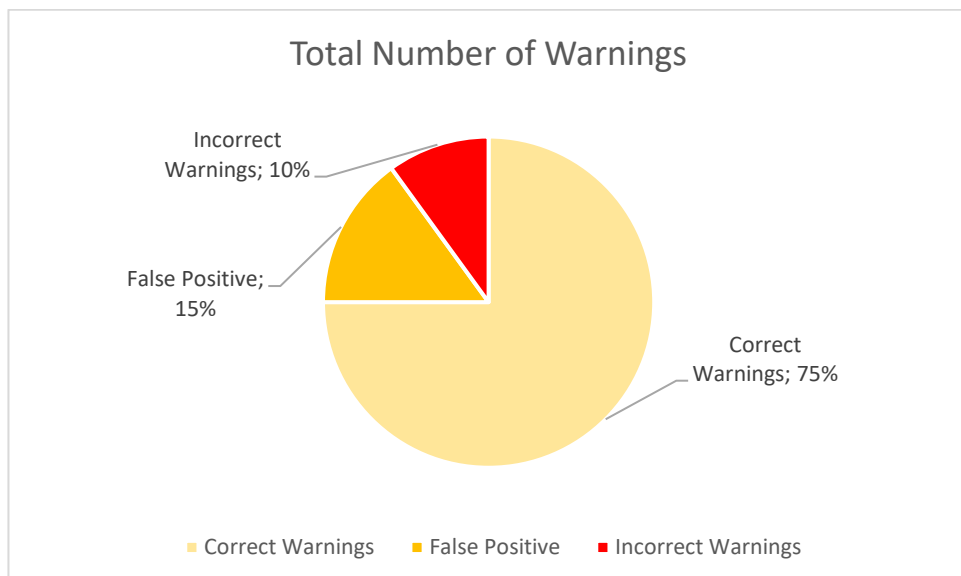
		<p>Type-0 Frame 268.</p>
		<p>Type-0 Frame 292.</p>
		<p>Type-2 Frame 310.</p>
		<p>Type-1 Frame 367.</p>



There are a total of 7 situations in which the algorithm returned an alert on test 3, and a total of 13 on test 4. In test 3, there is just one error, which is in frame 118. Here, there is a false positive from a type-0 alert. Likewise, the same error occurred in frames 241 and 292 from test 4, for which a type-1 and type-0 alerts were given respectively.

On the other hand, the situation in frame 268 from test 4 was set as a type-0 alert, when it was a type-2 situation. Something similar can be said from the frame 367, where a type-1 alert was given for a type-0 situation.

Therefore, there are a total of 20 alerts, for which 3 were not needed, and 2 returned the wrong type of alert. From these errors, the most important is the error on frame 267, which is classifying the situation as less dangerous than it is.



**Fig. 53.** Pie chart of warnings.

On the other hand, the safety areas sometimes are slightly shifted to a different sight, but in general terms, it has a good performance.



These results can be completely extrapolable for human-vehicles and vehicles-vehicles situations, if the detection model is trained in forklifts. Likewise, the security areas can be easily extended considering bigger angles and longer radius. Therefore, as a future work, I would like to improve the performance on the orientation of the security areas, as well as testing the algorithm in real-time, and train the detection model to be able of recognizing these type of vehicles, which in conclusion, is translated into a more robust collision avoidance algorithm.

## Conclusions

1. The aim of the project is achieved throughout two test, on which two people have walked around a predefined area simulating possible collision situations. Here, the algorithm, has been able to effectively classify most of them with the correct type of alert, depending on the distance between the individuals appeared.
2. After reading and comparing the performances in terms of speed and accuracy of several object detection models, the usage of YOLO instead of any other was a key factor. Even though it was not test in real time, YOLOv5 is extremely fast and allow a real-time implementation, which is crucial for this problematic.
3. The researches done in chapters 3, 4 and 5, were essential to understand the basis of a CNN, as well as the fundamentals of an object detector and object tracker respectively.
4. Due to the hardware limitations, Google Colaboratory helped to obtain the detection and tracking files needed for the development of the project. Therefore, it was another key factor in this project.
5. The collision avoidance algorithm has demonstrated to perform accurately, correctly returning a warning for all the 17 situations with a real hazard of collision, although one of those was classified as less dangerous.
6. According to the goal of the project, these results can be use for future work safety developments in the manufacturing industry.

## List of references

- [1] «Powered Industrial Truck Operator Training,» 14 03 1995. [On Line]. Available: <https://www.osha.gov/laws-regs/federalregister/1995-03-14>.
- [2] «Occupational Injuries, Illnesses, and Fatalities Involving Forklifts,» 10 6 2019. [On Line]. Available: <https://www.bls.gov/iif/oshwc/foi/forklifts-2017.htm>.
- [3] «Intel,» [On Line]. Available: [https://www.intel.com/content/www/us/en/robotics/autonomous-mobile-robots/overview.html#:~:text=An%20autonomous%20mobile%20robot%20\(AMR\)%20is%20a%20type%20of%20robot,to%20a%20fixed%2C%20predetermined%20path..](https://www.intel.com/content/www/us/en/robotics/autonomous-mobile-robots/overview.html#:~:text=An%20autonomous%20mobile%20robot%20(AMR)%20is%20a%20type%20of%20robot,to%20a%20fixed%2C%20predetermined%20path..)
- [4] E. Romaine, «Conveyco,» 27 August 2020. [On Line]. Available: <https://www.conveyco.com/types-and-applications-of-amrs/>.
- [5] «Viatech,» [On Line]. Available: <https://www.viatech.com/en/products/ai-systems/mobile360-forklift-safety-system/>.
- [6] «Bigmate,» [On Line]. Available: <https://bigmate.com.au/technologies/computer-vision/>.
- [7] V. Staff, «VentureBeat,» 29 September 2020. [On Line]. Available: <https://venturebeat.com/2020/09/29/applying-machine-learning-to-keep-employees-safe-and-save-lives/>.
- [8] «IBM,» [On Line]. Available: <https://www.ibm.com/topics/computer-vision>.
- [9] B. D. Vijay Kotu, Data Science (Second Edition), 2019.
- [10] «GeekforGeeks,» 29 July 2021. [On Line]. Available: <https://www.geeksforgeeks.org/cnn-introduction-to-pooling-layer/>.
- [11] Deepanshi, «Analytics Vidhya,» 25 May 2021. [On Line]. Available: <https://www.analyticsvidhya.com/blog/2021/05/all-you-need-to-know-about-your-first-machine-learning-model-linear-regression/>.
- [12] A. Saini, «Analytics Vidhya,» 3 August 2021. [On Line]. Available: <https://www.analyticsvidhya.com/blog/2021/08/conceptual-understanding-of-logistic-regression-for-data-science-beginners/>.
- [13] 48saily, «Analytics Vidhya,» 25 February 2021. [On Line]. Available: <https://www.analyticsvidhya.com/blog/2021/02/cost-function-is-no-rocket-science/>.
- [14] R. Kwiatkowski, 22 May 2021. [On Line]. Available: <https://towardsdatascience.com/gradient-descent-algorithm-a-deep-dive-cf04e8115f21>.
- [15] Z. Zhihua y J. Li, Big Data Mining for Climate Change, 2020.
- [16] S. Sharma, «Towards Data science,» 6 September 2017. [On Line]. Available: <https://towardsdatascience.com/activation-functions-neural-networks-1cbd9f8d91d6>.
- [17] V. Jain, «Towards Data Science,» 30 December 2019. [On Line]. Available: <https://towardsdatascience.com/everything-you-need-to-know-about-activation-functions-in-deep-learning-models->

84ba9f82c253#:~:text=Simply%20put%2C%20an%20activation%20function,fired%20to%20the%20next%20neuron..

- [18] R. Draelos, «Glass box,» 13 April 2019. [On Line]. Available: <https://glassboxmedicine.com/2019/04/13/a-short-history-of-convolutional-neural-networks/>.
- [19] R. Girshick, I. Forrester, D. Trevor y M. Jitendra, «Deformable Parts Models are Convolutional Neural Networks,» 1 October 2014.
- [20] U. J.R.R., K. van de Sande, T. Gevers y S. A. W.M., «Selective Search for Object Recognition,» 2012.
- [21] J. Redmon, S. Divvala, R. Girshick y A. Farhadi, «You Only Look Once: Unified, Real-Time Object Detection,» 9 May 2016.
- [22] J. Redmon y A. Farhadi, «YOLO9000: Better, Faster, Stronger,» 25 December 2016.
- [23] K. He, X. Zhang, R. Shaoqing y J. Sun, «Deep Residual Learning for Image Recognition,» 10 December 2015.
- [24] J. Redmon y A. Farhadi, «YOLOv3: An Incremental Improvement,» 8 April 2018.
- [25] A. Bochkovskiy, C.-Y. Wang y H.-Y. M. Liao, «YOLOv4: Optimal Speed and Accuracy of Object Detection,» 23 April 2020.
- [26] C.-Y. Wang, H.-Y. M. Liao, I.-H. Yeh, Y.-H. Wu, P.-Y. Chen y J.-W. Hsieh, «CSPNet: A New Backbone that can Enhance Learning Capability of CNN,» 27 November 2019.
- [27] S. L. Lu Qi, H. Qin, J. Shi y J. Jia, «Path Aggregation Network for Instance Segmentation,» 18 September 2018.
- [28] Y. Pei, D. S. Fussell, S. Biswas y K. Pingali, «An Elementary Introduction to Kalman Filtering,» 27 June 2019.
- [29] A. Bewley, Z. Ge, L. Ott, F. Ramos y B. Upcroft, «SIMPLE ONLINE AND REALTIME TRACKING,» 2017.
- [30] N. Wojke, A. Bewley y P. Drietrich, «Simple Online and Realtime Tracking with a Deep Association Metric,» 12 March 2017.
- [31] «Xtion Pro Live,» [On Line]. Available: <http://xtionprolive.com/asus-3d-depth-camera/asus-xtion-pro-live>.
- [32] «Python,» [On Line]. Available: <https://www.python.org/doc/essays/blurb/>.
- [33] I. Orsolice, «Camera Calibration: Explaining Camera Distortions,» [En línea]. Available: <https://ori.codes/artificial-intelligence/camera-calibration/camera-distortions/>.
- [34] «Open Source Computer Vision,» 2022. [On Line]. Available: [https://docs.opencv.org/4.x/d9/d0c/group\\_\\_calib3d.html#ga93efa9b0aa890de240ca32b11253dd4a](https://docs.opencv.org/4.x/d9/d0c/group__calib3d.html#ga93efa9b0aa890de240ca32b11253dd4a).
- [35] «Open Source Computer Vision,» 2022. [On Line]. Available: [https://docs.opencv.org/4.x/dd/d1a/group\\_\\_imgproc\\_\\_feature.html#ga354e0d7c86d0d9da75](https://docs.opencv.org/4.x/dd/d1a/group__imgproc__feature.html#ga354e0d7c86d0d9da75)

de9b9701a9a87e.

- [36] «Open Source Computer Vision,» 2022. [On Line]. Available:  
[https://docs.opencv.org/4.x/d9/d0c/group\\_\\_calib3d.html#ga3207604e4b1a1758aa66acb6ed5aa65d](https://docs.opencv.org/4.x/d9/d0c/group__calib3d.html#ga3207604e4b1a1758aa66acb6ed5aa65d).
- [37] «Open Source Computer Vision,» 2022. [On Line]. Available:  
[https://docs.opencv.org/4.x/d9/d0c/group\\_\\_calib3d.html#ga7a6c4e032c97f03ba747966e6ad862b1](https://docs.opencv.org/4.x/d9/d0c/group__calib3d.html#ga7a6c4e032c97f03ba747966e6ad862b1).
- [38] «Open Source Computer Vision,» 2022. [On Line]. Available:  
[https://docs.opencv.org/4.x/d9/d0c/group\\_\\_calib3d.html#ga69f2545a8b62a6b0fc2ee060dc30559d](https://docs.opencv.org/4.x/d9/d0c/group__calib3d.html#ga69f2545a8b62a6b0fc2ee060dc30559d).
- [39] «Open Source Computer Vision,» 2022. [On Line]. Available:  
[https://docs.opencv.org/4.x/d9/d0c/group\\_\\_calib3d.html#ga4abc2ece9fab9398f2e560d53c8c9780](https://docs.opencv.org/4.x/d9/d0c/group__calib3d.html#ga4abc2ece9fab9398f2e560d53c8c9780).
- [40] «Open Source Computer Vision,» 2022. [On Line] Available:  
[https://docs.opencv.org/4.x/da/d54/group\\_\\_imgproc\\_\\_transform.html#gaf73673a7e8e18ec6963e3774e6a94b87](https://docs.opencv.org/4.x/da/d54/group__imgproc__transform.html#gaf73673a7e8e18ec6963e3774e6a94b87).

## Appendices

### Appendix 1. Tracking file – Test 1.

3	1	388	475	260	391
4	1	384	474	256	400
5	1	380	476	250	408
6	1	376.5	477	233	415
7	1	374	478	220	424
8	1	371.5	478	205	437
9	1	367.5	479	201	448
10	1	363.5	477	199	451
11	1	360.5	476	197	455
12	1	357	464	200	455
13	1	359	451	194	449
14	1	361	448	194	448
15	1	363	446	192	446
16	1	368.5	445	191	445
17	1	375	445	190	445
18	1	385.5	444	189	444
19	1	394.5	440	187	440
20	1	401.5	429	185	429
21	1	405.5	419	183	419
22	1	407.5	415	179	415
23	1	408.5	414	175	414
24	1	405.5	412	169	412
25	1	402.5	412	167	412
26	1	399.5	412	161	412
27	1	396.5	412	157	412
28	1	390.5	412	157	412
29	1	371	410	162	410
30	1	357	412	160	411
31	1	342.5	412	163	412
32	1	328.5	415	163	414
33	1	304.5	417	201	417
34	1	284	415	198	415
35	1	268.5	414	195	414
36	1	247	439	156	439
37	1	228.5	457	175	457
38	1	220.5	463	183	462
39	1	206.5	464	213	461
40	1	197	464	232	459
41	1	190.5	464	241	457
42	1	181	466	256	455
43	1	170	465	274	448
44	1	152.5	463	287	445
45	1	142.5	465	283	447
46	1	135.5	467	271	448
47	1	123.5	469	247	445
48	1	113.5	469	227	443
49	1	103	467	206	437
50	1	94.5	465	189	431
51	1	93.5	469	187	419
52	1	93	468	186	413
53	1	92	469	184	415
54	1	92	469	184	418
55	1	89.5	464	179	418
56	1	83	467	164	425
57	1	80.5	464	161	423
58	1	73	460	146	422

59 1 62.5 455 121 424  
60 1 59 451 118 430  
61 1 59 443 118 432  
62 1 59.5 436 119 429  
63 1 59.5 435 119 429  
64 1 63 433 126 431  
65 1 65.5 429 131 427  
66 1 66.5 430 133 430  
67 1 66.5 428 133 428  
68 1 66 424 132 424  
69 1 63 398 126 398  
70 1 63.5 370 127 370  
71 1 65.5 347 131 347  
72 1 65.5 333 131 333  
73 1 66.5 327 133 327  
74 1 73.5 327 147 327  
75 1 75 327 150 327  
76 1 80 325 160 324  
77 1 81 322 162 322  
78 1 82 313 164 313  
79 1 83.5 302 159 302  
80 1 85 294 156 294  
81 1 88 279 154 279  
82 1 90.5 266 149 266  
83 1 93 255 146 255  
84 1 94.5 245 141 245  
85 1 98.5 242 131 242  
86 1 102.5 240 125 240  
87 1 105.5 239 121 239  
88 1 108.5 236 123 236  
89 1 111 234 124 234  
90 1 113 232 126 232  
91 1 116 229 124 229  
92 1 120 224 122 224  
93 1 121.5 220 121 220  
94 1 124 217 120 217  
95 1 125.5 200 121 200  
96 1 130.5 188 115 188  
97 1 138 186 120 186  
98 1 145 186 122 186  
99 1 149.5 185 119 185  
100 1 157 185 116 185  
101 1 164 183 108 183  
102 1 168 179 110 179  
103 1 170 175 110 175  
104 1 171.5 171 107 171  
105 1 173 167 102 167  
106 1 175 159 98 159  
107 1 184.5 151 83 151  
108 1 189.5 149 81 149  
109 1 194 148 78 148  
110 1 198 148 72 148  
111 1 201 148 70 148  
112 1 212.5 147 95 147  
113 1 223 147 96 147  
114 1 226.5 147 89 147  
115 1 233 147 100 147  
116 1 236 145 98 145  
117 1 239.5 141 93 140  
118 1 242.5 139 89 138  
119 1 250.5 133 81 132

120 1 260.5 128 65 128  
121 1 267 133 60 133  
122 1 283 133 88 133  
123 1 293 133 98 133  
124 1 299 131 106 131  
125 1 305 130 116 130  
126 1 309 130 114 130  
127 1 312 129 114 129  
128 1 316 130 104 130  
129 1 322 129 90 129  
130 1 326.5 129 83 129  
131 1 330.5 130 77 130  
132 1 336.5 129 75 129  
133 1 353.5 129 75 129  
134 1 364.5 129 79 129  
135 1 370.5 130 83 130  
136 1 374 129 88 129  
137 1 379 130 98 130  
138 1 380 130 96 130  
139 1 381.5 131 101 131  
140 1 383.5 131 105 130  
141 1 385 130 104 129  
142 1 394.5 127 73 127  
143 1 403.5 120 61 120  
144 1 409.5 125 53 125  
145 1 417.5 133 49 133  
146 1 426.5 138 67 138  
147 1 433.5 143 77 143  
148 1 437 148 78 148  
149 1 438.5 153 79 153  
150 1 440.5 158 75 158  
151 1 442.5 160 77 160  
152 1 445.5 160 77 160  
153 1 450 161 80 161  
154 1 453.5 160 79 160  
155 1 456.5 167 77 167  
156 1 459 177 78 177  
157 1 460 182 78 182  
158 1 461 188 76 188  
159 1 464.5 195 85 195  
160 1 467 202 88 202  
161 1 468.5 207 91 207  
162 1 472 210 94 210  
163 1 477.5 212 105 212  
164 1 479.5 212 109 212  
165 1 484.5 212 117 212  
166 1 486.5 211 117 210  
167 1 490 231 118 231  
168 1 492.5 245 119 245  
169 1 494.5 253 121 253  
170 1 496 263 118 263  
171 1 497 269 118 269  
172 1 498.5 279 121 279  
173 1 499.5 283 123 283  
174 1 502.5 284 125 284  
175 1 505.5 284 127 284  
176 1 509.5 285 125 285  
177 1 512.5 288 123 288  
178 1 515.5 310 121 310  
179 1 520 329 126 329  
180 1 525.5 350 135 350



181 1 535 359 160 359  
182 1 543 363 172 362  
183 1 546.5 365 171 364  
184 1 547 366 174 366  
185 1 550 365 178 365  
186 1 552.5 366 173 366  
187 1 554 371 170 371  
188 1 556 399 166 399  
189 1 556 408 166 408  
190 1 555.5 411 167 411  
191 1 554 415 170 415  
192 1 550 414 178 414  
193 1 549.5 430 179 430  
194 1 548 442 182 442  
195 1 547.5 444 183 444  
196 1 548.5 444 181 444  
197 1 550.5 443 175 443  
198 1 549 447 180 447  
199 1 526.5 446 169 446  
200 1 510.5 445 185 445  
201 1 496 448 188 448  
202 1 488.5 448 187 448  
203 1 486.5 446 193 446  
204 1 474.5 444 167 444  
205 1 462 443 156 443  
206 1 456.5 443 149 443  
207 1 453 439 144 439  
208 1 449.5 431 137 431  
209 1 440 409 136 409  
210 1 427.5 379 141 379  
211 1 416 360 142 360  
212 1 405.5 346 137 346  
213 1 389 335 150 335  
214 1 373.5 331 153 331  
215 1 360.5 329 149 329  
216 1 350 320 138 320  
217 1 342 310 128 310  
218 1 331 301 126 301  
219 1 317.5 280 129 280  
220 1 305 269 130 269  
221 1 292 269 128 269  
222 1 285 267 128 267  
223 1 281 266 124 266  
224 1 273.5 265 119 265  
225 1 269.5 264 117 264  
226 1 266.5 263 117 263  
227 1 258.5 258 109 258  
228 1 251.5 247 107 247  
229 1 245 237 104 237  
230 1 237.5 221 105 221  
231 1 234 213 100 213  
232 1 232 209 102 209  
233 1 229 208 94 208  
234 1 224.5 207 97 207  
235 1 222 207 96 207  
236 1 218 206 100 205  
237 1 216 205 104 204  
238 1 212.5 202 107 201  
239 1 207.5 198 111 197  
240 1 202.5 194 113 193  
241 1 196.5 186 113 186

242 1 185.5 175 107 175  
243 1 177.5 171 95 171  
244 1 174 170 94 170  
245 1 178.5 170 73 170  
246 1 180.5 170 69 170  
247 1 174.5 169 89 169  
248 1 173.5 168 91 168  
249 1 171.5 166 85 166  
250 1 171 164 86 164  
251 1 173 161 94 161  
252 1 174 155 94 155  
253 1 174.5 150 91 150  
254 1 176.5 146 89 146  
255 1 179 145 82 145  
256 1 181 142 80 142  
257 1 182 141 80 141  
258 1 181.5 141 77 141  
259 1 180.5 141 73 141  
260 1 180 139 70 139  
261 1 181 137 74 137  
262 1 192.5 135 87 135  
263 1 200.5 134 89 134  
264 1 210.5 134 103 134  
265 1 216 134 106 134  
266 1 218.5 134 107 134  
267 1 221 134 110 134  
268 1 223.5 133 107 133  
269 1 226.5 132 103 132  
270 1 230 133 96 133  
271 1 232.5 132 91 131  
272 1 237.5 133 79 132  
273 1 249.5 133 65 132  
274 1 255 133 64 132  
275 1 268.5 134 81 133  
276 1 273.5 135 83 134  
277 1 277 136 76 135  
278 1 281.5 136 71 135  
279 1 283.5 137 81 136  
280 1 286 139 92 138  
281 1 291.5 143 81 142  
282 1 295.5 147 79 147  
283 1 296 159 80 158  
284 1 296.5 163 81 162  
285 1 294.5 170 79 169  
286 1 293.5 175 81 174  
287 1 293 181 86 181  
288 1 292 185 82 185  
289 1 292.5 187 83 187  
290 1 293 188 92 188  
291 1 288.5 188 107 188  
292 1 286 189 106 189  
293 1 285.5 202 103 202  
294 1 285 213 104 213  
295 1 285 225 108 225  
296 1 285.5 239 109 239  
297 1 285.5 246 111 246  
298 1 285.5 248 115 247  
299 1 285.5 249 117 248  
300 1 285.5 249 117 248  
301 1 285.5 249 117 248  
302 1 285 257 114 256

303 1 284.5 269 113 269  
304 1 282 285 116 285  
305 1 280 300 118 300  
306 1 278 314 118 314  
307 1 275.5 319 121 319  
308 1 273 322 128 322  
309 1 270.5 323 135 323  
310 1 267.5 322 143 322  
311 1 263.5 330 145 330  
312 1 261.5 347 145 347  
313 1 261.5 362 147 362  
314 1 261.5 374 149 374  
315 1 262.5 382 149 382  
316 1 264 386 150 386  
317 1 266 388 154 388  
318 1 269.5 388 159 388  
319 1 271.5 386 163 386  
320 1 273 385 166 384  
321 1 274.5 401 165 401  
322 1 275.5 406 165 406  
323 1 276 409 164 409  
324 1 275.5 410 161 410  
325 1 275.5 411 151 411  
326 1 276 412 140 412  
327 1 277.5 411 131 411  
328 1 280 413 130 413  
329 1 280 415 126 415  
330 1 278 414 126 414  
331 1 275.5 416 123 416  
332 1 275 415 128 415  
333 1 278.5 417 135 417  
334 1 284 417 144 417  
335 1 289.5 415 147 415  
336 1 296 413 150 413  
337 1 301 413 152 413  
338 1 306 411 150 411  
339 1 309.5 408 149 408  
340 1 311 407 148 407  
341 1 312.5 403 143 403  
342 1 314.5 387 141 387  
343 1 316.5 367 137 367  
344 1 318.5 344 133 344  
345 1 322 333 126 333  
346 1 325 331 122 331  
347 1 327.5 328 121 328  
348 1 332 328 122 327  
349 1 337.5 327 117 326  
350 1 343 324 118 323  
351 1 348.5 318 119 317  
352 1 355 308 118 308  
353 1 359 301 118 301  
354 1 361 294 118 294  
355 1 364.5 276 121 276  
356 1 367.5 263 119 263  
357 1 369.5 253 117 253  
358 1 373 249 114 249  
359 1 376.5 249 115 249  
360 1 378.5 249 115 249  
361 1 381 249 112 249  
362 1 383.5 248 109 247  
363 1 384.5 241 109 240

364 1 385.5 236 107 235  
365 1 386 231 106 230  
366 1 386 227 106 226  
367 1 385.5 220 109 220  
368 1 389 200 102 200  
369 1 391 192 96 192  
370 1 393 190 92 190  
371 1 394 190 90 190  
372 1 397 189 88 189  
373 1 400 189 88 189  
374 1 403 188 88 188  
375 1 407.5 187 87 187  
376 1 409.5 183 85 183  
377 1 408.5 179 77 179  
378 1 410 175 82 175  
379 1 411 169 82 169  
380 1 411 159 78 159  
381 1 414.5 152 85 152  
382 1 417.5 150 85 150  
383 1 417 149 72 149  
384 1 419 149 68 149  
385 1 422.5 148 65 148  
386 1 423 147 66 147  
387 1 421.5 145 61 145  
388 1 421 144 60 143  
389 1 418 144 54 143  
390 1 413.5 144 47 143  
391 1 412 144 46 143  
392 1 417 145 66 145  
393 1 417.5 146 71 146  
394 1 412.5 145 63 145  
395 1 412.5 145 93 145  
396 1 406.5 145 77 145  
397 1 409 144 96 144  
398 1 403 144 78 144  
399 1 403.5 144 85 144  
400 1 402 145 80 144  
401 1 402 146 74 145  
402 1 403.5 146 73 145  
403 1 405.5 146 73 145  
404 1 407 147 72 146  
405 1 407.5 148 77 147  
406 1 409 154 76 153  
407 1 411 160 86 160  
408 1 413 166 94 166  
409 1 414 171 92 171  
410 1 417.5 177 87 177  
411 1 420 180 86 180  
412 1 420 181 88 181  
413 1 420.5 182 93 182  
414 1 422 183 94 183  
415 1 423.5 183 95 183  
416 1 424.5 185 97 185  
417 1 426 196 94 196  
418 1 431 208 94 208  
419 1 435 217 96 216  
420 1 439 230 98 229  
421 1 444.5 238 107 238  
422 1 448.5 241 109 241  
423 1 452.5 241 117 241  
424 1 457.5 242 125 242

425 1 460.5 243 127 243  
426 1 470 269 122 269  
427 1 476 285 128 285  
428 1 478.5 295 131 295  
429 1 481 308 132 308  
430 1 482 320 134 320  
431 1 484.5 325 141 325  
432 1 486 326 144 326  
433 1 488.5 326 145 326  
434 1 489.5 325 143 325  
435 1 490.5 326 143 326  
436 1 493 331 144 331  
437 1 497.5 367 141 367  
438 1 502 392 148 392  
439 1 507 410 156 410  
440 1 510.5 421 157 421  
441 1 515.5 432 163 432  
442 1 524 436 186 436  
443 1 532 440 204 440  
444 1 536 443 206 443  
445 1 537.5 444 203 444  
446 1 539.5 452 199 452  
447 1 539.5 470 199 467  
448 1 538.5 479 201 472  
449 1 534.5 479 209 461  
450 1 530 479 218 448  
451 1 525 479 228 440  
452 1 518.5 479 241 429  
453 1 508 479 262 416  
454 1 503 479 272 405  
455 1 500 479 278 395  
456 1 495.5 479 287 385  
457 1 486.5 479 305 366  
458 1 484.5 479 309 354  
459 1 474.5 479 329 318  
460 1 472.5 478 333 283  
461 1 471.5 479 335 267  
462 1 469 479 340 250  
463 1 467.5 479 339 242  
464 1 464.5 479 345 238  
465 1 461.5 479 347 241

## Appendix 2. Tracking file – Test 2.

3	1	281.5	478	349	207
4	1	290	478	336	221
5	1	300	478	336	234
6	1	307	478	334	243
7	1	313	479	332	251
8	1	320.5	478	325	260
9	1	330	478	320	268
10	1	340.5	478	317	276
11	1	355	479	316	282
12	1	365.5	479	313	284
13	1	382	479	314	284
14	1	397	479	310	286
15	1	404	479	310	288
16	1	406.5	479	309	289
17	1	409.5	479	299	294
18	1	409	479	298	300
19	1	406	479	290	310
20	1	398.5	479	245	343
21	1	392	479	236	363
22	1	386	479	230	376
23	1	383	479	228	383
24	1	382	479	216	393
25	1	384	478	192	403
26	1	389.5	478	189	410
27	1	397	476	182	416
28	1	402	477	182	429
29	1	401	479	194	441
30	1	400.5	479	197	446
31	1	395.5	479	203	450
32	1	389	479	204	451
33	1	378.5	479	199	456
34	1	365.5	478	195	460
35	1	356.5	479	193	464
36	1	346.5	479	193	467
37	1	339.5	478	193	468
38	1	329.5	478	193	470
39	1	321	476	192	473
40	1	314.5	467	195	467
41	1	308.5	452	193	452
42	1	302.5	448	181	448
43	1	299	446	178	446
44	1	298	440	168	440
45	1	297.5	430	165	430
46	1	298	422	162	422
47	1	298.5	414	159	414
48	1	298.5	406	155	406
49	1	298.5	368	153	368
50	1	298.5	343	147	343
51	1	298	322	142	322
52	1	298	314	134	314
53	1	297	311	130	310
54	1	296	309	126	309
55	1	296	310	126	310
56	1	294.5	311	123	311
57	1	294	307	122	307
58	1	292.5	299	123	299
59	1	291	294	124	294
60	1	291	285	126	285

61 1 290 257 132 257  
62 1 290 242 124 242  
63 1 290 235 120 235  
64 1 289.5 234 117 234  
65 1 290.5 234 113 234  
66 1 290.5 233 113 232  
67 1 292 231 112 229  
68 1 296 228 110 228  
69 1 299 222 108 222  
70 1 302 213 104 213  
71 1 304 200 106 200  
72 1 304.5 191 103 191  
73 1 303 181 96 181  
74 1 301.5 177 77 177  
75 1 298.5 176 69 176  
76 1 296.5 176 69 176  
77 1 295.5 177 69 177  
78 1 294.5 176 67 176  
79 1 293 176 72 176  
80 1 291.5 169 75 168  
81 1 290 161 74 160  
82 1 288.5 152 77 152  
83 1 285.5 149 79 149  
84 1 283.5 148 69 148  
85 1 276.5 147 61 147  
86 1 272 147 64 146  
87 1 269 148 70 148  
88 1 266 148 72 148  
89 1 264.5 146 75 146  
90 1 263 145 76 145  
91 1 261.5 141 75 141  
92 1 255.5 139 69 139  
93 1 246 141 62 141  
94 1 240 145 58 145  
95 1 234 151 54 151  
96 1 231.5 160 53 160  
97 1 229 167 60 167  
98 1 227.5 170 65 170  
99 1 225 172 70 172  
100 1 216 175 96 175  
101 1 203 178 124 178  
102 1 198 180 94 180  
103 1 195 182 78 182  
104 1 189.5 182 77 182  
105 1 187 182 80 182  
106 1 184 184 82 184  
107 1 180.5 194 85 194  
108 1 178.5 201 89 201  
109 1 173.5 207 93 207  
110 1 168.5 216 103 216  
111 1 165.5 222 105 222  
112 1 156.5 229 121 229  
113 1 137.5 231 133 231  
114 1 126 235 128 235  
115 1 117.5 252 125 252  
116 1 112.5 265 125 265  
117 1 109 276 124 276  
118 1 107 283 126 283  
119 1 107 289 126 289  
120 1 107.5 300 129 300  
121 1 106.5 303 133 303

122 1 105.5 304 137 304  
123 1 104.5 305 137 305  
124 1 101 306 138 306  
125 1 99.5 306 141 306  
126 1 94 335 142 335  
127 1 90 353 152 353  
128 1 85.5 366 159 366  
129 1 83.5 375 163 375  
130 1 81 387 162 387  
131 1 82 392 164 392  
132 1 82 394 164 394  
133 1 83.5 395 167 395  
134 1 83 394 166 394  
135 1 78.5 394 155 394  
136 1 76.5 394 153 394  
137 1 77.5 395 155 395  
138 1 77.5 395 155 395  
139 1 91 395 182 395  
140 1 103 394 186 394  
141 1 113.5 394 181 394  
142 1 119.5 395 175 393  
143 1 131.5 393 147 392  
144 1 138.5 370 141 369  
145 1 142 357 132 356  
146 1 153.5 333 133 333  
147 1 174.5 323 157 323  
148 1 192.5 319 169 317  
149 1 205 319 166 318  
150 1 215.5 318 161 317  
151 1 224 316 158 314  
152 1 227.5 312 151 310  
153 1 251.5 275 139 274  
154 1 265.5 261 133 260  
155 1 276 256 132 255  
156 1 284.5 254 129 253  
157 1 290 253 128 252  
158 1 297.5 252 123 251  
159 1 303.5 247 119 246  
160 1 307 244 114 243  
161 1 310 239 106 238  
162 1 312.5 233 99 232  
163 1 315 206 102 206  
164 1 317 196 98 196  
165 1 330 194 86 194  
166 1 339.5 193 85 193  
167 1 346 193 88 193  
168 1 352 192 90 192  
169 1 354.5 191 89 191  
170 1 356 185 88 185  
171 1 358.5 182 89 182  
172 1 360.5 177 85 177  
173 1 364 173 90 173  
174 1 367.5 167 91 167  
175 1 373 160 96 160  
176 1 384 154 94 154  
177 1 390 153 90 153  
178 1 395.5 153 87 153  
179 1 399 153 86 153  
180 1 403.5 152 81 152  
181 1 405 152 80 152  
182 1 406 151 78 151



183 1 405 149 80 149  
184 1 403.5 148 79 148  
185 1 400 143 70 143  
186 1 398.5 139 65 139  
187 1 401 138 58 138  
188 1 406 138 50 138  
189 1 409.5 139 47 139  
190 1 415 141 54 141  
191 1 417 143 54 143  
192 1 418 145 54 144  
193 1 421.5 148 65 148  
194 1 424.5 149 67 149  
195 1 429 153 78 153  
196 1 433 157 82 157  
197 1 435.5 159 83 159  
198 1 437.5 159 85 159  
199 1 442 160 82 160  
200 1 451 161 80 160  
201 1 455 160 80 160  
202 1 458 163 82 163  
203 1 459.5 172 79 172  
204 1 463 181 82 181  
205 1 466.5 186 87 186  
206 1 471 198 86 198  
207 1 476.5 203 95 203  
208 1 480 206 102 206  
209 1 481.5 207 105 207  
210 1 482.5 207 107 207  
211 1 484.5 207 111 207  
212 1 487 206 114 206  
213 1 490.5 206 119 206  
214 1 492.5 206 119 206  
215 1 498 227 110 227  
216 1 501 238 114 238  
217 1 502 243 114 243  
218 1 503 246 116 246  
219 1 502 249 120 249  
220 1 501.5 249 123 249  
221 1 500.5 248 127 248  
222 1 499.5 248 131 248  
223 1 497.5 246 135 245  
224 1 497 248 136 247  
225 1 496.5 260 135 259  
226 1 495.5 269 141 268  
227 1 494 275 142 274  
228 1 494.5 277 139 276  
229 1 496 278 132 277  
230 1 496.5 279 123 279  
231 1 495 280 124 280  
232 1 464 279 158 279  
233 1 439.5 279 167 279  
234 1 420.5 280 175 280  
235 1 414 280 172 280  
236 1 403 276 160 276  
237 1 393.5 273 147 273  
238 1 381 270 118 270  
239 1 358.5 274 111 274  
240 1 337.5 273 107 273  
241 1 320 277 114 277  
242 1 310.5 284 119 284  
243 1 304 283 128 283

244 1 291.5 281 159 281  
245 1 291 282 150 281  
246 1 283.5 286 163 286  
247 1 280.5 288 159 288  
248 1 277 288 150 288  
249 1 267 288 138 288  
250 1 251.5 287 111 287  
251 1 240 287 110 287  
252 1 214.5 288 107 288  
253 1 203 288 114 287  
254 1 194.5 287 131 287  
255 1 188 286 142 286  
256 1 175 286 170 286  
257 1 172.5 287 169 287  
258 1 169 287 172 287  
259 1 161.5 287 169 287  
260 1 158 287 166 287  
261 1 148.5 293 153 293  
262 1 142.5 301 157 301  
263 1 138 307 166 307  
264 1 138 310 170 310  
265 1 138.5 312 171 312  
266 1 140.5 316 167 315  
267 1 143.5 317 161 316  
268 1 147 317 154 316  
269 1 151.5 316 155 315  
270 1 154.5 316 155 315  
271 1 159.5 320 153 320  
272 1 166.5 349 155 349  
273 1 170 362 160 362  
274 1 172.5 379 163 379  
275 1 174 389 168 389  
276 1 175 396 172 395  
277 1 175.5 399 173 399  
278 1 175.5 399 179 399  
279 1 176.5 400 183 400  
280 1 178 400 188 400  
281 1 179 401 190 401  
282 1 181.5 400 197 400  
283 1 184.5 398 201 398  
284 1 186.5 398 199 398  
285 1 188.5 401 195 401  
286 1 192 402 190 402  
287 1 195 402 190 402  
288 1 199 401 188 401  
289 1 202 400 188 400  
290 1 206 401 190 401  
291 1 210.5 405 189 405  
292 1 212 410 188 410  
293 1 213.5 420 187 420  
294 1 214.5 422 185 422  
295 1 215 423 184 423  
296 1 215.5 424 173 424  
297 1 216 425 168 425  
298 1 218 423 154 423  
299 1 220 422 148 422  
300 1 222.5 422 143 422  
301 1 224.5 424 139 424  
302 1 224 428 144 428  
303 1 221.5 429 145 429  
304 1 223 429 158 429

305 1 225.5 430 167 430  
306 1 226.5 430 177 430  
307 1 227.5 430 179 430  
308 1 227 431 180 431  
309 1 226.5 430 183 430  
310 1 225 430 184 430  
311 1 222 433 182 433  
312 1 219.5 430 179 430  
313 1 217 421 178 421  
314 1 215 406 174 406  
315 1 214.5 402 169 402  
316 1 214.5 401 167 401  
317 1 216.5 399 165 399  
318 1 218.5 395 161 395  
319 1 220.5 394 159 394  
320 1 230 384 154 384  
321 1 237 373 146 373  
322 1 241 366 144 366  
323 1 244.5 354 143 354  
324 1 247.5 339 141 339  
325 1 253.5 302 137 302  
326 1 256.5 290 129 290  
327 1 258 285 124 285  
328 1 258.5 283 121 283  
329 1 258.5 281 119 281  
330 1 258.5 273 117 273  
331 1 258.5 263 117 263  
332 1 259 247 118 247  
333 1 259 235 118 235  
334 1 258.5 223 117 223  
335 1 258.5 214 113 214  
336 1 258 211 108 211  
337 1 258.5 210 105 210  
338 1 259 210 104 210  
339 1 259 210 104 210  
340 1 261.5 194 99 194  
341 1 262.5 181 95 181  
342 1 263.5 173 93 173  
343 1 264.5 165 93 164  
344 1 265 162 88 161  
345 1 263 162 84 160  
346 1 263.5 162 83 160  
347 1 265 161 84 159  
348 1 263 161 76 161  
349 1 265.5 157 81 157  
350 1 266.5 154 75 154  
351 1 266.5 151 67 151  
352 1 266 149 66 149  
353 1 264.5 147 65 147  
354 1 263.5 144 61 144  
355 1 263.5 143 59 143  
356 1 263.5 142 55 142  
357 1 264 142 56 142  
358 1 264 142 56 142  
359 1 264.5 142 55 142  
360 1 266.5 143 55 143  
361 1 269.5 143 59 143  
362 1 274 142 62 142  
363 1 275.5 142 61 142  
364 1 277 142 60 142  
365 1 278.5 142 55 142

366 1 280 142 56 142  
367 1 282 143 56 143  
368 1 284.5 143 55 142  
369 1 295 142 72 142  
370 1 303 143 80 143  
371 1 311.5 143 95 143  
372 1 318 144 102 144  
373 1 322 143 112 143  
374 1 324.5 143 113 143  
375 1 326.5 142 113 142  
376 1 327.5 143 111 143  
377 1 330.5 143 103 143  
378 1 333.5 142 97 142  
379 1 337.5 138 81 138  
380 1 344 131 68 131  
381 1 359 136 56 136  
382 1 375.5 137 79 137  
383 1 385 139 86 139  
384 1 389 140 90 140  
385 1 391.5 140 89 140  
386 1 391.5 141 89 141  
387 1 394 141 82 141  
388 1 397.5 142 75 142  
389 1 410 142 60 142  
390 1 419.5 142 61 142  
391 1 423.5 142 61 142  
392 1 428 142 64 142  
393 1 429 141 64 141  
394 1 428.5 141 61 141  
395 1 429.5 141 63 141  
396 1 432.5 141 69 141  
397 1 437.5 143 73 143  
398 1 440.5 145 79 144  
399 1 442 150 84 149  
400 1 443.5 158 85 158  
401 1 443.5 166 85 166  
402 1 444 172 80 172  
403 1 447.5 176 87 176  
404 1 451 181 84 181  
405 1 452 185 84 185  
406 1 453 187 80 186  
407 1 454.5 187 91 186  
408 1 456 187 90 186  
409 1 456 187 94 186  
410 1 457 187 94 186  
411 1 456.5 187 93 186  
412 1 460.5 204 93 204  
413 1 463 214 96 214  
414 1 469 226 98 226  
415 1 472 236 102 236  
416 1 475.5 246 107 246  
417 1 477 248 110 248  
418 1 487 251 132 251  
419 1 493 252 134 252  
420 1 499 267 132 267  
421 1 502.5 279 135 279  
422 1 507 296 132 296  
423 1 509.5 311 131 311  
424 1 511.5 326 135 326  
425 1 512.5 332 137 332  
426 1 514 335 142 335

427 1 515.5 335 145 334  
428 1 518.5 334 147 333  
429 1 520.5 335 147 334  
430 1 523 335 148 334  
431 1 525.5 350 145 350  
432 1 533 379 150 379  
433 1 540 398 160 398  
434 1 543.5 407 163 407  
435 1 545 413 166 413  
436 1 547.5 418 169 418  
437 1 551 425 176 425  
438 1 551.5 428 175 428  
439 1 550 431 178 431  
440 1 549.5 432 179 432  
441 1 549 432 180 432  
442 1 548.5 429 181 429  
443 1 549 429 180 429  
444 1 548 429 182 429  
445 1 546.5 431 185 431  
446 1 542 432 194 432  
447 1 537 430 204 428  
448 1 533 429 212 427  
449 1 529 426 220 423  
450 1 522.5 425 219 422  
451 1 513.5 424 215 421  
452 1 502 423 220 420  
453 1 488 420 222 415  
454 1 463 415 214 408  
455 1 447 413 192 405  
456 1 434 412 184 406  
457 1 427.5 413 181 408  
458 1 415.5 407 159 403  
459 1 405.5 405 151 404  
460 1 380 413 148 413  
461 1 364 431 152 431  
462 1 346 425 162 425  
463 1 328 428 162 428  
464 1 314.5 422 169 422  
465 1 296 421 202 420  
466 1 289 421 200 420  
467 1 284 425 206 424  
468 1 274 427 216 426  
469 1 257.5 429 229 429  
470 1 239 428 230 428  
471 1 215.5 427 233 426  
472 1 195.5 430 215 429  
473 1 176 428 200 427  
474 1 159 431 202 430  
475 1 151 431 210 429  
476 1 141 430 230 428  
477 1 136.5 429 233 427  
478 1 131.5 431 249 430  
479 1 129.5 434 251 434  
480 1 115 429 224 429  
481 1 103.5 429 203 429  
482 1 87 431 166 429  
483 1 83 431 166 428  
484 1 83 430 166 425  
485 1 83.5 423 167 417  
486 1 83 418 166 413  
487 1 83 416 166 413

488 1 83 415 166 412  
489 1 82.5 414 165 410  
490 1 81.5 415 163 411  
491 1 78 418 156 416  
492 1 74.5 417 149 416  
493 1 73 419 146 419  
494 1 73.5 418 147 418  
495 1 76 418 152 418  
496 1 76.5 416 153 416  
497 1 81.5 416 163 416  
498 1 84.5 419 169 419  
499 1 86.5 422 173 422  
500 1 91 421 182 421  
501 1 95 419 190 419  
502 1 97.5 417 195 417  
503 1 98 415 196 415  
504 1 100 411 200 411  
505 1 100.5 401 197 401  
506 1 106.5 389 183 389  
507 1 112 368 174 368  
508 1 117 355 170 355  
509 1 126.5 334 171 334  
510 1 134 326 162 326  
511 1 142.5 322 155 322  
512 1 149.5 320 153 320  
513 1 155 315 146 314  
514 1 162.5 305 145 305  
515 1 166.5 297 145 297  
516 1 169.5 282 145 282  
517 1 174.5 265 137 265  
518 1 179.5 249 133 249  
519 1 182 245 128 245  
520 1 184.5 244 131 244  
521 1 192 245 130 245  
522 1 198.5 245 125 245  
523 1 203.5 245 119 245  
524 1 211 235 108 235  
525 1 216 227 108 227  
526 1 221.5 215 109 215  
527 1 228 196 114 196  
528 1 233 190 110 190  
529 1 236 187 108 187  
530 1 238.5 186 103 186  
531 1 242.5 181 97 181  
532 1 248.5 176 85 176  
533 1 250.5 164 95 164  
534 1 255.5 155 89 155  
535 1 254.5 152 87 152  
536 1 256 151 82 151  
537 1 255.5 151 85 151  
538 1 255 150 88 150  
539 1 255 150 90 150  
540 1 256 149 88 149  
541 1 257 148 86 148  
542 1 260.5 147 75 147  
543 1 265.5 145 67 145  
544 1 271 143 54 142  
545 1 275.5 142 47 141  
546 1 278 142 48 142  
547 1 279 142 50 142  
548 1 280 142 46 142

549 1 280 142 60 142  
550 1 279 142 66 142  
551 1 278.5 143 73 143  
552 1 278.5 143 73 143  
553 1 288 143 76 143  
554 1 291 143 76 143  
555 1 293.5 142 79 141  
556 1 295 144 72 143  
557 1 293.5 148 73 147  
558 1 291.5 154 77 154  
559 1 289.5 157 73 157  
560 1 287 161 74 161  
561 1 280.5 171 77 171  
562 1 277.5 175 81 175  
563 1 273 177 88 177  
564 1 270.5 177 81 176  
565 1 263.5 178 95 177  
566 1 260.5 178 97 177  
567 1 258.5 179 97 179  
568 1 257 183 96 183  
569 1 254.5 194 97 194  
570 1 252.5 202 101 202  
571 1 252 209 100 209  
572 1 252 212 104 212  
573 1 252.5 217 103 217  
574 1 252.5 228 105 228  
575 1 252 234 106 234  
576 1 253 237 110 237  
577 1 253 239 114 239  
578 1 253.5 239 113 239  
579 1 254.5 239 115 239  
580 1 253.5 241 115 241  
581 1 253 260 112 260  
582 1 252.5 272 115 272  
583 1 250.5 285 117 285  
584 1 249.5 294 117 294  
585 1 247.5 308 121 308  
586 1 242.5 315 131 315  
587 1 240 317 138 317  
588 1 239 316 144 316  
589 1 238.5 316 145 316  
590 1 240 362 144 362  
591 1 240.5 380 151 380  
592 1 244 400 152 400  
593 1 248.5 408 159 408  
594 1 253.5 413 167 413  
595 1 260 415 176 415  
596 1 266 414 184 414  
597 1 270 412 188 412  
598 1 273 425 188 425  
599 1 275 445 190 445  
600 1 277 465 192 465  
601 1 278.5 477 195 475  
602 1 280.5 479 201 472  
603 1 282 479 206 468  
604 1 282.5 479 211 464  
605 1 283.5 479 229 459  
606 1 284.5 479 233 454  
607 1 294 479 284 429  
608 1 297.5 479 279 415  
609 1 305.5 479 287 396

610	1	309.5	479	281	385
611	1	327	479	298	370
612	1	344	479	308	357
613	1	359	479	322	345
614	1	371.5	479	327	336
615	1	383	479	342	326
616	1	388.5	479	343	320
617	1	392.5	479	347	312



### Appendix 3. Tracking file – Test 3.

```
3 1 167.5 478 311 302
3 2 587.5 356 103 355
4 1 166.5 478 311 306
4 2 583 351 112 350
5 1 166 479 312 308
5 2 578.5 344 121 343
6 1 166 479 308 307
6 2 575.5 340 127 340
7 1 164.5 479 301 307
7 2 572.5 338 133 338
8 1 164.5 479 293 306
8 2 570 336 138 335
9 1 164 479 280 308
9 2 568 335 142 333
10 1 162 479 268 312
10 2 567.5 333 143 331
11 1 161.5 479 253 319
11 2 567.5 332 141 329
12 1 160.5 479 247 327
12 2 568 332 140 329
13 1 158.5 478 231 336
13 2 568.5 331 139 328
14 1 154.5 479 207 354
14 2 568.5 332 141 328
15 1 152 478 204 363
15 2 568 332 142 326
16 1 150 478 186 375
16 2 568.5 333 141 324
17 1 148 478 184 388
17 2 568.5 334 139 328
18 1 146 479 190 396
18 2 568.5 335 141 333
19 1 145.5 479 267 421
19 2 568 335 142 329
20 1 139 479 270 432
20 2 568.5 335 139 332
21 1 131 479 258 438
21 2 568.5 335 141 330
22 1 129 479 258 445
22 2 568 334 142 332
23 1 132 479 264 451
23 2 567 333 144 333
24 1 125 479 246 458
24 2 555 333 168 333
25 1 122 479 244 461
25 2 542.5 331 193 331
26 1 121 479 242 462
26 2 536 330 206 330
27 1 120.5 479 241 463
27 2 532.5 330 211 330
28 1 119.5 479 239 464
28 2 530 330 214 330
29 1 118 479 236 465
29 2 525 331 208 331
30 1 115 479 228 468
30 2 519.5 333 195 333
31 1 114.5 479 223 471
31 2 515 333 188 333
```

32 1 113.5 479 217 473  
32 2 511 333 180 333  
33 1 112.5 479 211 478  
33 2 507.5 333 177 332  
34 1 112 467 208 467  
34 2 504 333 170 332  
35 1 112 456 200 456  
35 2 502 333 170 332  
36 1 111.5 429 197 429  
36 2 499 339 160 339  
37 1 111.5 416 191 416  
37 2 491.5 345 175 344  
38 1 111 406 182 406  
38 2 482 361 168 360  
39 1 111 401 178 401  
39 2 475.5 379 167 379  
40 1 110.5 399 173 399  
40 2 472 390 166 390  
41 1 110 397 174 397  
41 2 471 397 166 397  
42 1 109.5 390 173 390  
42 2 470 401 166 401  
43 1 108.5 380 175 380  
43 2 466.5 404 175 404  
44 1 106 365 172 365  
44 2 462 407 178 407  
45 1 106 354 174 354  
45 2 457 411 170 411  
46 1 106 320 176 320  
46 2 454.5 412 165 412  
47 1 107 309 168 309  
47 2 451.5 413 165 413  
48 1 109 304 162 304  
48 2 443 417 174 417  
49 1 112.5 303 157 303  
49 2 432 421 182 421  
50 1 113.5 302 151 302  
50 2 425 421 188 421  
51 1 117 301 148 301  
51 2 418.5 422 189 422  
52 1 120.5 298 139 298  
52 2 412 421 188 421  
53 1 124.5 290 135 290  
53 2 405 420 186 420  
54 1 128 281 134 281  
54 2 391 421 206 421  
55 1 131.5 267 133 267  
55 2 378.5 420 211 420  
56 1 136.5 248 135 248  
56 2 364 421 212 421  
57 1 139.5 236 133 236  
57 2 354.5 422 205 422  
58 1 142.5 232 129 232  
58 2 346.5 422 195 422  
59 1 144.5 231 127 231  
59 2 339 426 178 426  
60 1 144.5 231 125 231  
60 2 334.5 430 173 430  
61 1 146 231 122 231  
61 2 330.5 431 169 431  
62 1 147.5 233 123 233

62 2 328.5 433 177 433  
63 1 147.5 231 121 231  
63 2 325 432 184 432  
64 1 149.5 228 121 228  
64 2 319.5 430 189 430  
65 1 150 224 120 224  
65 2 309.5 430 199 430  
66 1 150.5 217 113 217  
66 2 293.5 428 197 428  
67 1 150 210 108 210  
67 2 277 439 196 439  
68 1 151 194 100 194  
68 2 260 452 184 446  
69 1 153 184 96 184  
69 2 247.5 462 169 451  
70 1 156 179 90 179  
70 2 238.5 462 157 450  
71 1 159.5 177 91 177  
71 2 236 459 146 452  
72 1 161.5 178 89 177  
72 2 233 453 148 448  
73 1 159 178 68 177  
73 2 231 449 152 447  
74 1 160.5 174 65 173  
74 2 219 440 182 440  
75 2 213.5 435 189 435  
76 2 201 431 214 431  
77 2 196.5 432 217 432  
78 2 187.5 429 227 429  
79 2 177.5 427 249 427  
80 2 169.5 427 253 427  
80 3 221 144 74 144  
81 2 157 431 264 431  
81 3 229.5 149 77 149  
82 2 150 433 268 433  
82 3 235.5 151 81 151  
83 2 139 430 272 430  
83 3 243.5 151 85 151  
84 2 132 429 264 429  
84 3 249.5 151 87 151  
85 2 124.5 433 247 433  
85 3 257 152 96 152  
86 2 115 432 230 432  
86 3 262 150 100 150  
87 2 105.5 429 211 429  
87 3 264.5 148 101 147  
88 2 99 429 198 429  
88 3 267 146 96 145  
89 2 98.5 431 197 431  
89 3 272 139 82 138  
90 2 98 435 196 435  
90 3 279 132 66 130  
91 2 98 439 196 437  
91 3 288.5 127 59 127  
92 2 98 438 196 435  
92 3 297 131 56 131  
93 2 97.5 436 195 433  
93 3 304 133 66 133  
94 2 97 435 194 432  
94 3 314 133 86 133  
95 2 96.5 436 193 434

95 3 323.5 131 101 131  
96 2 96.5 436 193 435  
96 3 327.5 129 105 129  
97 2 95.5 437 191 437  
97 3 330.5 130 105 130  
98 2 93.5 438 187 438  
98 3 332.5 132 107 132  
99 2 93 436 186 436  
99 3 334 132 106 132  
100 2 92 434 184 434  
100 3 336 132 98 132  
101 2 91.5 427 183 427  
101 3 340.5 133 89 133  
102 2 91.5 412 183 412  
102 3 359 133 64 133  
103 2 91.5 399 183 399  
103 3 371 132 60 132  
104 2 94 367 188 367  
104 3 387.5 132 89 132  
105 2 95.5 356 183 356  
105 3 394.5 132 93 132  
106 2 98 351 180 351  
106 3 396.5 136 91 136  
107 2 100.5 348 179 348  
107 3 398 138 92 138  
108 2 104 348 178 348  
108 3 399.5 139 89 138  
109 2 107 345 174 344  
109 3 406.5 140 85 139  
110 2 107.5 341 173 340  
110 3 411 140 82 139  
111 2 105 327 166 327  
111 3 424.5 144 87 144  
112 2 103 314 162 314  
112 3 433 152 92 152  
113 2 103 297 160 297  
113 3 439 161 94 161  
114 2 103.5 284 159 284  
114 3 442 165 96 165  
115 2 104 277 158 277  
115 3 443 168 94 168  
116 2 106.5 270 161 270  
116 3 439.5 170 75 170  
117 2 111.5 268 165 267  
117 3 442.5 179 89 179  
118 2 113 267 162 266  
118 3 444 184 90 184  
119 2 117 267 160 266  
119 3 444.5 186 87 186  
120 2 120 268 158 267  
120 3 444 186 90 186  
121 2 124.5 267 151 266  
121 3 444.5 186 91 186  
122 2 129 266 144 265  
122 3 447 187 94 187  
123 2 130.5 264 145 263  
123 3 448 187 92 187  
124 2 132.5 258 143 257  
124 3 450 188 96 188  
125 2 136 252 134 252  
125 3 451 199 92 199

126 2 138 247 132 247  
126 3 453 207 98 207  
127 2 139.5 243 133 243  
127 3 455.5 214 99 214  
128 2 143 235 138 235  
128 3 457 219 96 219  
129 2 148 223 140 223  
129 3 460.5 226 99 225  
130 2 153.5 216 135 216  
130 3 465.5 237 101 237  
131 2 158.5 213 131 213  
131 3 471 244 108 244  
132 2 160.5 212 131 212  
132 3 476.5 247 119 247  
133 2 162.5 212 127 212  
133 3 480.5 249 125 249  
134 2 163.5 213 129 213  
134 3 483 250 130 250  
135 2 165.5 213 127 213  
135 3 486.5 249 135 249  
136 2 167 214 122 214  
136 3 489.5 247 135 247  
137 2 167.5 213 117 213  
137 3 493.5 247 135 247  
138 2 166.5 213 113 213  
138 3 495.5 254 133 254  
139 2 167.5 206 87 206  
139 3 502.5 283 125 283  
140 2 169 201 82 201  
140 3 506 302 130 302  
141 2 170.5 196 87 196  
141 3 508 319 134 319  
142 2 172 191 86 191  
142 3 509.5 326 143 326  
143 2 172 188 88 188  
143 3 510.5 329 145 329  
144 2 175.5 187 97 187  
144 3 513 331 150 331  
145 2 180.5 188 109 188  
145 3 516 331 152 331  
146 2 185.5 189 113 189  
146 3 519 330 154 329  
147 2 191 192 116 192  
147 3 523.5 354 151 354  
148 2 195.5 194 115 194  
148 3 528.5 379 153 379  
149 2 201.5 198 105 198  
149 3 537 406 164 406  
150 2 204.5 199 103 199  
150 3 543 425 176 425  
151 2 207.5 201 97 201  
151 3 545.5 431 187 431  
152 2 210.5 201 95 201  
152 3 546 431 186 431  
153 2 211.5 201 93 201  
153 3 547 434 184 434  
154 2 212.5 201 91 201  
154 3 548 435 182 435  
155 2 214 201 90 201  
155 3 549 434 180 434  
156 2 218.5 200 85 200

156 3 549.5 432 179 432  
157 2 221 200 84 200  
157 3 545 429 188 429  
158 2 233.5 200 109 200  
158 3 532.5 428 213 428  
159 2 246.5 200 123 200  
159 3 521.5 431 235 431  
160 2 257 200 130 200  
160 3 515.5 430 247 430  
161 2 268 203 126 202  
161 3 492 432 254 432  
162 2 275 205 120 204  
162 3 475 431 240 431  
163 2 279.5 207 115 206  
163 3 460 431 220 431  
164 2 283.5 207 111 206  
164 3 451.5 432 191 432  
165 2 287 207 104 206  
165 3 442 436 174 436  
166 2 294.5 208 91 207  
166 3 429.5 438 153 438  
167 2 305 211 106 210  
167 3 418.5 441 157 441  
168 2 305 213 80 212  
168 3 407 447 160 447  
169 2 307.5 218 79 217  
169 3 397.5 454 165 454  
170 2 307.5 219 77 218  
170 3 389 455 166 455  
171 2 312.5 210 71 209  
171 3 376.5 456 167 455  
172 2 316 206 66 205  
172 3 368 453 166 451  
173 2 320.5 205 65 204  
173 3 351.5 451 157 451  
174 3 341.5 447 157 447  
175 3 334.5 441 157 441  
176 3 331.5 438 153 438  
177 3 333 438 144 438  
178 3 329.5 439 155 439  
179 3 323 439 160 439  
180 3 316.5 440 161 440  
181 2 381 230 84 230  
181 3 300 440 170 440  
182 2 390 231 80 231  
182 3 279 440 180 440  
183 2 398.5 231 89 231  
183 3 268.5 439 183 439  
184 2 406 232 108 232  
184 3 262 439 182 439  
185 2 415.5 232 113 232  
185 3 257.5 439 183 439  
186 2 419.5 232 117 231  
186 3 255 437 180 437  
187 2 422 232 118 231  
187 3 251.5 437 175 437  
188 2 421.5 232 117 232  
188 3 246.5 436 169 436  
189 2 420.5 231 111 231  
189 3 242.5 432 165 432  
190 2 418 231 110 231

190 3 240 425 162 425  
191 2 417.5 231 111 231  
191 3 238 419 160 419  
192 2 417.5 232 109 232  
192 3 232.5 396 155 396  
193 2 417.5 232 113 231  
193 3 229.5 378 151 378  
194 2 419 232 122 231  
194 3 224 344 148 344  
195 2 421.5 231 125 230  
195 3 219.5 333 139 333  
196 2 423.5 225 129 224  
196 3 216 328 136 325  
197 2 424 217 126 216  
197 3 212 326 132 324  
198 2 423 212 126 211  
198 3 209 327 134 326  
199 2 422.5 208 119 207  
199 3 205.5 325 133 324  
200 2 420.5 205 113 204  
200 3 202 321 134 320  
201 2 420 203 110 202  
201 3 199.5 313 139 312  
202 2 418.5 203 111 203  
202 3 195.5 306 141 306  
203 2 419 203 112 203  
203 3 191 300 138 300  
204 2 418 203 108 203  
204 3 185.5 283 141 283  
205 2 416 204 112 204  
205 3 180 260 140 260  
206 2 415.5 203 113 203  
206 3 175.5 252 135 252  
207 2 415 200 114 200  
207 3 173 249 132 249  
208 2 416.5 195 109 195  
208 3 171.5 247 129 247  
209 2 414.5 191 99 190  
209 3 169.5 248 125 247  
210 2 414 189 92 189  
210 3 168.5 247 119 247  
211 2 414 185 86 185  
211 3 167.5 243 115 243  
212 2 414.5 182 79 182  
212 3 166 240 112 240  
213 2 414.5 180 75 180  
213 3 166 231 110 231  
214 2 415 175 74 175  
214 3 165.5 219 111 219  
215 2 414 172 72 172  
215 3 165.5 206 111 206  
216 2 414 170 70 170  
216 3 165.5 200 109 200  
217 2 415.5 169 65 169  
217 3 166 194 110 194  
218 2 414 168 72 168  
218 3 165.5 191 107 191  
219 2 411 169 84 169  
219 3 163 190 104 190  
220 2 410.5 171 85 171  
220 3 162.5 189 101 189

221 2 412.5 174 79 174  
221 3 160 186 106 186  
222 2 411.5 176 85 176  
222 3 161.5 182 95 182  
223 2 414.5 179 77 179  
223 3 159.5 179 101 179  
224 2 414.5 181 79 181  
224 3 158.5 175 103 175  
225 2 415 183 76 183  
225 3 160 170 98 170  
226 2 411 187 84 187  
226 3 159 162 98 162  
227 2 410 189 86 189  
227 3 157.5 159 101 159  
228 2 409.5 192 75 192  
228 3 159.5 158 103 158  
229 2 409.5 193 71 193  
229 3 164 157 106 157  
230 2 408.5 193 73 193  
230 3 169 157 100 157  
231 2 404.5 193 71 192  
231 3 172 157 98 157  
232 2 401 193 72 192  
232 3 174.5 157 95 157  
233 2 397.5 193 77 193  
233 3 176 158 96 158  
234 2 393.5 193 81 193  
234 3 178 157 90 157  
235 2 390 193 82 193  
235 3 179 154 88 154  
236 2 382 195 92 195  
236 3 180 148 84 148  
237 2 376 199 98 199  
237 3 180.5 143 83 143  
238 2 363 208 122 208  
238 3 183.5 143 79 143  
239 2 358 214 120 214  
239 3 186 142 78 142  
240 2 349.5 227 109 227  
240 3 188 142 78 141  
241 2 344.5 232 107 232  
241 3 189 142 72 141  
242 2 340 234 104 234  
242 3 190.5 143 71 142  
243 2 339 235 102 234  
243 3 191.5 143 69 142  
244 2 330 234 118 233  
244 3 191.5 143 65 142  
245 2 326 235 108 234  
245 3 192.5 143 63 142  
246 2 314.5 251 95 251  
246 3 193 141 62 140  
247 2 291.5 272 97 272  
247 3 192 142 54 141  
248 2 282 284 96 284  
248 3 192 142 52 141  
249 2 268 290 104 290  
249 3 190.5 142 59 142  
250 2 258.5 293 99 293  
250 3 189 142 60 142  
251 2 250 293 98 293



251 3 189.5 142 59 142  
252 2 242 293 102 293  
253 2 231 292 110 292  
254 2 220.5 300 113 300  
255 2 214.5 310 117 310  
256 2 209.5 317 125 317  
257 2 203.5 329 133 329  
258 2 185 342 180 342  
259 2 179.5 350 179 350  
260 2 174.5 353 181 353  
261 2 174.5 354 177 354  
262 2 171.5 356 173 356  
262 3 221.5 158 77 158  
263 2 160.5 356 179 355  
263 3 224.5 156 91 156  
264 2 138.5 358 199 357  
264 3 232 161 114 161  
265 2 124.5 360 199 359  
265 3 240 166 112 166  
266 2 121 367 200 366  
266 3 243.5 169 113 169  
267 2 121 376 206 375  
267 3 246.5 179 105 179  
268 2 126 379 220 379  
268 3 248 183 102 183  
269 2 130.5 383 219 383  
269 3 251 184 98 183  
270 2 133.5 387 213 386  
270 3 255.5 185 95 185  
271 2 135.5 389 211 387  
271 3 260 186 104 186  
272 2 138 389 206 386  
272 3 266.5 187 111 187  
273 2 141 388 200 385  
273 3 271.5 190 109 190  
274 2 143.5 387 197 386  
274 3 276 202 108 202  
275 2 146 386 196 386  
275 3 280 214 108 214  
276 2 148 393 192 393  
276 3 284.5 220 111 220  
277 2 150 401 190 401  
277 3 287 225 110 225  
278 2 152 407 186 407  
278 3 289.5 229 111 229  
279 2 152.5 410 189 410  
279 3 291 234 110 234  
280 2 152.5 414 187 414  
280 3 293.5 238 109 236  
281 2 154 416 188 416  
281 3 296 239 112 235  
282 2 156.5 423 175 423  
282 3 304.5 240 113 239  
283 2 157.5 427 173 427  
283 3 310.5 239 113 238  
284 2 157.5 427 175 427  
284 3 317 239 116 238  
285 2 159 426 182 426  
285 3 323.5 240 113 239  
286 2 162 427 192 427  
286 3 334.5 251 125 251

287 2 164 427 194 427  
287 3 342.5 259 127 259  
288 2 164.5 426 195 426  
288 3 345.5 264 121 264  
289 2 164.5 425 193 425  
289 3 354.5 278 113 278  
290 2 161 426 190 426  
290 3 360 283 112 283  
291 2 158.5 426 187 426  
291 3 364 286 114 286  
292 2 153 426 186 426  
292 3 374 287 122 287  
293 2 150 427 188 427  
293 3 386.5 287 121 287  
294 2 148 426 188 426  
294 3 394 286 124 286  
295 2 146.5 425 191 425  
295 3 406 296 130 296  
296 2 145.5 427 193 427  
296 3 419 322 132 322  
297 2 145 428 194 428  
297 3 426 335 136 335  
298 2 144 428 196 428  
298 3 431 344 136 344  
299 2 144 427 198 427  
299 3 435 352 138 351  
300 2 142 427 200 427  
300 3 441 362 140 362  
301 2 140 427 202 427  
301 3 444 369 142 369  
302 2 136.5 427 201 427  
302 3 450 373 144 373  
303 2 133.5 428 199 428  
303 3 457 372 142 372  
304 2 130.5 427 203 427  
304 3 470 373 136 373  
305 2 128 423 204 423  
305 3 477.5 374 137 374  
306 2 120 395 204 395  
306 3 493 374 148 374  
307 2 115 375 200 375  
307 3 503 375 152 375  
308 2 113 364 196 364  
308 3 511 377 158 377  
309 2 113.5 360 193 360  
309 3 517.5 388 157 388  
310 2 115.5 358 187 358  
310 3 525 413 164 413  
311 2 119 358 182 358  
311 3 537 433 190 433  
312 2 122 359 178 359  
312 3 541.5 438 195 438  
313 2 124 359 178 359  
313 3 542.5 441 193 441  
314 2 128 353 172 353  
314 3 545.5 441 187 441  
315 2 131 341 168 341  
315 3 546 442 186 442  
316 2 133 328 168 328  
316 3 545.5 442 187 442  
317 2 136 315 166 315

317 3 546 446 186 446  
318 2 140.5 292 165 292  
318 3 552.5 446 173 443  
319 2 142 278 162 278  
319 3 556.5 445 165 439  
320 2 145 273 152 273  
320 3 557.5 443 163 434  
321 2 146.5 272 147 272  
321 3 557 439 164 430  
322 2 147.5 272 145 272  
322 3 558 441 162 432  
323 2 147 272 144 272  
323 3 555.5 433 167 421  
324 2 147 272 144 272  
324 3 556.5 439 165 429  
325 2 147 272 144 272  
325 3 554.5 437 169 427  
326 2 145 264 144 264  
326 3 547.5 439 183 432  
327 2 142 255 144 255  
327 3 534 429 210 423  
328 2 140 247 138 247  
328 3 535 431 208 427  
329 2 138.5 232 135 232  
329 3 526.5 434 225 431  
330 2 138 223 130 223  
330 3 522.5 435 233 432  
331 2 139 219 124 219  
331 3 525 436 226 433  
332 2 140 217 124 217  
332 3 517.5 433 239 432  
333 2 140.5 216 119 216  
333 3 508.5 431 217 431  
334 2 141 216 118 216  
334 3 505.5 425 209 425  
335 2 141.5 216 115 216  
335 3 498.5 425 197 425  
336 2 143 216 112 215  
336 3 493.5 419 179 419  
337 2 143 217 114 216  
337 3 487.5 416 169 416  
338 2 144 216 110 215  
338 3 472.5 422 173 422  
339 2 145 215 110 214  
339 3 461 422 180 422  
340 2 146 210 108 209  
340 3 445.5 439 177 439  
341 2 149.5 195 111 195  
341 3 408.5 437 193 437  
342 2 152.5 186 109 186  
342 3 388 433 194 433  
343 2 155 176 106 176  
343 3 369.5 430 193 430  
344 2 156.5 173 107 173  
344 3 362.5 427 191 427  
345 2 162.5 172 99 172  
345 3 357.5 430 185 430  
346 2 165 172 104 172  
346 3 355 430 176 430  
347 2 165.5 172 103 172  
347 3 354 430 168 430

348 2 168 173 98 173  
348 3 346.5 430 159 430  
349 2 170 172 90 172  
349 3 317 430 150 430  
350 2 170.5 172 85 172  
350 3 293.5 430 141 430  
351 2 170 170 78 170  
351 3 271.5 433 141 433  
352 2 169.5 167 77 167  
352 3 261.5 434 147 434  
353 2 171 162 76 162  
353 3 253.5 436 159 436  
354 2 175 156 60 156  
354 3 246.5 438 171 438  
355 2 176.5 153 57 153  
355 3 241.5 439 185 439  
356 3 237.5 438 193 438  
357 3 233.5 438 203 438  
358 3 229 437 210 437  
359 3 222 433 214 433  
360 3 212.5 430 223 430  
361 3 201 421 204 420  
362 3 179.5 419 183 417  
363 3 159 419 176 417  
364 3 140 420 154 418  
364 6 218.5 148 101 148  
365 3 132.5 417 159 414  
365 6 220 147 100 147  
366 3 125 411 176 409  
366 6 224.5 147 83 146  
367 3 118.5 409 189 407  
367 6 227 147 86 146  
368 3 111 410 202 409  
368 6 230.5 148 81 147  
369 3 107.5 410 207 410  
369 6 233.5 149 75 148  
370 3 105.5 409 211 409  
370 6 234.5 149 71 148  
371 3 104.5 408 209 408  
371 6 241.5 149 69 148  
372 3 101.5 409 203 409  
372 6 247.5 149 73 148  
373 3 95 405 190 405  
373 6 261.5 150 91 149  
374 3 91 403 182 403  
374 6 272 150 100 149  
375 3 88 402 176 402  
375 6 279 151 100 150  
376 3 87.5 403 175 403  
376 6 283 151 100 150  
377 3 87.5 403 175 403  
377 6 284 151 100 150  
378 3 87 406 174 406  
378 6 285 149 98 148  
379 3 87.5 408 175 408  
379 6 286.5 147 97 146  
380 3 90 405 180 405  
380 6 294 141 78 140  
381 3 90.5 402 181 402  
381 6 301.5 138 69 137  
382 3 91.5 394 183 394

382 6 308 139 62 138  
383 3 92 385 182 385  
383 6 315 143 64 142  
384 3 97 366 174 366  
384 6 330 141 86 141  
385 3 101 347 170 347  
385 6 338 139 90 139  
386 3 105 328 164 328  
386 6 344.5 139 97 139  
387 3 108.5 312 159 312  
387 6 349 141 102 141  
388 3 110.5 306 151 306  
388 6 350.5 143 103 143  
389 3 112.5 303 145 303  
389 6 353 144 104 144  
390 3 113.5 302 141 302  
390 6 354.5 144 97 144  
391 3 115 300 140 300  
391 6 357 144 92 144  
392 3 117 298 138 298  
392 6 360 144 84 144  
393 3 119 296 138 296  
393 6 364 144 78 143  
394 3 119.5 293 139 293  
394 6 368 144 72 143  
395 3 122 284 142 284  
395 6 381.5 144 59 144  
396 3 123.5 277 141 277  
396 6 388.5 144 59 144  
397 3 125 265 140 265  
397 6 396.5 143 75 143  
398 3 126.5 246 139 246  
398 6 404 143 88 143  
399 3 131.5 236 145 236  
399 6 410 145 92 145  
400 3 135 235 144 235  
400 6 411 146 90 146  
401 3 137.5 234 139 234  
401 6 412 149 92 149  
402 3 139.5 234 139 234  
402 6 413.5 150 93 150  
403 3 141 234 136 234  
403 6 414.5 151 93 151  
404 3 142.5 234 129 234  
404 6 420 151 106 151  
405 3 145 234 130 234  
405 6 422 151 98 151  
406 3 146 234 128 234  
406 6 425.5 151 101 151  
407 3 148 231 120 231  
407 6 428 151 92 151  
408 3 150.5 226 121 226  
408 6 434 151 88 151  
409 3 152.5 221 117 221  
409 6 442 155 92 155  
410 3 156 213 112 213  
410 6 450 161 94 161  
411 3 160.5 204 109 204  
411 6 453.5 169 89 169  
412 3 162.5 197 109 197  
412 6 456 174 96 174

413 3 163 186 104 186  
413 6 456.5 176 97 176  
414 3 166 180 102 180  
414 6 456 178 98 178  
415 3 173 179 92 179  
415 6 456.5 182 97 182  
416 3 176.5 178 89 178  
416 6 456 185 100 185  
417 3 178.5 178 87 178  
417 6 455.5 185 101 185  
418 3 181.5 179 81 179  
418 6 455 186 104 186  
419 3 184.5 178 77 178  
419 6 455.5 186 107 186  
420 3 185 178 78 178  
420 6 455.5 185 107 185  
421 3 186 175 76 175  
421 6 455.5 185 107 185  
422 3 186 172 70 172  
422 6 455.5 185 105 185  
423 3 186 170 68 170  
423 6 455 185 102 185  
424 3 185 170 68 170  
424 6 456.5 195 99 195  
425 3 183.5 170 65 170  
425 6 459.5 204 101 204  
426 3 183 167 70 167  
426 6 461 211 108 211  
427 3 184.5 165 73 165  
427 6 463 216 108 216  
428 3 184.5 166 77 166  
428 6 466.5 225 107 225  
429 3 184 166 80 166  
429 6 469.5 232 109 232  
430 3 183 167 82 167  
430 6 473.5 235 113 235  
431 3 182 166 88 166  
431 6 478.5 236 119 236  
432 3 181 166 90 166  
432 6 483 236 126 236  
433 3 180.5 167 93 167  
433 6 486.5 236 131 235  
434 3 180 166 94 166  
434 6 489 235 130 234  
435 3 179.5 167 93 167  
435 6 488.5 236 129 235  
436 3 180.5 168 93 168  
436 6 491 236 134 235  
437 3 181 170 94 170  
437 6 493.5 244 135 244  
438 3 182 170 92 170  
438 6 495.5 251 135 251  
439 3 185 170 90 170  
439 6 497 265 136 265  
440 3 187.5 170 89 170  
440 6 498.5 273 135 273  
441 3 188.5 170 89 170  
441 6 500.5 281 137 281  
442 3 191.5 171 107 171  
442 6 504.5 291 141 291  
443 3 198 171 122 171

443 6 507.5 297 141 297  
444 3 203 171 128 171  
444 6 509 299 140 299  
445 3 210 175 132 175  
445 6 514 299 148 299  
446 3 215 179 128 179  
446 6 518 300 148 300  
447 3 218.5 183 121 183  
447 6 519.5 301 149 301  
448 3 221.5 190 117 189  
448 6 517.5 301 139 301  
449 3 226 193 112 193  
449 6 523 301 156 301  
450 3 227.5 194 107 194  
450 6 525.5 312 153 312  
451 3 230 195 104 195  
451 6 528.5 323 159 323  
452 3 236 195 104 195  
452 6 534.5 345 171 345  
453 3 239.5 195 105 195  
453 6 537.5 357 173 357  
454 3 244.5 196 107 196  
454 6 540 364 178 364  
455 3 248 200 110 200  
455 6 541.5 366 181 366  
456 3 251.5 211 111 211  
456 6 546.5 367 183 366  
457 3 257.5 222 115 222  
457 6 551 368 176 367  
458 3 263 228 116 228  
458 6 554 366 170 364  
459 3 267.5 235 119 235  
459 6 555.5 367 167 365  
460 3 271 239 120 238  
460 6 556 366 166 364  
461 3 275.5 242 119 241  
461 6 557 368 164 367  
462 3 279.5 243 115 242  
462 6 557 366 164 365  
463 3 282.5 244 117 243  
463 6 557 366 164 366  
464 3 285.5 244 117 243  
464 6 557 367 164 367  
465 3 292 244 112 244  
465 6 558 367 162 367  
466 3 297 243 116 243  
466 6 558.5 366 161 365  
467 3 302 242 114 242  
467 6 559.5 368 159 367  
468 3 306 242 112 242  
468 6 559 370 160 370  
469 3 309 242 114 242  
469 6 559 370 160 370  
470 3 314 242 112 242  
470 6 555.5 367 167 367  
471 3 319.5 241 109 241  
471 6 545.5 365 187 365  
472 3 323 241 106 241  
472 6 540 363 198 363  
473 3 330 240 102 239  
473 6 527.5 365 223 365

474 3 333.5 240 103 239  
474 6 522.5 363 233 362  
475 3 338 240 106 239  
475 6 516.5 363 245 362  
476 3 341 240 106 239  
476 6 510 362 252 361  
477 3 346.5 240 107 239  
477 6 500.5 364 249 362  
478 3 356 243 106 243  
478 6 485 365 224 365  
479 3 361 251 108 251  
479 6 475.5 366 221 364  
480 3 364.5 258 107 258  
480 6 465.5 367 197 367  
481 3 367.5 263 107 263  
481 6 460 368 190 368  
482 3 366.5 269 87 269  
482 6 449.5 366 167 366  
483 3 366.5 263 85 263  
483 6 443 366 154 366  
484 3 366.5 240 69 240  
484 6 433 371 132 371  
485 3 363.5 233 55 233  
485 6 418.5 373 151 373  
486 3 366 231 50 231  
486 6 393 372 156 372  
487 6 381.5 383 159 381  
488 6 363 383 160 379  
489 3 423.5 287 95 287  
489 6 348.5 380 169 378  
490 3 436.5 294 107 294  
490 6 342.5 382 189 382  
491 3 443 297 112 297  
491 6 335.5 384 165 384  
492 3 448.5 302 111 302  
492 6 326.5 384 163 384  
493 3 454 316 114 316  
493 6 313.5 384 159 384  
494 3 458 324 122 324  
494 6 305 384 154 384  
495 3 461 329 130 329  
495 6 296.5 385 153 385  
496 3 471.5 347 151 347  
496 6 264 385 138 385  
497 3 483 354 168 354  
497 6 241 384 150 384  
498 3 494.5 357 183 357  
498 6 230 385 154 385  
499 3 504 357 186 356  
499 6 221.5 386 169 386  
500 3 508 357 184 356  
500 6 217.5 387 177 387  
501 3 534 383 174 383  
501 6 202 384 196 383  
502 3 545 399 174 399  
502 6 193.5 379 185 379  
503 3 549.5 405 179 405  
503 6 186.5 371 181 371  
504 3 550.5 408 177 408  
504 6 180.5 368 175 368  
505 3 551 408 176 408



505 6 163.5 367 159 367  
506 3 551 410 176 409  
506 6 152 366 150 366  
507 3 550.5 412 177 410  
507 6 131 361 172 361  
508 3 551 415 176 414  
508 6 122 356 180 356  
509 3 551 420 176 419  
509 6 119 353 190 353  
510 3 550.5 430 177 430  
510 6 118 353 196 353  
511 3 550 438 178 438  
511 6 118 352 204 352  
512 3 550 443 178 443  
512 6 110 352 214 352  
513 3 549.5 444 179 444  
513 6 103 352 204 352  
514 3 549.5 446 179 446  
514 6 99.5 352 199 352  
515 3 550 445 178 445  
515 6 96 350 192 350  
516 3 550.5 444 177 444  
516 6 95 347 190 347  
517 3 553 444 172 444  
517 6 92.5 343 185 343  
518 3 555 441 168 441  
518 6 90 339 180 339  
519 3 562 441 150 441  
519 6 89.5 339 179 339  
520 3 557.5 443 163 443  
520 6 87.5 338 175 338  
521 3 554 445 170 445  
521 6 88 338 176 338  
522 3 551.5 445 175 445  
522 6 89 338 178 338  
523 3 547.5 445 183 445  
523 6 90 338 180 338  
524 3 544 451 190 451  
524 6 91 339 182 339  
525 3 526.5 451 225 451  
525 6 92.5 338 185 338  
526 3 521 449 236 449  
526 6 96.5 336 179 336  
527 3 510.5 451 231 451  
527 6 100 331 174 331  
528 3 499.5 448 197 448  
528 6 105 321 164 321  
529 3 493 449 184 449  
529 6 108 313 162 312  
530 3 490 449 184 449  
530 6 111 307 160 307  
531 3 478 447 156 447  
531 6 118 288 168 288  
532 3 469 443 148 443  
532 6 122 278 166 278  
533 3 457 422 150 422  
533 6 126 272 166 272  
534 3 444.5 409 143 409  
534 6 129 271 164 271  
535 3 433.5 404 139 404  
535 6 131 271 162 271

536 3 426.5 398 135 398  
536 6 132 270 160 270  
537 3 419.5 393 135 393  
537 6 132.5 270 159 270  
538 3 399 389 166 389  
538 6 133 271 152 271  
539 3 389.5 385 161 385  
539 6 133.5 272 151 272  
540 3 368 380 184 380  
540 6 131 268 146 268  
541 3 359.5 378 179 378  
541 6 130.5 265 145 265  
542 3 354 376 184 376  
542 6 133 258 132 258  
543 3 351.5 375 179 375  
543 6 134 253 132 253  
544 3 347 372 172 372  
544 6 135 241 130 241  
545 3 335 367 170 367  
545 6 137.5 225 129 225  
546 3 327 364 166 364  
546 6 138.5 216 125 216  
547 3 319 363 164 363  
547 6 138.5 213 123 213  
548 3 309.5 364 157 364  
548 6 140.5 211 125 211  
549 3 265 368 144 368  
549 6 145 210 110 210  
550 3 247.5 369 151 369  
550 6 147.5 210 111 210  
551 3 238.5 367 165 367  
551 6 150 208 108 208  
552 3 235 366 166 366  
552 6 145 206 88 206  
553 3 226.5 361 173 361  
553 6 146 203 84 203  
554 3 216.5 357 165 357  
555 3 208 354 158 354  
556 3 196 344 152 344  
557 3 179 334 138 334  
558 3 166.5 332 127 332  
559 3 160 325 136 325  
560 3 158.5 319 135 319  
561 3 158 317 136 317  
562 3 155 312 142 311  
563 3 152 311 146 310  
564 3 149 310 152 309  
564 8 211.5 166 81 165  
565 3 146.5 310 157 309  
565 8 211 169 90 168  
566 3 141.5 307 171 306  
566 8 213.5 170 93 170  
567 3 136.5 304 179 303  
567 8 215 170 90 170  
568 3 133 302 174 302  
568 8 214 169 84 169  
569 3 130 299 180 299  
569 8 217.5 168 85 168  
570 3 118 295 182 295  
570 8 220.5 158 81 157  
571 3 108.5 292 181 292

571 8 222 153 76 153  
572 3 98.5 289 177 289  
572 8 224.5 149 73 149  
573 3 89.5 288 171 288  
573 8 226 145 72 144  
574 3 84.5 288 167 288  
574 8 227.5 143 69 142  
575 3 77.5 288 153 288  
575 8 235.5 145 83 144  
576 3 74 288 148 288  
576 8 241 144 86 142  
577 3 73 288 146 288  
577 8 247 145 94 145  
578 3 73 289 146 289  
578 8 252.5 143 99 143  
579 3 73.5 289 147 289  
579 8 257.5 142 105 142  
580 3 73.5 289 147 289  
580 8 263 141 112 141  
581 3 74 290 146 290  
581 8 270 142 108 142  
582 3 74 290 146 290  
582 8 274.5 143 105 143  
583 3 75 288 150 288  
583 8 279 145 104 145  
584 3 75.5 287 151 287  
584 8 281.5 146 103 146  
585 3 75.5 288 151 288  
585 8 283.5 145 99 144  
586 3 74 288 148 288  
586 8 287 145 86 144  
587 3 72.5 289 145 289  
587 8 294.5 145 75 144  
588 3 72 288 144 288  
588 8 302 145 74 145  
589 3 74.5 285 149 285  
589 8 311.5 145 73 145  
590 3 75 281 150 281  
590 8 317 145 72 145  
591 3 75.5 276 151 276  
591 8 322 145 76 145  
592 3 80.5 263 161 263  
592 8 333.5 145 93 145  
593 3 81 258 162 258  
593 8 338 144 94 144  
594 3 81.5 257 163 256  
594 8 340 145 94 145  
595 3 82.5 257 163 256  
595 8 342 145 94 145  
596 3 83 258 164 257  
596 8 343.5 144 89 144  
597 3 83 257 166 256  
597 8 346.5 143 83 143  
598 3 82.5 257 165 256  
598 8 351.5 141 75 141  
599 3 83 257 164 257  
599 8 366 142 70 142  
600 3 83 258 164 258  
600 8 375 143 72 143  
601 3 83.5 257 161 257  
601 8 380.5 145 73 145

602 3 86 258 154 258  
602 8 386.5 145 79 145  
603 3 87.5 259 153 259  
603 8 390 146 80 146  
604 3 89.5 260 149 260  
604 8 392 148 78 148  
605 3 92.5 257 141 257  
605 8 389 148 70 148  
606 3 94 255 134 254  
606 8 389 149 72 149  
607 3 98 252 130 252  
607 8 391 149 70 149  
608 3 105 250 134 250  
608 8 394 148 72 148  
609 3 117.5 248 153 248  
609 8 399.5 147 65 147  
610 3 132.5 245 165 245  
610 8 405.5 148 61 148  
611 3 142.5 243 167 243  
611 8 409.5 148 61 148  
612 3 148 242 168 242  
612 8 410.5 149 61 149  
613 3 158 242 160 242  
613 8 413 148 78 147  
614 3 166 244 154 244  
614 8 418.5 148 87 148  
615 3 171.5 245 151 245  
615 8 422 148 92 148  
616 3 178 245 138 245  
616 8 423 148 106 148  
617 3 181.5 245 137 245  
617 8 424 148 108 148  
618 3 187 245 124 245  
618 8 425.5 148 113 148  
619 3 190.5 246 119 246  
619 8 426 148 114 148  
620 3 204.5 246 99 246  
620 8 429.5 147 93 147  
621 3 221.5 246 123 246  
621 8 432 145 100 145  
622 3 241.5 245 135 245  
622 8 427 145 100 145  
623 3 254.5 245 141 245  
623 8 421.5 144 93 144  
624 3 267.5 245 145 245  
624 8 422.5 144 109 144  
625 3 273.5 245 149 245  
625 8 420.5 145 109 145  
626 3 278.5 243 139 243  
626 8 417 145 102 145  
627 3 283 242 134 242  
627 8 413.5 145 97 145  
628 3 291.5 240 119 240  
628 8 410 146 92 146  
629 3 304 238 88 238  
629 8 406.5 146 83 146  
630 3 319 238 74 238  
630 8 403.5 146 79 146  
631 3 329 243 70 243  
631 8 402.5 144 77 144  
632 3 339 244 76 244

632 8 401 144 62 144  
633 3 365 240 146 240  
633 8 399.5 143 59 143  
634 3 378 242 152 242  
635 3 382 245 146 245  
636 3 387 246 152 246  
636 8 343 140 64 140  
637 3 392.5 246 135 246  
637 8 340.5 141 85 141  
638 3 396.5 247 129 247  
638 8 342 143 90 143  
639 3 406 247 128 246  
639 8 343.5 145 99 145  
640 3 426 246 124 245  
640 8 341.5 145 89 145  
641 3 446.5 246 107 245  
641 8 337 145 78 145  
642 3 459.5 246 107 245  
642 8 318.5 145 63 145  
643 3 464.5 246 107 245  
643 8 307 145 68 145  
644 3 471 247 122 247  
644 8 298 144 76 144  
645 3 471.5 246 113 246  
645 8 289.5 144 91 144  
646 3 471.5 246 115 246  
646 8 285 144 96 143  
647 3 473 248 120 248  
647 8 283 143 98 142  
648 3 476 252 130 252  
648 8 282.5 145 95 144  
649 3 485 253 146 253  
649 8 283 147 94 146  
650 3 489.5 254 143 254  
650 8 282 147 94 146  
651 3 497 255 142 255  
651 8 280.5 149 89 148  
652 3 506.5 255 141 255  
652 8 275 149 92 149  
653 3 515.5 256 135 256  
653 8 269 150 84 150  
654 3 521.5 257 139 257  
654 8 263.5 150 81 150  
655 3 524.5 256 143 256  
655 8 261.5 152 79 152  
656 3 525.5 256 145 256  
656 8 259 155 78 155  
657 3 528 256 152 256  
657 8 254.5 166 75 166  
658 3 529.5 258 153 258  
658 8 251.5 175 75 175  
659 3 530.5 260 157 260  
659 8 249 179 82 179  
660 3 529 267 162 267  
660 8 247.5 183 83 183  
661 3 524.5 275 171 275  
661 8 247.5 184 85 184  
662 3 521.5 279 173 279  
662 8 245.5 183 89 183  
663 3 518 284 174 284  
663 8 238.5 184 107 184

664 3 514.5 288 173 288  
664 8 235.5 184 107 184  
665 3 513 292 170 292  
665 8 234 184 108 184  
666 3 510 295 164 295  
666 8 234 183 104 183  
667 3 508.5 296 161 296  
667 8 234.5 183 103 183  
668 3 504.5 296 151 296  
668 8 237 183 94 183  
669 3 502 296 148 296  
669 8 236 184 100 184  
670 3 492.5 296 155 296  
670 8 236 194 96 194  
671 3 484.5 296 161 296  
671 8 234 205 100 205  
672 3 480.5 297 161 297  
672 8 233.5 210 103 210  
673 3 478 300 162 300  
673 8 233 211 106 211  
674 3 475.5 319 155 319  
674 8 233.5 215 101 215  
675 3 473.5 341 153 341  
675 8 232.5 220 107 220  
676 3 472 359 154 359  
676 8 232 221 110 221  
677 3 470.5 369 157 369  
677 8 232 223 112 223  
678 3 470 376 158 376  
678 8 233 222 112 221  
679 3 468.5 381 159 381  
679 8 232.5 222 117 221  
680 3 468 387 160 387  
680 8 233 222 114 221  
681 3 467 392 166 392  
681 8 235.5 222 109 221  
682 3 466.5 394 173 394  
682 8 229.5 223 127 223  
683 3 465.5 395 177 395  
683 8 227 223 128 223  
684 3 463 395 186 395  
684 8 225.5 223 127 223  
685 3 462 395 188 395  
685 8 226.5 223 129 223  
686 3 459.5 398 187 398  
686 8 231.5 224 133 224  
687 3 458.5 398 187 398  
687 8 235.5 225 133 224  
688 3 457 400 188 400  
688 8 240 226 142 225  
689 3 452.5 412 193 412  
689 8 242.5 225 145 225  
690 3 434.5 457 203 456  
690 8 249.5 228 137 228  
691 3 428.5 474 195 470  
691 8 254.5 231 131 231  
692 3 423 479 196 473  
692 8 258 231 126 231  
693 3 419 479 196 472  
693 8 260.5 231 121 230  
694 3 412 479 206 469

694 8 263.5 230 113 229  
695 3 407.5 479 213 466  
695 8 266 230 112 229  
696 3 403 479 218 464  
696 8 268 230 106 229  
697 3 393.5 479 243 455  
697 8 278 235 108 235  
698 3 387 479 266 440  
698 8 288.5 239 99 239  
699 3 384 479 278 419  
699 8 295.5 234 89 234  
700 3 385 479 284 405  
700 8 300 231 86 231  
701 3 388 479 294 393  
701 8 310 231 96 231  
702 3 391.5 479 295 384  
702 8 314.5 231 93 230  
703 3 400.5 479 301 372  
703 8 316 231 76 230  
704 3 408.5 479 303 365  
704 8 317.5 231 81 229  
705 3 419.5 479 321 351  
705 8 323 232 94 231  
706 3 423.5 479 323 340  
706 8 328.5 233 99 232  
707 3 425 479 330 329  
707 8 337.5 232 109 231

#### Appendix 4. Tracking file – Test 4.

```
3 1 136 479 264 336
3 2 540 308 144 307
4 1 127.5 479 247 350
4 2 544.5 304 151 303
5 1 116.5 479 227 364
5 2 547 303 154 301
6 1 108 479 216 372
6 2 548.5 302 157 300
7 1 95.5 479 187 381
7 2 548.5 300 157 298
8 1 96 479 192 391
8 2 548 298 154 297
9 1 93.5 479 187 400
9 2 545.5 297 147 296
10 1 95 479 190 406
10 2 543.5 298 145 297
11 1 97 479 194 411
11 2 542.5 298 145 298
12 1 100.5 478 201 419
12 2 542 298 144 298
13 1 102.5 478 205 428
13 2 542 297 142 297
14 1 103.5 479 207 434
14 2 541 298 140 298
15 1 110.5 479 221 436
15 2 541.5 299 143 299
16 1 117 479 234 438
16 2 542.5 301 147 301
17 1 120.5 479 241 439
17 2 543 303 146 303
18 1 123 479 246 441
18 2 543.5 304 147 304
19 1 125 478 250 450
19 2 545 304 152 304
20 1 126 478 252 454
20 2 546.5 305 153 305
21 1 125 479 246 459
21 2 548 306 156 306
22 1 121.5 479 241 463
22 2 550.5 306 159 306
23 1 119.5 479 239 465
23 2 552 307 162 307
24 1 117.5 479 235 465
24 2 553 307 164 307
25 1 114.5 479 229 466
25 2 554.5 307 165 307
26 1 112.5 479 225 469
26 2 556 306 164 306
27 1 110 479 220 473
27 2 560 306 156 306
28 1 108.5 479 217 475
28 2 563.5 308 149 308
29 1 107 478 214 475
29 2 567 306 144 306
30 1 108 478 216 477
30 2 570.5 307 137 307
31 1 106.5 474 213 474
31 2 571 306 136 306
```



32 1 104 458 208 458  
32 2 571 313 136 313  
33 1 100.5 448 201 448  
33 2 571 315 136 315  
34 1 91.5 428 179 428  
34 2 573 314 132 314  
35 1 87 414 174 414  
35 2 576.5 319 119 319  
36 1 85.5 410 171 410  
36 2 577.5 326 123 326  
37 1 84.5 409 169 409  
37 2 574.5 338 129 338  
38 1 84 408 168 408  
38 2 568.5 348 141 346  
39 1 84 406 168 406  
39 2 560.5 357 157 354  
40 1 83.5 405 167 404  
40 2 559 363 160 359  
41 1 83.5 401 167 401  
41 2 559 368 160 358  
42 1 83.5 396 167 396  
42 2 559 371 160 364  
43 1 84 392 168 392  
43 2 558.5 373 159 367  
44 1 85 384 170 384  
44 2 558.5 371 161 365  
45 1 89.5 360 179 360  
45 2 554 375 170 372  
46 1 93 337 174 337  
46 2 548.5 373 181 372  
47 1 97 321 170 321  
47 2 546 374 186 373  
48 1 99 315 166 315  
48 2 544 381 188 379  
49 1 102.5 313 161 313  
49 2 542 402 188 399  
50 1 104.5 309 157 309  
50 2 539.5 422 189 421  
51 1 108.5 306 151 306  
51 2 538 442 196 442  
52 1 110.5 304 147 304  
52 2 536.5 450 201 450  
53 1 113.5 300 147 300  
53 2 533.5 454 211 454  
54 1 117 294 148 294  
54 2 528.5 455 211 455  
55 1 118 290 146 290  
55 2 526 456 208 456  
56 1 118.5 281 143 281  
56 2 521.5 457 197 457  
57 1 119 276 140 276  
57 2 518.5 458 191 458  
58 1 121.5 244 137 244  
58 2 503 453 196 453  
59 1 123.5 234 129 234  
59 2 492.5 456 197 456  
60 1 131 231 130 231  
60 2 462 456 226 456  
61 1 136.5 229 123 229  
61 2 430 452 236 452  
62 1 139.5 228 119 228

62 2 413 451 232 451  
63 1 143.5 224 113 224  
63 2 398 449 212 449  
64 1 146.5 218 111 218  
64 2 388.5 453 197 453  
65 1 149.5 214 107 214  
65 2 384.5 451 197 451  
66 1 152.5 206 105 206  
66 2 377.5 445 187 445  
67 1 157 191 110 191  
67 2 364.5 440 165 440  
68 1 162.5 181 105 181  
68 2 340.5 446 155 446  
69 1 167 178 102 178  
69 2 324.5 450 155 450  
70 1 166 177 82 177  
70 2 301.5 447 151 445  
71 1 169.5 176 73 176  
71 2 277 451 164 451  
72 1 172 175 72 175  
72 2 263.5 451 183 451  
73 1 175 171 68 171  
73 2 256.5 450 191 450  
74 2 238.5 451 225 451  
75 2 228.5 453 239 453  
76 2 207.5 456 249 456  
77 2 183.5 460 255 460  
78 2 152.5 460 251 460  
78 3 221.5 127 67 127  
79 2 136 460 248 460  
79 3 229.5 138 77 138  
80 2 118.5 465 229 465  
80 3 244.5 142 103 142  
81 2 116 466 232 466  
81 3 256.5 142 123 142  
82 2 116 466 232 466  
82 3 262 139 126 139  
83 2 116 463 232 463  
83 3 266 138 122 138  
84 2 117 463 234 459  
84 3 270 138 112 137  
85 2 111 464 222 462  
85 3 279 137 92 136  
86 2 105 464 210 463  
86 3 292 137 84 137  
87 2 100.5 461 201 460  
87 3 305.5 136 79 136  
88 2 92.5 450 185 448  
88 3 314 135 72 135  
89 2 80.5 444 159 442  
89 3 316 135 64 134  
90 2 75 440 150 437  
90 3 316.5 134 59 133  
91 2 72.5 432 145 426  
91 3 327.5 133 91 133  
92 2 73 426 146 396  
92 3 335.5 133 103 133  
93 2 71.5 411 143 369  
93 3 344 133 116 133  
94 2 71 406 142 360  
94 3 347.5 133 113 133

95 2 69.5 401 139 353  
95 3 355.5 131 97 131  
96 2 69 398 138 348  
96 3 359.5 131 91 131  
97 2 67.5 395 135 345  
97 3 362.5 131 91 131  
98 2 64.5 391 127 341  
98 3 371.5 132 89 132  
99 2 62.5 389 125 339  
99 3 376.5 133 83 133  
100 2 63.5 387 127 334  
100 3 378.5 136 57 136  
101 2 63.5 390 127 335  
101 3 381.5 142 53 142  
102 2 66 391 132 340  
102 3 385 149 52 149  
103 2 68.5 393 137 346  
103 3 386 154 60 154  
104 2 71.5 391 143 351  
104 3 387.5 155 63 155  
105 2 73 387 144 372  
105 3 391 156 78 156  
106 2 73.5 380 145 376  
106 3 390.5 156 79 156  
107 2 74 370 148 369  
107 3 392 156 82 156  
108 2 74 358 148 358  
108 3 387 157 82 157  
109 2 74.5 350 149 350  
109 3 386 162 84 162  
110 2 75 338 150 338  
110 3 383.5 169 85 169  
111 2 76.5 324 153 324  
111 3 381 179 90 179  
112 2 77 316 154 316  
112 3 381.5 183 97 183  
113 2 77.5 308 155 308  
113 3 380 188 98 188  
114 2 76.5 305 153 305  
114 3 376.5 197 101 197  
115 2 76 304 152 304  
115 3 374 201 102 201  
116 2 76 304 152 304  
116 3 372 203 102 203  
117 2 75.5 305 151 305  
117 3 371 203 100 203  
118 2 75 303 150 303  
118 3 369 202 98 202  
119 2 75 287 150 287  
119 3 356.5 207 101 207  
120 2 74 269 148 269  
120 3 341.5 215 113 215  
121 2 74.5 254 149 254  
121 3 333 222 112 222  
122 2 77 250 154 250  
122 3 327 235 106 235  
123 2 79 248 158 248  
123 3 323.5 242 107 242  
124 2 81 248 154 248  
124 3 319 244 104 244  
125 2 83.5 248 147 248

125 3 309 245 106 245  
126 2 85.5 248 143 248  
126 3 300 245 106 245  
127 2 90 246 140 246  
127 3 286 245 114 245  
128 2 93.5 243 139 243  
128 3 279.5 249 111 249  
129 2 97 236 132 236  
129 3 266.5 261 123 261  
130 2 99 232 130 232  
130 3 260.5 278 121 278  
131 2 101.5 223 125 223  
131 3 249 293 136 293  
132 2 105 210 126 210  
132 3 240 301 144 301  
133 2 107.5 195 127 195  
133 3 234.5 315 147 315  
134 2 109.5 187 129 187  
134 3 231.5 322 141 322  
135 2 111.5 186 123 186  
135 3 228.5 324 127 324  
136 2 112.5 186 117 186  
136 3 224.5 325 121 325  
137 2 115 186 106 186  
137 3 216 324 108 323  
138 2 115 186 96 186  
138 3 206.5 326 109 325  
139 2 116.5 186 89 186  
139 3 201 324 106 323  
140 2 118.5 183 85 183  
140 3 190 325 112 324  
141 3 179 325 126 324  
142 3 165 340 152 340  
143 3 159 353 162 353  
144 3 156.5 358 169 358  
145 3 145.5 378 183 377  
146 3 134 386 200 385  
147 3 119 389 214 387  
147 4 135 83 68 83  
148 3 108.5 388 217 384  
148 4 138.5 121 81 121  
149 3 100 389 200 383  
149 4 139 140 98 140  
150 3 95 389 190 384  
150 4 139.5 148 111 147  
151 3 91 392 182 387  
151 4 140.5 152 117 151  
152 3 89 395 178 390  
152 4 141 165 110 165  
153 3 91 403 182 398  
153 4 142 171 118 171  
154 3 92 412 184 409  
154 4 144.5 172 107 172  
155 3 92 410 184 408  
155 4 145 172 100 172  
156 3 93.5 414 187 414  
156 4 150 167 76 167  
157 3 93.5 413 187 413  
157 4 152 158 74 158  
158 3 94 417 188 416  
158 4 150.5 150 79 150

159 3 97.5 435 195 434  
159 4 150 145 80 145  
160 3 100 444 200 441  
160 4 151 145 74 145  
161 3 103.5 444 207 441  
161 4 155 150 64 150  
162 3 114.5 451 211 447  
162 4 156.5 156 63 156  
163 3 138 456 238 452  
164 3 158 457 238 452  
165 3 180.5 464 225 459  
166 3 196.5 468 203 461  
167 3 207.5 470 195 463  
168 3 214 471 182 462  
169 3 224 467 166 458  
170 3 238.5 469 161 462  
171 3 258.5 468 183 462  
171 5 125.5 214 99 214  
172 3 288 467 208 463  
172 5 124 216 98 216  
173 3 305 467 212 464  
173 5 121 216 100 216  
174 3 317.5 467 211 462  
174 5 118 216 106 216  
175 3 330.5 466 209 460  
175 5 113.5 217 113 217  
176 3 339.5 465 211 459  
176 5 114 232 104 231  
177 3 355 453 154 451  
177 5 108 251 122 251  
178 3 383.5 457 127 457  
178 5 96.5 267 147 267  
179 3 399.5 448 125 447  
179 5 91.5 272 155 272  
180 3 417.5 437 129 437  
180 5 86.5 273 161 273  
181 3 428.5 434 133 434  
181 5 83.5 274 161 274  
182 3 441.5 426 147 426  
182 5 81 274 160 274  
183 3 457.5 414 175 414  
183 5 77 275 154 275  
184 3 470.5 409 193 409  
184 5 73 275 146 275  
185 3 479 411 200 411  
185 5 69.5 278 139 278  
186 3 503 417 226 417  
186 5 62 299 116 299  
187 3 519 417 232 417  
187 5 59.5 314 119 314  
188 3 523.5 416 231 416  
188 5 60 324 120 324  
189 3 528 412 222 412  
189 5 60 330 120 330  
190 3 534 412 210 412  
190 5 58.5 332 117 332  
191 3 537 413 204 413  
191 5 58 332 116 332  
192 3 536.5 412 193 412  
192 5 56.5 331 113 331  
193 3 531 411 186 411

193 5 54 330 108 330  
194 3 518 404 200 404  
194 5 52.5 333 105 333  
195 3 508 400 206 400  
195 5 51.5 346 103 346  
196 3 500.5 398 207 398  
196 5 51.5 359 103 358  
197 3 493 397 204 397  
197 5 52 369 104 366  
198 3 484 399 200 399  
198 5 52.5 381 105 373  
199 3 475 399 192 399  
199 5 51.5 387 103 375  
200 3 468.5 399 191 399  
200 5 52 390 104 375  
201 3 460 390 166 390  
201 5 52.5 393 105 370  
202 3 455.5 380 143 380  
202 5 52.5 393 105 362  
203 3 448 374 130 374  
203 5 52 393 104 358  
204 3 440 373 134 373  
204 5 52 392 104 352  
205 3 432 371 138 371  
205 5 52 390 104 347  
206 3 400.5 373 149 373  
206 5 56.5 390 113 335  
207 3 378.5 375 151 375  
207 5 65 390 130 330  
208 3 363.5 375 147 375  
208 5 74.5 389 149 327  
209 3 354 372 150 372  
209 5 82.5 390 165 331  
210 3 346 366 150 366  
210 5 86 394 168 368  
211 3 327 348 132 348  
211 5 92.5 398 185 362  
212 3 316.5 332 127 332  
212 5 93 397 182 385  
213 3 300 320 120 319  
213 5 94.5 398 187 395  
214 3 287.5 307 109 305  
214 5 94 397 186 397  
215 3 279.5 305 107 303  
215 5 93.5 394 187 392  
216 3 273.5 306 105 305  
216 5 94.5 398 189 398  
217 3 268.5 305 105 305  
217 5 95 399 188 399  
218 3 256.5 303 131 303  
218 5 97 408 192 408  
219 3 251 302 138 302  
219 5 102.5 416 205 416  
220 3 248.5 298 137 298  
220 5 113.5 424 223 424  
221 3 243 294 146 294  
221 5 140 436 252 436  
222 3 236 287 140 287  
222 5 162 442 254 442  
223 3 230 279 114 279  
223 5 181 445 246 445

224 3 226.5 262 89 262  
224 5 196 447 236 447  
225 3 219.5 255 85 255  
225 5 206 448 224 448  
226 5 215 446 204 446  
227 5 220.5 447 197 447  
228 3 152.5 204 101 204  
228 5 229 445 170 445  
229 3 150 224 110 224  
229 5 244 446 184 446  
230 3 149 253 114 253  
230 5 261 443 200 443  
231 3 148 263 116 263  
231 5 272.5 445 203 445  
232 3 149 268 128 268  
232 5 286 442 202 442  
233 3 144 265 124 265  
233 5 300.5 444 201 444  
234 3 138.5 255 117 255  
234 5 307.5 443 189 443  
235 3 132.5 245 117 245  
235 5 313 442 170 442  
236 3 130.5 241 115 241  
236 5 316.5 441 167 441  
237 3 128.5 237 117 237  
237 5 320.5 439 159 439  
238 3 126.5 232 121 232  
238 5 328.5 438 151 438  
239 3 124.5 231 119 231  
239 5 337 437 152 437  
240 3 123.5 231 117 231  
240 5 345 415 158 415  
241 3 125 229 114 229  
241 5 356.5 381 159 381  
242 3 126 229 112 229  
242 5 362.5 368 155 368  
243 3 129 229 110 229  
243 5 370 361 152 361  
244 3 132 227 112 227  
244 5 376 361 150 361  
245 3 134.5 224 111 224  
245 5 380 361 148 361  
246 3 136.5 222 111 222  
246 5 382.5 360 149 360  
247 3 138 219 110 219  
247 5 385.5 360 149 360  
248 3 140.5 216 103 216  
248 5 393.5 358 147 358  
249 3 142 214 100 214  
249 5 401 350 148 350  
250 3 145 214 98 214  
250 5 408.5 342 153 342  
251 3 152.5 214 107 214  
251 5 418.5 314 163 314  
252 3 158 212 114 212  
252 5 425.5 299 159 299  
253 3 161 212 118 212  
253 5 429 294 154 294  
254 3 163.5 211 123 211  
254 5 434.5 293 151 293  
255 3 168.5 212 123 212

255 5 439.5 293 145 293  
256 3 170.5 212 121 212  
256 5 441.5 293 141 293  
257 3 172 213 120 213  
257 5 442.5 293 139 293  
258 3 174 214 120 214  
258 5 440.5 291 131 291  
259 3 175.5 215 119 215  
259 5 439 285 128 285  
260 3 177 215 114 215  
260 5 438.5 277 125 277  
261 3 180 215 108 215  
261 5 437.5 267 125 266  
262 3 182.5 215 103 215  
262 5 437.5 256 125 255  
263 3 187 215 94 215  
263 5 437 236 126 235  
264 3 188 215 90 215  
264 5 437.5 228 119 227  
265 3 193 214 90 214  
265 5 437 225 118 224  
266 3 203 214 104 214  
266 5 439 225 112 224  
267 3 218 214 124 214  
267 5 439.5 225 111 224  
268 3 233.5 214 145 214  
268 5 439.5 225 113 224  
269 3 244.5 215 137 215  
269 5 440 224 116 223  
270 3 252.5 215 131 215  
270 5 440 217 116 216  
271 3 256 215 128 215  
271 5 439.5 211 115 211  
272 3 260.5 215 119 215  
272 5 440 206 116 206  
273 3 274.5 216 81 216  
273 5 439 189 110 189  
274 3 284.5 225 79 225  
274 5 437 180 102 180  
275 3 297 227 90 227  
275 5 433 177 100 177  
276 3 316 232 116 232  
276 5 425.5 176 105 176  
277 3 328 233 126 233  
277 5 420.5 175 107 175  
278 3 337.5 231 135 231  
278 5 415.5 176 107 176  
279 3 343 231 138 231  
279 5 413 176 104 176  
280 3 345 232 140 232  
280 5 412.5 177 99 177  
281 3 347.5 233 141 233  
281 5 413 176 86 176  
282 3 356.5 233 115 233  
282 5 413.5 166 57 166  
283 3 370.5 233 111 232  
283 5 412.5 162 53 162  
284 3 380 234 100 233  
285 3 394.5 234 109 234  
286 3 402.5 234 133 234  
287 3 409 233 130 233



288 3 419.5 233 113 233  
289 3 423 233 108 233  
290 3 423 234 104 233  
290 5 358 153 80 153  
291 3 423 234 104 233  
291 5 341.5 144 43 144  
292 3 426.5 234 101 233  
292 5 349 150 78 150  
293 3 429.5 235 101 234  
293 5 350 152 86 152  
294 3 436 238 92 238  
294 5 350 152 80 152  
295 3 442 236 90 236  
295 5 349 152 84 152  
296 3 451.5 246 79 246  
296 5 343.5 152 89 152  
297 3 458 250 74 250  
297 5 337.5 151 93 151  
298 3 463 253 80 253  
298 5 333 152 102 152  
299 3 465.5 255 83 255  
299 5 332.5 154 101 154  
300 3 468.5 258 87 258  
300 5 340.5 156 71 156  
301 3 483 262 124 261  
301 5 333 160 88 160  
302 3 491 264 136 263  
302 5 327.5 164 89 164  
303 3 496 264 140 263  
303 5 324.5 169 87 169  
304 3 501.5 265 147 264  
304 5 322.5 174 99 174  
305 3 502 265 154 264  
305 5 318.5 176 103 176  
306 3 499.5 265 153 264  
306 5 307 178 84 178  
307 3 497 266 148 265  
307 5 306.5 178 101 178  
308 3 494.5 268 145 267  
308 5 304 183 100 183  
309 3 492.5 268 145 267  
309 5 304 190 100 190  
310 3 489.5 268 139 268  
310 5 301.5 203 95 203  
311 3 483.5 267 135 267  
311 5 300 219 90 219  
312 3 480.5 267 135 267  
312 5 295 231 100 231  
313 3 477 267 132 267  
313 5 290 236 104 236  
314 3 475 266 130 266  
314 5 286.5 237 111 237  
315 3 473 267 130 267  
315 5 279.5 239 125 239  
316 3 471 267 126 267  
316 5 275 239 128 239  
317 3 469.5 266 125 266  
317 5 268.5 238 137 238  
318 3 468.5 266 123 266  
318 5 264 240 138 240  
319 3 467 266 122 266

319 5 261.5 244 141 244  
320 3 464.5 261 119 261  
320 5 257 262 132 262  
321 3 463 255 120 255  
321 5 257.5 275 133 275  
322 3 458 245 114 245  
322 5 259.5 288 133 288  
323 3 457.5 240 119 240  
323 5 261.5 295 135 295  
324 3 453.5 218 119 218  
324 5 265 299 138 299  
325 3 451 207 114 207  
325 5 267 300 142 300  
326 3 448 204 114 204  
326 5 268.5 300 151 300  
327 3 446.5 203 115 203  
327 5 268.5 300 153 300  
328 3 442 201 104 201  
328 5 269.5 311 155 311  
329 3 438 199 98 199  
329 5 269.5 332 153 332  
330 3 434.5 193 95 193  
330 5 269.5 347 153 347  
331 3 432.5 187 95 187  
331 5 268.5 355 151 355  
332 3 430.5 178 99 178  
332 5 266 362 150 362  
333 3 429 167 96 167  
333 5 262.5 368 149 368  
334 3 425.5 161 91 161  
334 5 255 371 162 371  
335 3 424.5 159 89 159  
335 5 252 372 162 372  
336 3 422.5 158 85 158  
336 5 247.5 373 167 372  
337 3 419 159 80 159  
337 5 242 371 174 370  
338 3 417.5 159 81 159  
338 5 238.5 371 175 370  
339 3 414.5 159 79 159  
339 5 233 373 174 372  
340 3 413.5 160 77 160  
340 5 231 372 172 371  
341 3 409.5 159 71 159  
341 5 216 385 164 385  
342 3 406.5 160 69 160  
342 5 201 398 174 398  
343 3 405 159 66 159  
343 5 195.5 413 175 413  
344 3 405 156 62 156  
344 5 186 417 204 417  
345 3 406 153 58 153  
345 5 179 414 214 414  
346 3 406.5 152 55 152  
346 5 176 413 216 413  
347 3 407.5 152 55 152  
347 5 173.5 416 221 416  
348 3 407.5 152 53 152  
348 5 154.5 415 261 415  
349 3 408 152 54 152  
349 5 136.5 415 259 415

350 3 406.5 153 61 153  
350 5 126 419 246 419  
351 3 402.5 154 73 154  
351 5 115.5 420 227 420  
352 3 400 155 76 155  
352 5 108 420 216 420  
353 3 396 156 84 156  
353 5 94.5 417 187 417  
354 3 394 157 88 157  
354 5 93 418 186 418  
355 3 391.5 158 93 158  
355 5 93 420 186 420  
356 3 390 158 98 158  
356 5 93 418 186 418  
357 3 389.5 162 97 162  
357 5 92.5 418 185 417  
358 3 390 164 98 164  
358 5 93 417 186 415  
359 3 393 164 92 164  
359 5 90.5 415 181 412  
360 3 394.5 165 91 165  
360 5 88.5 414 177 411  
361 3 395.5 165 91 165  
361 5 79 411 154 409  
362 3 391.5 165 95 165  
362 5 68 397 134 395  
363 3 386 169 102 169  
363 5 65.5 392 131 391  
364 3 382 175 104 175  
364 5 65 390 130 390  
365 3 378 182 102 182  
365 5 66.5 386 133 386  
366 3 376.5 186 105 186  
366 5 67.5 384 135 384  
367 3 374 194 100 194  
367 5 69.5 384 139 384  
368 3 372 202 96 202  
368 5 70.5 385 141 385  
369 3 370 206 96 206  
369 5 71 383 142 383  
370 3 364 209 96 208  
370 5 69.5 377 139 377  
371 3 357.5 209 101 209  
371 5 68.5 365 137 361  
372 3 352 209 104 209  
372 5 66.5 353 133 349  
373 3 346 208 110 208  
373 5 67 329 134 327  
374 3 342 214 110 214  
374 5 67 311 134 310  
375 3 335 234 112 234  
375 5 67 306 134 306  
376 3 331.5 245 115 245  
376 5 68 305 136 305  
377 3 329 250 118 250  
377 5 71 305 142 305  
378 3 327 253 120 253  
378 5 72.5 306 145 306  
379 3 325 258 120 258  
379 5 73.5 305 147 305  
380 3 322 268 118 268

380 5 74 306 148 306  
381 3 320.5 274 119 274  
381 5 74.5 306 149 306  
382 3 319 275 118 275  
382 5 76 302 152 302  
383 3 317 276 116 276  
383 5 77 295 154 295  
384 3 315.5 276 115 276  
384 5 77 288 154 288  
385 3 312.5 275 113 275  
385 5 79 277 154 277  
386 3 308.5 275 111 275  
386 5 83 260 154 260  
387 3 301 291 120 291  
387 5 88 242 156 242  
388 3 295 300 128 300  
388 5 91 236 150 235  
389 3 287 312 126 311  
389 5 95 234 144 233  
390 3 282 328 118 328  
390 5 100 233 142 232  
391 3 275.5 340 119 340  
391 5 103.5 234 141 233  
392 3 266.5 346 129 346  
392 5 106.5 233 137 232  
393 3 260.5 347 133 347  
393 5 109.5 233 135 232  
394 3 248 348 154 348  
394 5 110 225 130 224  
395 3 237 350 166 349  
395 5 107.5 218 119 217  
396 3 229 360 172 358  
396 5 112 202 104 202  
397 3 224.5 390 171 389  
397 5 117 191 100 191  
398 3 221.5 426 173 426  
398 5 119 185 96 185  
399 3 220.5 452 181 451  
399 5 131 169 94 169  
400 3 222 467 184 466  
400 5 135 165 92 165  
401 3 226.5 474 205 470  
401 5 140.5 137 79 137  
402 3 228.5 477 213 471  
402 5 144 128 64 128  
403 3 229.5 479 221 469  
403 5 147.5 118 59 118  
404 3 230 479 224 468  
405 3 231 479 234 464  
406 3 231.5 479 249 451  
407 3 231.5 479 251 442  
408 3 231 479 258 431  
409 3 225.5 479 287 412  
410 3 222 479 302 397  
411 3 220 479 314 384  
411 9 225 158 114 158  
412 3 223 479 328 373  
412 9 237 157 112 157  
413 3 225.5 479 331 363  
413 9 242.5 157 111 157  
414 3 237.5 479 353 347

414	9	248	157	108	157
415	3	246.5	479	351	339
415	9	249	157	108	157
416	3	260	479	358	329
416	9	252.5	155	99	154
417	3	286.5	479	367	318
417	9	260	150	82	150
418	3	301	479	364	312
418	9	264	147	76	147
419	3	316	479	370	305
419	9	269.5	146	75	145